



# Analysis of the water-power nexus in the North, Eastern and Central African Power Pools

Authors:

PAVIČEVIĆ, M., QUOILIN, S.,

Editors:

DE FELICE, M.,

BUSCH, S.,

HIDALGO GONZÁLEZ, I.

2020



This publication is a report prepared by the Katholieke Universiteit Leuven for the Joint Research Centre (JRC), the European Commission's science and knowledge service. It aims to provide evidence-based scientific support to the European policymaking process. The scientific output expressed does not imply a policy position of the European Commission. Neither the European Commission nor any person acting on behalf of the Commission is responsible for the use that might be made of this publication. For information on the methodology and quality underlying the data used in this publication for which the source is neither Eurostat nor other Commission services, users should contact the referenced source. The designations employed and the presentation of material on the maps do not imply the expression of any opinion whatsoever on the part of the European Union concerning the legal status of any country, territory, city or area or of its authorities, or concerning the delimitation of its frontiers or boundaries.

#### Contact information

Name: Ignacio Hidalgo González

Address: European Commission, Joint Research Centre (JRC), P.O. Box 2, NL-1755 ZG Petten, The Netherlands

Email: [Ignacio.HIDALGO-GONZALEZ@ec.europa.eu](mailto:Ignacio.HIDALGO-GONZALEZ@ec.europa.eu)

Tel.: +31224565103

#### EU Science Hub

<https://ec.europa.eu/jrc>

JRC121098

EUR 30310 EN

PDF

ISBN 978-92-76-20874-7

ISSN 1831-9424

doi:10.2760/12651

Luxembourg: Publications Office of the European Union, 2020

© European Union, 2020



The reuse policy of the European Commission is implemented by the Commission Decision 2011/833/EU of 12 December 2011 on the reuse of Commission documents (OJ L 330, 14.12.2011, p. 39). Except otherwise noted, the reuse of this document is authorised under the Creative Commons Attribution 4.0 International (CC BY 4.0) licence (<https://creativecommons.org/licenses/by/4.0/>). This means that reuse is allowed provided appropriate credit is given and any changes are indicated. For any use or reproduction of photos or other material that is not owned by the EU, permission must be sought directly from the copyright holders.

All content © European Union 2020

How to cite this report: Pavičević, M. and Quoilin, S., *Analysis of the water-power nexus in the North, Eastern and Central African Power Pools*, De Felice, M., Busch, S. and Hidalgo Gonzalez, I., editor(s), EUR 30310 EN, Publications Office of the European Union, Luxembourg, 2020, ISBN 978-92-76-20874-7, doi:10.2760/12651, JRC121098.

# Contents

Foreword.....	1
Acknowledgements.....	2
Abstract.....	3
1 Introduction.....	4
1.1 Overview of the African power pools .....	4
1.2 Policy context.....	5
1.3 Data uncertainty.....	6
1.4 Structure of the report.....	6
2 Modelling framework.....	7
2.1 Models used within this study.....	7
2.1.1 LISFLOOD .....	7
2.1.2 TEMBA – OSeMOSYS .....	8
2.1.3 Dispa-SET .....	8
2.2 Methods and assumptions.....	9
2.2.1 Hydro inflows and availability factors .....	9
2.2.2 Wind and solar availability factors.....	10
2.2.3 Fuel prices .....	10
2.3 Power system metrics and indicators.....	11
2.3.1 RES curtailment.....	11
2.3.2 Shed load and lost load .....	11
2.3.3 Shadow price .....	11
2.3.4 Water stress .....	11
2.3.5 Water exploitation index.....	12
2.3.6 Water value.....	12
2.3.7 Start-ups.....	12
2.3.8 CO <sub>2</sub> emissions .....	12
3 Input data and assumptions.....	13
3.1 African power pools.....	13
3.2 Fuel prices.....	13
3.2.1 Local resource availability (biomass/biogas, peat and coal) .....	14
3.3 Hourly load profiles .....	14
3.4 Supply .....	15
3.5 Hydropower units.....	17
3.5.1 Evapotranspiration .....	19
3.5.2 Inflows .....	19
3.6 Thermal units.....	20

3.7 Grid infrastructure .....	20
<b>4 Scenarios .....</b>	<b>23</b>
4.1 Reference scenario.....	23
4.2 Connected scenario.....	24
<b>5 Results and discussion of the Reference and Connected scenarios .....</b>	<b>25</b>
5.1 Storage levels computed by Dispa-SET MTS .....	25
5.2 Total system costs .....	27
5.3 Shadow prices .....	27
5.3.1 Reference scenario .....	27
5.3.2 Connected scenario .....	28
5.4 Electricity generation .....	29
5.4.1 Reference scenario .....	31
5.4.2 Connected scenario .....	31
5.5 Curtailment and spillage .....	31
5.6 Load shedding .....	32
5.6.1 Reference scenario .....	32
5.6.2 Connected scenario .....	34
5.7 Start-ups .....	34
5.8 Water stress and water value .....	37
5.8.1 Reference scenario .....	37
5.8.2 Connected scenario .....	40
5.9 Water values .....	41
5.10 CO <sub>2</sub> emissions .....	42
<b>6 Long-term simulations: soft linking with TEMBA.....</b>	<b>44</b>
6.1 PV, Wind and CSP .....	44
6.2 TEMBA Scenarios .....	44
6.3 Power supply .....	45
6.3.1 NTC .....	46
6.4 Results and discussion from TEMBA scenarios .....	47
6.4.1 Generation .....	47
6.4.2 Curtailment .....	48
6.4.3 Load shedding .....	48
6.4.4 Fresh water withdrawal and consumption .....	49
6.4.5 CO <sub>2</sub> emissions .....	50
6.4.6 Adequacy of the TEMBA system .....	51
<b>7 Conclusions .....</b>	<b>52</b>
<b>8 References .....</b>	<b>53</b>
List of abbreviations and definitions .....	55
List of figures .....	56

List of tables .....	59
Annexes .....	60
Annex 1. Fuel price estimation .....	60
Annex 2. Hydro units statistics .....	64
Annex 3. Typical units .....	65
Annex 4. Renewable capacity factors .....	66
Annex 5. Historical inflows .....	68
Annex 6. Shadow prices .....	71
Annex 7. Generation .....	75
Annex 8. Curtailment .....	78
Annex 9. Load shedding .....	80
Annex 10. Water indicators .....	83
Annex 11. CO <sub>2</sub> emissions .....	89

## **Foreword**

Increasing water stress will intensify competition between water uses. A lack or an excess of water may undermine the functioning of the energy and food production sectors with societal and economic effects. Energy and water are inextricably linked: we need “water for energy” for cooling thermal power plants, energy storage, biofuels production, hydropower, enhanced oil recovery, etc., and we need “energy for water” to pump, treat and desalinate. Without energy and water, we cannot satisfy basic human needs, produce food for a rapidly growing population and achieve economic growth. Producing more crops per drop to meet present and future food demands means developing new water governance approaches.

The Water Energy Food and Ecosystem Nexus (WEFE Nexus) flagship project addresses in an integrated way the interdependencies and interactions between water, energy, agriculture, as well as household demand. These interactions have been so far largely underappreciated. The WEFE-Nexus can be depicted as a way to overcome stakeholders' view of resources as individual assets by developing an understanding of the broader system. It is the realization that acting from the perspective of individual sectors cannot help tackle future societal challenges.

The overall objective of the Water-Energy-Food-Ecosystems Nexus flagship project (WEFE-Nexus) is to help in a systemic way the design and implementation of European policies with water dependency. By combining expertise and data from across the JRC it will inform cross-sectoral policy making on how to improve the resilience of water-using sectors such as energy, agriculture and ecosystems.

### **WEFE-NEXUS objectives**

- Analyse the most significant interdependencies by testing strategies, policy options and technological solutions under different socio-economic scenarios for Europe and beyond.
- Evaluate the impacts of changing availability of water due to climate change, land use, urbanization, demography in Europe and geographical areas of strategic interest for the EU.
- Deliver country and regional scale reports, outlooks on anomalies in water availability, a toolbox for scenario-based decision making, and science-policy briefs connecting the project's recommendations to the policy process.

### **How is the analysis done?**

JRC experts use a broad range of models and sources to ensure a robust analysis. This includes water resources and climate models to understand current and future availability of water resources, and energy models and scenario employed to understand and forecast current and future energy demands and the related water footprint of the energy sector.

The results from these models are expected to provide i) understanding the impacts of water resources on the operation of the energy system, and vice versa, ii) spatial analysis and projection of water and energy requirements of agricultural and urban areas in different regions, iii) producing insights for a better management of water and energy resources.

### **What is this report about?**

The WEFE projects aims to provide a detailed insight of the water-power nexus in all African power pools, since the power system is the most water-intensive part of the energy industry. This report provides the results of the model-based analyses carried out for the North (NAPP), Central (CAPP) and Eastern (EAPP) African Power Pool according to the approach used by the JRC for the West African Power Pool (De Felice et al., 2018), and the Iberian Peninsula (Fernandez Blanco Carramolino et al., 2017).

## **Acknowledgements**

This report has been prepared by the Mechanical Engineering Technology unit of The Katholieke Universiteit Leuven (KUL) for the European Commission's Joint Research Centre, under service contract 938088, therefore the content of this study does not reflect the official opinion of the European Union. Responsibility for the information and views expressed in the study lies entirely with the authors.

We thank you the comments and suggestions from our colleagues Andreas Uihlein and Stathis Petevs.

### ***Authors (KUL)***

Matija Pavičević

Sylvain Quoilin

### ***Editors (JRC)***

Sebastian Busch

Matteo De Felice

Ignacio Hidalgo González

## **Abstract**

This report describes the results of applying an open-source modelling framework to three African power pools<sup>1</sup>: the Central African Power Pool, the Eastern Africa Power Pool and the North African Power Pool. The modelling framework is used to analyse results at country level - where insights regarding the power generation, system adequacy, total operational costs, freshwater consumption and withdrawals, water values (hydro storage shadow price), and CO<sub>2</sub> emissions linked to the power sector are assessed. The model source code and the input data are provided together with the report for transparency purposes to facilitate further exploitation and analysis of the results.

Water-energy nexus indicators such as the water exploitation index, or water withdrawal and consumption related to power generation, are computed for the three power pools and for major individual power plants. The indicators show that these three African Power Pools are strongly dependent on the availability of freshwater resources. The variation between wet and dry years significantly impacts the final energy mix, the total operational costs, the total carbon emissions and the water stress index of the system. The relative impact of water consumption<sup>2</sup> over water withdrawals<sup>3</sup> is low because of the predominance of once-through cooling systems in the most vulnerable countries.

Furthermore, several isolated countries within each power pool exhibit a power system which is not adequate, leading to significant amounts of load not served. The importance of increasing the reliability as well as the capacity of interconnection lines is thereby highlighted. A well interconnected grid reduces the need for variable renewable energy (VRES) curtailment and water spillage in hydropower units, allows higher integration of renewable sources, and reduces the need for load shedding<sup>4</sup>, especially in extremely dry years. A higher degree of interconnection also has a positive impact on water stress indicators since water consumption and water withdrawal can be significantly reduced.

Africa presents an important potential of variable renewable energy sources (mainly wind and solar) which is still largely untapped. The addition of new VRES capacity can reduce the potential carbon emissions by more than 32% by 2045 compared to a business-as-usual scenario. However, this is only possible by reducing the congestion when energy flows from southern countries (hydro-rich), and energy flows from the northern countries (VRES-abundant) are enabled. This is particularly the case in future low carbon scenarios, in which power generation from thermal units is lower, resulting in a lack of flexibility and therefore in higher curtailment and load shedding.

---

<sup>1</sup> Regional cooperation entities aimed to developing a common power grid and a common market between their members.

<sup>2</sup> Water lost due to evaporation, leakages, or rendered unusable through other thermo-chemical processes.

<sup>3</sup> Thermal pollution due to the increased water temperature caused by cooling processes inside the power plants.

<sup>4</sup> An additional safety mechanism that can be enforced to prevent system blackouts, usually provided by large industrial facilities which can decrease their production for a certain amount of time.

# 1 Introduction

Access to a stable and secure supply of energy is a fundamental driver of economic growth in Africa. More than two-thirds of the population, approximately 600 million people, especially in Sub-Saharan Africa, lacked access to electricity in 2016, and 850 million people had no access to clean cooking facilities such as natural gas, liquefied petroleum gas, electricity and biogas, or improved biomass cook stoves (International Energy Agency, 2017). Africa's gross economic activity is, according to (African Development Bank Group, 2019), expected to continue its rapid growth. The economic growth is estimated at 4.1% in 2019 compared to 2.4% in 2018 and is set to increase between 2.1 and 4.1% annually in the next decade<sup>5</sup>. In order to meet this growing demand, and take advantage of trade opportunities, five regional power pools (regional cooperation entities aimed to developing a common power grid and a common market between their members) have been established.

## 1.1 Overview of the African power pools

The geographical overview of the power pools studied in this report is presented in Figure 1, while their statistical data are shown in Table 1. This study complements similar analyses carried out directly by the JRC and therefore focuses only on three power pools, namely:

- the Central African Power Pool (CAPP)<sup>6</sup> Angola, Cameroon, Central African Republic, Chad, Congo, Democratic Republic of Congo (DRC), Equatorial Guinea and Gabon;
- the East African Power Pool (EAPP)<sup>7</sup>, DRC, Djibouti, Egypt, Ethiopia, Kenya, Rwanda, Somalia, Sudan, Tanzania, Libya, Uganda and South Sudan; and
- the North African Power Pool (NAPP)<sup>8</sup> Algeria, Libya, Mauritania, Morocco and Tunisia.

**Figure 1** Organization of African power pools



Source: (Medinilla, Byieres, and Karaki, 2019)

<sup>5</sup> The World Bank: <https://data.worldbank.org/indicator/NY.GDP.MKTP.KD.ZG?locations=ZG>

<sup>6</sup> CAPP Geographic Information System: <https://www.peac-sig.org/en/>

<sup>7</sup> East African Power Pool: <http://eappool.org/>

<sup>8</sup> Comité Maghrébin de l'Électricité (COMELEC): <https://comelec-net.org/index-en.php>

**Table 1** Statistics for the three power pools.

Power Pool	Country names and corresponding ISO-2 code	Population 2018 (change from 2010), millions	GDP per capita 2018 (change from 2010), USD	Electricity consumption per capita 2015 (change from 2010), kWh	Electricity use rate 2017 (total, urban and rural) %
CAPP	Angola (AO)	30.8 (+7.4)	3 432 (-155)	312 (+105)	41.8 / 72.7 / 0.0
	Cameroon (CM)	25.2 (+4.9)	1 533 (+248)	275 (+14)	61.4 / 93.2 / 21.3
	Central African Republic (CF)	4.7 (+0.3)	475 (-12)		29.9 / 52.1 / 14.6
	Chad (TD)	15.5 (+3.5)	728 (-163)		10.8 / 39.1 / 2.4
	Congo (CG)	5.2 (+1.0)	2 147 (-661)	203 (+63)	66.2 / 87.4 / 24.2
	Democratic Republic of the Congo (CD)	84.0 (+19.5)	561 (+228)	108 (+4)	19.1 / 49.2 / 0.0
	Equatorial Guinea (QE)	1.3 (+0.4)	10 261 (-7,001)		67.1 / 91.3 / 6.0
	Gabon (GA)	2.1 (+0.5)	7 952 (-888)	1 168 (+210)	92.2 / 97.5 / 49.1
	Burundi (BI)	11.2 (+2.5)	272 (+38)		9.3 / 61.8 / 1.7
EAPP	Djibouti (DJ)	1.0 (+0.1)	3 083 (+1,740)		
	Egypt (EG)	98.4 (+15.7)	2 549 (-96)	1 683 (+107)	100 / 100 / 100
	Eritrea (ER)	3.2 (+0.0)	332 (-336)		
	Ethiopia (ET)	109.2 (+21.6)	772 (+431)	69 (+21)	44.3 / 96.6 / 31
	Kenya (KE)	51.4 (+9.4)	1 711 (+759)	164 (+16)	63.8 / 81.1 / 57.6
	Rwanda (RW)	12.3 (+2.3)	773 (+190)		34.1 / 84.8 / 23.6
	Somalia (SO)	15.0 (+3.0)	315 (+47)		
	South Sudan (SS)	11.0 (+1.5)	353 (-1,182)		
	Sudan (SD)	41.8 (+7.3)	977 (-513)	190 (+59)	56.5 / 82.5 / 42.8
NAPP	Tanzania (TZ)	56.3 (+12.0)	1 050 (+307)		
	Uganda (UG)	42.7 (+10.3)	643 (+20)		
	Algeria (DZ)	42.2 (+6.3)	4,115 (-366)	1 363 (+346)	100 / 100 / 100
	Libya (LY)*	6.7 (+0.5)	7 242 (-4,823)	1 811 (-1,551)	70.1 / 70.1 / 70.1
	Mauritania (MR)	4.4 (+0.9)	1 189 (-53)		42.9 / 82.6 / 0
	Morocco (MA)	36.0 (+3.7)	3 238 (+398)	904 (+128)	100 / 100 / 100
	Tunisia (TN)	11.6 (+0.9)	3,448 (-694)	1 455 (+90)	100 / 100 / 100

Source: The World Bank Data

The renewable and fossil potentials vary significantly between the power pools. NAPP is mostly dominated by fossil while CAPP and EAPP are dominated by water. Most diverse, by per country basis is EAPP where some countries are either entirely fossil or almost entirely renewable powered.

## 1.2 Policy context

The European Commission's Comprehensive Strategy with Africa (European Commission, 2020), the United Nation's Sustainable Energy for All<sup>9</sup> and the Power Africa<sup>10</sup> initiatives aim to electrify some 60 million homes and support the investment of 30 GW of clean power generation in the near future. Despite this, however, there is no coherent 'by country' and 'by region' set of concrete scenarios besides the ones proposed in (Taliotis et al., 2016; Pappis et al., 2019), nor an open energy system analysis platform that may be used to carry out a more detailed investigation of the proposed long term power generation expansion scenarios. However, there are several studies based on non-open modelling frameworks such as JRC's GECO (Keramidas et al., 2020) and IEA's WEO (IEA, 2020) among others.

<sup>9</sup> Sustainable Energy for All (SEforALL) - an international organization working with leaders in government, the private sector and civil society to drive further, faster action toward achievement of Sustainable Development Goal 7 (SDG7), which calls for universal access to sustainable energy by 2030, and the Paris Agreement, which calls for reducing greenhouse gas emissions to limit climate warming to below 2° Celsius. <https://www.seforall.org/about-us>

<sup>10</sup> Power Africa - project development in sub-Saharan Africa's energy sector. [www.usaid.gov/powerafrica](http://www.usaid.gov/powerafrica)

The term “water-energy nexus” refers to the complex interactions between water resources (especially freshwater) and the energy sector. The combined effect of increased water consumption, for energy and non-energy purposes, with lower availability of water resources due to climate change is expected to lead to monetary losses, power curtailments, temporary shutdowns and demand restrictions in power grids across the world (Fernandez Blanco Carramolino et al., 2017). These consequences highlight the need for an integrated modelling framework for the water and power sectors capable of analysing such cross-sectoral interactions. According to some analyses (The World Bank, 2014), electricity and water demands in Africa are projected to grow by 700% and 500% by 2050, with respect to 2012. In most African energy systems hydropower remains the dominant renewable energy source (IHA, 2016). Other salient characteristics of these systems are their small sizes, the low electrification rates, the high shares of oil in the power generation mix, and the lack of significant power and gas interconnections.

The overall objectives of this study are to:

- Propose a methodology for the analysis of the water-power nexus.
- Describe the available data sources used for modelling of the three African Power Pools.
- Investigate synergies between the water and power sectors by assessing the hydro potential in the proposed region through several what-if scenarios with regard to the availability of water for energy purposes in dry and wet seasons.
- Examine the potential for and relationship between current and future electricity situation and power trade between countries in selected power pools, by increasing the temporal and technological granularity of the previously-developed model TEMBA – OSeMOSYS (The Electricity Model Base for Africa)<sup>11</sup>.
- Identify areas where grid extensions would be beneficial for the African electricity supply system.

### **1.3 Data uncertainty**

Significant effort has been made to obtain the best possible data for the modelling and scenario analyses. The demand forecasts are uncertain and have significant impact on the modelling results. A number of scenarios and projections regarding the hydro inflows and other key parameters have been made in this analysis, and the accuracy of the results is function of the uncertainty linked to these projections, especially regarding the cross-border interconnection lines, technical and costs assumptions of the power plant fleet as well as fuel prices.

When data was unavailable or obviously erroneous, corrections had to be performed and best-guess assumptions had to be formulated to fill the gaps. In order to ensure full traceability in the data processing, all the scripts used to process the raw data are documented and provided as electronic annex to this report.

### **1.4 Structure of the report**

This report is structured as follows: In Section 2 the modelling framework applied to this study is introduced, in Section 3 the assumptions regarding the input data are explained, in Section 4 the scenarios used within this study are defined, in Section 5 the main findings from the historic and Connected scenarios are presented, in Section 6 the findings from the TEMBA scenarios are presented, and finally Section 7 concludes the report with a summary of the key outcomes and suggestions for further research.

---

<sup>11</sup> TEMBA – the open source model of African electricity supply that represents each continental African country's electricity supply system and transmission links between them. <http://www.osemosys.org/temba-the-electricity-model-base-for-africa.html>

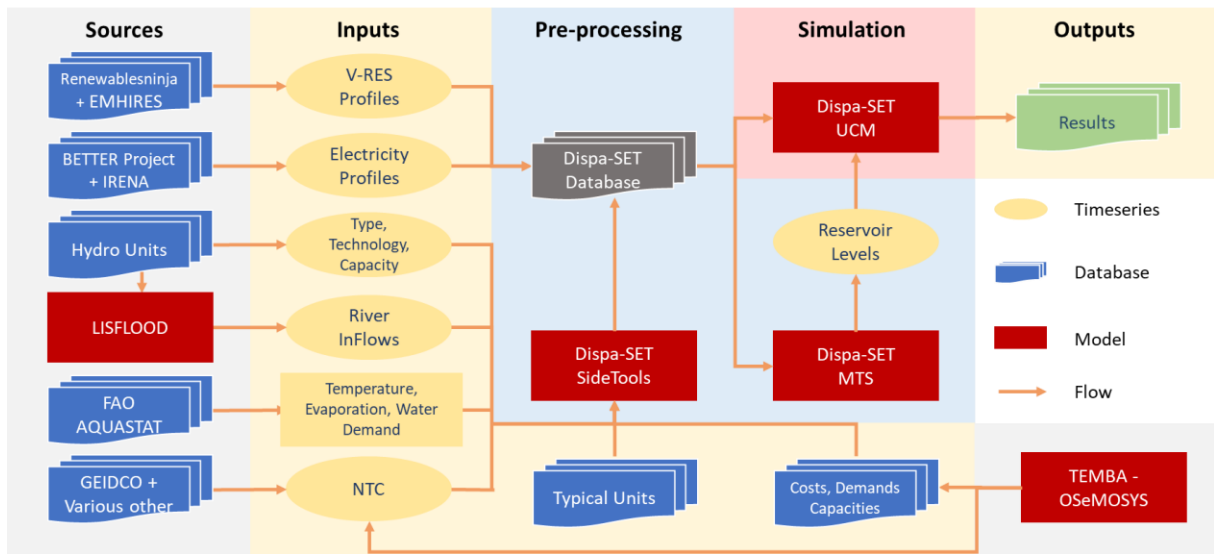
## 2 Modelling framework

This section describes the different tools, techniques and methods used in this work. Figure 2 highlights all possible links and data flows within the modelling framework. It consists of the following five elements: sources, inputs, pre-processing, simulation and outputs. The usual measured historical or simulated input data, such as hourly time series, are complemented with data from other models (LISFLOOD, TEMBA) or reports. These inputs include costs, demand projections and capacities (aggregated only per fuel type), net cross border interconnection capacities (NTC), yearly energy generation from which time series are generated for unit availabilities, demand profiles and energy flow limits between zones.

The proposed framework consists of five models:

- LISFLOOD is used for generation of multiannual hydro profiles;
- TEMBA is used for long term generation expansion planning;
- Data translation models between the LISFLOOD and TEMBA outputs and the Dispa-SET standard input database format;
- The Dispa-SET mid-term scheduling (MTS) module is used for the pre-allocation of large storage units, and the main Dispa-SET UCM model is used to compute the short-term unit commitment and optimal dispatch within all zones;
- Results obtained from the Dispa-SET UCM model are used as main outputs of this study.

**Figure 2** Relational block-diagram between models and various data sources used within this study.



Source: JRC, 2020

TEMBA - OSeMOSYS inputs are complemented with historical (where applicable) and computed hourly time series profiles. Unit commitment and power dispatch is solved with Dispa-SET.

### 2.1 Models used within this study

#### 2.1.1 LISFLOOD

LISFLOOD (Burek, Van der Knijff, and De Roo, 2013) is a rainfall-runoff hydrological model capable of simulating the hydrological processes in a particular catchment area. It was developed by the Joint Research Centre (JRC) of the European Commission, with the specific objective to produce a tool that can be used in large and trans-national catchments for a variety of applications, including flood forecasting, assessing the effects of river regulation measures, the effects of land-use change and the effects of climate change. Within this study, LISFLOOD was used for estimating historical discharge rates in river basins on which hydro units are located.

## 2.1.2 TEMBA – OSeMOSYS

The Electricity Model Base for Africa (TEMBA) was initially developed with the United Nations Economic Commission for Africa (UNECA) to provide a foundation for the analysis of the continental-scale African energy system (Taliotis et al., 2016). For the purpose of this analysis, the results from the TEMBA model are used as inputs for assessing the long-term scenarios in the three African power pools. The input data and modelling framework used within the TEMBA model are described in more detail by (Pappis et al., 2019). The main model outputs are: capacity data (as investment in energy supply in Africa has been growing), cost and performance data, fuel price projections, new energy demand projections. The main limitation of the long term planning models in general is the low temporal resolution. In this study, TEMBA was run with four time intervals: two seasons (summer and winter) and two times of the day (day and night).

## 2.1.3 Dispa-SET

The Dispa-SET model is an open-source unit commitment and optimal dispatch model focused on the balancing and flexibility problems in integrated energy systems with high shares of VRES. It is mainly developed within the JRC of the EU Commission, in close collaboration with the University of Liège and the KU Leuven. The core formulation of the model is an efficient MILP formulation of the UCM problem (Carrion and Arroyo, 2006). A simplified hydro-thermal allocation (MTS) module is available, and is defined as a linear programming approximation (i.e. integer variables are relaxed) of the core UCM model with a lower time resolution. The MTS is used to pre-allocate reservoir levels of seasonal storage units. The main purpose of using the Dispa-SET model is the possibility of analysing large interconnected power systems with a high level of detail. In this study, demands are assumed to be inelastic to the price signal. The MILP objective function is therefore, the total generation cost over the optimization period and can be summarized by:

$$\text{Min TotalSystemCost} = \sum_{\forall u,i} \left( \begin{array}{l} \text{CostStartUp}_{i,u} + \text{CostShutDown}_{i,u} + \\ \text{CostFixed}_u \cdot \text{Committed}_{i,u} + \\ \text{CostVariable}_{i,u} \cdot \text{Power}_{i,u} + \\ \text{CostRampUp}_{i,u} + \text{CostRampDown}_{i,u} + \\ \text{PriceTransmission}_{i,l} \cdot \text{Flow}_{i,l} + \\ \sum_n (\text{CostLoadShedding}_{i,n} \cdot \text{ShedLoad}_{i,n}) + \\ \text{VOLL}_{\text{Power}} \cdot (\text{LL}_{\text{MaxPower},i,n} + \text{LL}_{\text{MinPower},i,n}) + \\ \text{VOLL}_{\text{Reserve}} \cdot (\text{LL}_{2U,i,n} + \text{LL}_{2D,i,n} + \text{LL}_{3U,i,n}) + \\ \text{VOLL}_{\text{Ramp}} \cdot (\text{LL}_{\text{RampUp},u,i} + \text{LL}_{\text{RampDown},u,i}) \end{array} \right) \quad (1)$$

where the terms linked to the heating and cooling sector and the gas sector have been removed since they are not considered in this work.

The main constraint to be met is the power supply-demand balance, for each period and each zone, in the day-ahead market:

$$\begin{aligned} \sum_u (\text{Power}_{u,i} \cdot \text{Location}_{u,n}) + \sum_l (\text{Flow}_{l,i} \cdot \text{LineNode}_{l,n}) &= \text{Demand}_{DA,n,h} \\ + \sum_r (\text{StorageInput}_{s,h} \cdot \text{Location}_{s,n}) - \text{ShedLoad}_{n,i} - \text{LL}_{\text{MaxPower},n,i} \\ + \text{LL}_{\text{MinPower},n,i} \end{aligned} \quad (2)$$

According to this restriction, the sum of the power generated by all the units present in the node (including the power generated by the storage units), the power injected from neighbouring nodes, and the curtailed power from intermittent sources is equal to the day ahead load in that node. Large continental power systems usually consist of hundreds or thousands of power plants of various types, sizes and operational characteristics. To ensure computational tractability, the Dispa-SET UCM model uses efficient clustering and computational relaxation techniques (Pavičević et al., 2019) which reduce the number of continuous and binary variables and

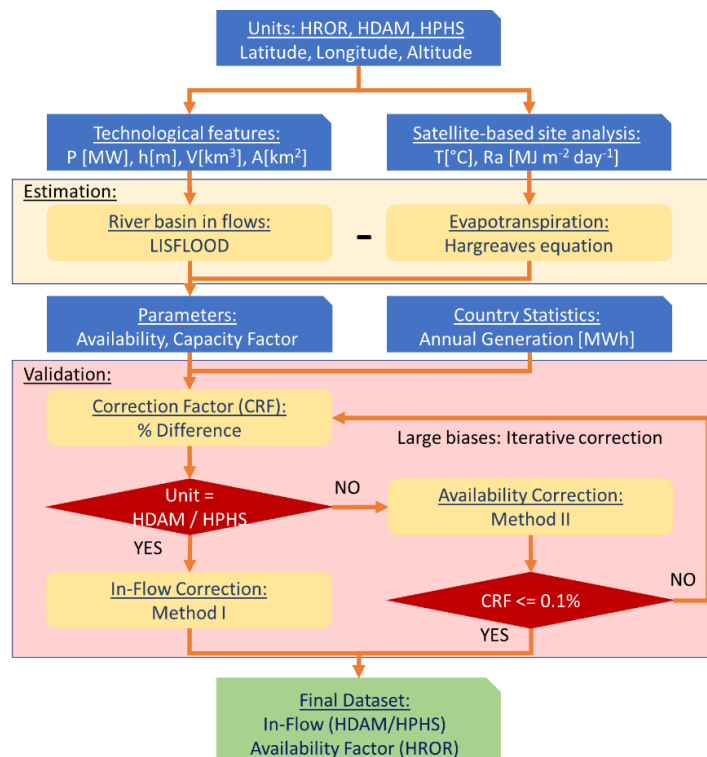
can, in certain conditions, be performed without significant loss of accuracy. A more detailed description regarding the model formulations in the Dispa-SET model is available in (Pavičević et al., 2019).

## 2.2 Methods and assumptions

### 2.2.1 Hydro inflows and availability factors

Hydro inflows resulting from the LISFLOOD model, in  $\text{m}^3/\text{s}$ , are given for a particular basin and geographical location. This usually results in excessive water availability for the considered location. In order to assess the actual water availability for hydro generation, technological features, such as nominal head, maximum power capacity, volume and surface area of the reservoirs (for hydro dams (HDAM) or pumped storage (PHPS) units), as well as satellite-based data such as average, minimal and maximal daily air temperatures and daily solar irradiation, need to be assessed. Evapotranspiration is calculated for each unit/location individually as proposed by (Hargreaves and Samani, 1982) and subtracted from the LISFLOOD outputs. For some hydro units, the computed inflows (potential energy in accumulation reservoirs behind the dams, in MWh) are orders of magnitude higher than the historical generation. This is due to inaccuracies in the definition of the catchment basins for these units and in the limited quality of the input data. In order to correct this, parameters such as hourly availability factors<sup>12</sup> for hydro run-of-river (HROR) units and capacity factors<sup>13</sup> for HDAM and PHPS units need to be adjusted. To that aim, an iterative two-stage calibration method is introduced as presented in Figure 3.

**Figure 3** Flowchart for generating availability factors time series for run-of-river (HROR) and scaled inflows time series for hydro dams (HDAM) units.



Source: JRC, 2020

In a first iteration, the difference between annual generation and computed inflows is evaluated. Based on the unit type, one of the two scaling methods is selected. For HDAM and PHPS units, inflows are scaled based on the correction factor. As such, units are usually built on large storage reservoirs, each containing several hundreds of hours of storage, no additional adjustments are necessary. In case of HROR units, a second method

<sup>12</sup> The availability factor is the unitless ratio of an actual electrical energy output in each time period to the maximum possible electricity output of particular unit

<sup>13</sup> The capacity factor is the unitless ratio of an actual electrical energy output over a given period of time to the maximum possible electrical energy output over that period

is applied to account for the higher importance of spillage (typically occurring when inflows are higher than the nominal capacity of the turbine). In that case, a five-step iterative methodology is introduced:

- I)  $InFlow_{u,i} = InFlow_{u,i} \cdot (1 + Correction)$
  - II)  $Spill_{u,i} = InFlow_{u,i} - PowerCapacity_u$
  - III)  $Spill_{u,i}(Spill_{u,i} < 0) = 0$
  - IV)  $InFlow_{u,i} = InFlow_{u,i} - Spill_{u,i}$
  - V)  $Correction = \frac{HistoricGeneration_u - \sum_{i=1}^n InFlow_{u,i}}{\sum_{i=1}^n InFlow_{u,i}}$
- (3)

After the spillage is assigned, new inflows and correction factors are computed. If newly computed inflows are within the historical values, the iteration stops, otherwise new correction factors and newly computed inflows are used as new inputs for the next loop.

### 2.2.2 Wind and solar availability factors

Wind and solar availability factors (AF) are estimated as weighted averages of potential and feasible wind and solar PV sites. Capacity factors for renewable technologies are computed as follows:

$$CF_{tr,z} = \frac{TP_{tr} \cdot \bar{x}_{tr,z}}{8760} \quad (4)$$

where  $CF_{tr,z}$  is the capacity factor of VRES technologies in each zone, in MWh/MW<sub>el</sub>;  $TP_{tr}$  is the technical potential of renewable technologies, in %; and  $\bar{x}_{tr,z}$  is the weighted average number of peak load hours in each zone, in h.

$$\bar{x}_{tr,z} = \frac{\sum_{i=1}^n A_{tr,i,z} x_{tr,i,z}}{\sum_{i=1}^n A_{tr,i,z}} \quad (5)$$

where  $A_{tr,i,z}$  is the available area with particular VRES potential for a specific renewable technology and zone, in km<sup>2</sup>;  $x_{tr,i,z}$  refers to the peak load hours for a specific VRES potential, renewable technology and zone, in h. A similar method is applied when generation from individual hydro units is unknown, but the total annual generation for the whole country is available from annual energy reports and statistical databases. The corrections from Eq. (4) are necessary since the raw VRES data from EMHIRES dataset (Gonzalez Aparicio et al., 2016; Gonzalez Aparicio et al., 2017) results in unrealistically high or low CF (e.g.  $CF_{wind} > 90\%$  in Somalia,  $CF_{wind} < 0.5\%$  in Democratic Republic of the Congo and  $CF_{solar} < 0.02\%$  in Central African Republic). The time-profile of solar and wind generation from the raw data is conserved, but rescaled to match the capacity factors provided in (Hermann, Miketa, and Fichaux, 2014).

### 2.2.3 Fuel prices

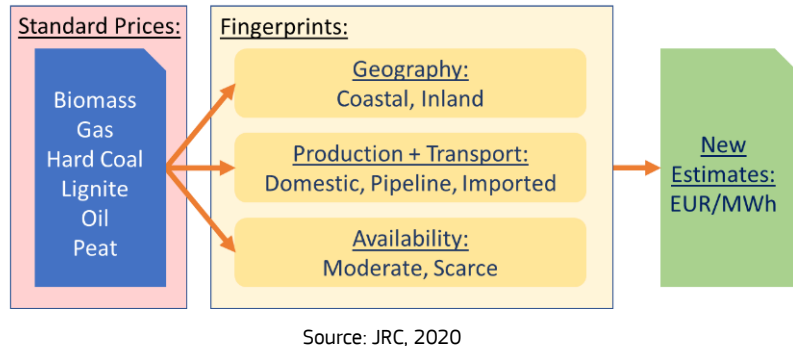
Variations in fuel prices are estimated based on a fingerprinting<sup>14</sup> algorithm. For each fuel type, one fingerprint per category is used to either increase or decrease the final fuel price, as proposed in (ECOWAS, 2011). Each country fingerprint is defined by: access to the sea (yes/no), local fuel production (yes/no), import and/or transport (this category mainly refers to local oil, gas and coal production and its means of transportation which can either be by ship, rail and/or truck or through international pipelines), and local resource availability

---

<sup>14</sup> Fingerprinting algorithm maps large data (in this case geography, local production and transportation and resource availability) to a much shorter sequence of bytes (in this case fuel price). Such a sequence is called the fingerprint. While fingerprints may identify the original data, the original data cannot be derived from its fingerprint. <https://devopedia.org/fingerprinting-algorithms>

(this category mainly refers to biomass, gas and peat scarcity/availability). A summary of the proposed fingerprinting algorithm is presented in **Figure 4**.

**Figure 4** Fuel price estimation based on three fingerprint types: geography, fuel production and availability.



Source: JRC, 2020

## 2.3 Power system metrics and indicators

### 2.3.1 RES curtailment

In the context of this work, RES curtailment refers to the reduction of renewable generation due to grid constraints. The total curtailed energy and the maximum hourly curtailed energy are both computed and reflect the flexibility of the proposed system. Excessive curtailed power is an indication of a poorly optimized system with excess generation capacity and a lack of flexibility.

### 2.3.2 Shed load and lost load

The amount of shed load highlights the adequacy of the system. It is defined as the demand of the system that must be reduced to match the available generation supply. Load shedding is used to prevent an imbalance and subsequent failure of the system. A maximum value of the load shedding capacity is defined for each simulated country. This value can be associated to the load-shedding plans of the transmission system operator (TSO) or to the contracted load suitable for shedding in large industries. In case load shedding does not allow to match generation and demand, an additional lost load (LL) relaxing variable is added to the market clearing equation. LL is given a very high price and ensures that no infeasibility occurs in the optimization problem. It should however not be activated (optimizations with  $LL > 0$  are discarded since the system is inadequate).

### 2.3.3 Shadow price

Shadow prices, expressed as EUR/MWh, are computed for each time step  $i$ , and for each zone  $n$ . The shadow price of electricity is the dual value of the energy balance equation. It can be interpreted as the clearing price of an ideal wholesale market. Other shadow prices are defined in the model, such as the shadow price of heat or of the reserve requirements, but are not used in this study.

### 2.3.4 Water stress

The water withdrawal factor is defined as the amount of water withdrawn per MWh of generated electricity. (Macknick et al., 2012) provide estimations of the water withdrawal factors per electricity generating technologies in the United States. (Fernández-Blanco, Kavvadias, and Hidalgo González, 2017) provide these values for Iberian power plants, while (Pappis et al., 2019) proposed withdrawal factors for African countries. This study complements the previous ones in case of missing technologies, mainly bio and gas-powered units, and introduces a cooling technology assignment matrix for units where the cooling system is not known, as presented in Table 2.

**Table 2** Selection algorithm for cooling systems and different fuel and technology combinations

Fuel	Cooling	GTUR	STUR	ICEN	COMC
<b>Biomass (BIO), Geothermal (GEO), Waste (WST)</b>	<b>AIR</b>	< 15	< 15	< 15	< 15
	<b>MDT</b>	>= 15	>= 15	>= 15	>= 15
	<b>AIR</b>	----	< 200	----	----
<b>Hard coal (HRD)</b>	<b>MDT</b>	----	200-450	----	----
	<b>OTS</b>	----	>= 450	----	----
	<b>AIR</b>	> 0	----	< 15	200-250
<b>Natural gas (GAS)</b>	<b>MDT</b>	----	< 20	----	> 0
	<b>OTS</b>	----	>= 20	>= 15	180-720
	<b>AIR</b>	> 0	< 15	> 0	< 15
<b>Fuel oil (OIL), Other (OTH)</b>	<b>MDT</b>	----	>= 720	----	>= 720
	<b>OTS</b>	----	15-720	----	15-720
	<b>Peat (PEA)</b>	<b>MDT</b>	> 0	> 0	----

Source: JRC, 2020

Values in the table indicate installed power plant capacities

According to (Fernandez Blanco Carramolino et al., 2017), once the water withdrawal factors are known and the water runoff is measured, computed, or estimated, the water stress index is calculated for each power plant and for each period of time as the water withdrawn divided by the water runoff. This index varies between 0 if the plant is not stressed at all and 1 if all the water available is used for cooling.

### 2.3.5 Water exploitation index

The water exploitation index is an indicator of water stress, relating water uses to water availability as proposed by (Adamovic et al., 2019). Within this study the water exploitation index refers to the ratio of water withdrawal and water consumption to water availability. It typically ranges between 0 and 1, but values above 1 are also possible (e.g. when water withdrawal and consumptions are higher than the local water availability). Values above 0.2 are ‘critical’ in terms of water scarcity. To meet the requirements of this study the water exploitation index of the energy sector only is also defined. It stands for water abstractions of the energy sector as a ratio of the sum of available internal (local) water.

### 2.3.6 Water value

The water value is given as the shadow price of the water balance constraint when minimising the total system-wide generation cost and is computed by the Dispa-SET MTS module. It attributes a monetary value to the water present in a reservoir for power generation purposes and can be used as an indicator of the possible arbitrage between various water usages (e.g. agriculture, drinking water). The water values in the catchments, considered for this analysis, correspond to the variable costs assumed for the thermal clusters and their values depend on the marginal unit in each time period.

### 2.3.7 Start-ups

The number of start-up events is the sum over one year of all commitment events for each thermal unit. It reflects the amount of flexibility provided by thermal units and is also an important indicator to calculate the wear and ageing of the power plant (not considered in this work).

### 2.3.8 CO<sub>2</sub> emissions

In this study, the carbon footprint is computed using standard emission factors of different combinations of fuel and technologies (European Investment Bank, 2018). It relates to emissions from power generation and operation of thermal units only (life cycle emissions are not considered) and is disaggregated per country.

### 3 Input data and assumptions

#### 3.1 African power pools

There are five power pools on the African continent. The main goal of these associations is to interconnect the electricity grids of the member countries in order to facilitate trading of electric power and take advantage of excess capacity within the network. This paper focuses on three of them: Central African Power Pool (CAPP), East African Power Pool (EAPP) and North African Power Pool (NAPP), also known as Comité Maghrébin de l'Électricité (COMELEC). A list of participating member states in each power pool is listed in Table 3. Since several countries are members of two or more power pools, and this study is carried out for all three power pools simultaneously, each country is assigned to a single power pool (the main one). This avoids double counting of electricity generation and aggregate results for individual power pools are more intuitive.

**Table 3** African power pools and participating member states.

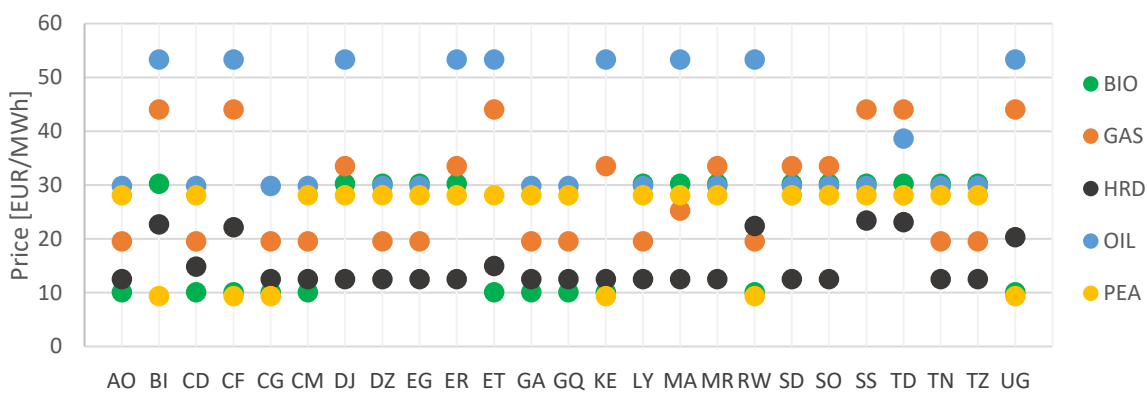
Power Pool	Number of states	Member states (ISO-2 country code)
CAPP	8	Angola (AO) <sup>15</sup> , Cameroon (CM), Central African Republic (CF), Republic of the Congo (CG), Chad (TD), Gabon (GA), Equatorial Guinea (GQ), Democratic Republic of the Congo (CD) <sup>16</sup>
EAPP	12	Burundi (BI), Djibouti (DJ), Egypt (EG), Ethiopia (ET), Eritrea (ER), Kenya (KE), Rwanda (RW), Somalia (SO), Sudan (SD), South Sudan (SS), Tanzania (TZ) <sup>17</sup> , Uganda (UG)
NAPP	5	Algeria (DZ), Libya (LY) <sup>18</sup> , Morocco (MA), Mauritania (MR), Tunisia (TN)

Source: JRC, 2020

#### 3.2 Fuel prices

A summary of the final fuel prices is presented in Figure 5. Variability of prices across zones and regions is based on the fingerprints (Section 2.2.3), thereby taking into account the influence of geographic location, local availability, and local fuel supply. A more detailed summary of the final fuel prices is presented in Table 10, Table 11, Table 12 and Table 13, located in the Annex 1 of this study. The marginal price of renewable sources (VRES, geothermal and hydro) is assumed to be zero.

**Figure 5** Fuel prices in different zones. Variability is based on the proposed price modification fingerprints.



Source: JRC, 2020

<sup>15</sup> Angola is participating in two power pools, namely CAPP and South African Power Pool (SAPP). In this study AO is member of CAPP.

<sup>16</sup> Due to its huge size, Democratic Republic of the Congo is member of three power pools, namely CAPP and EAPP as well as SAPP, which is not part of this study. In this study CD is member of CAPP.

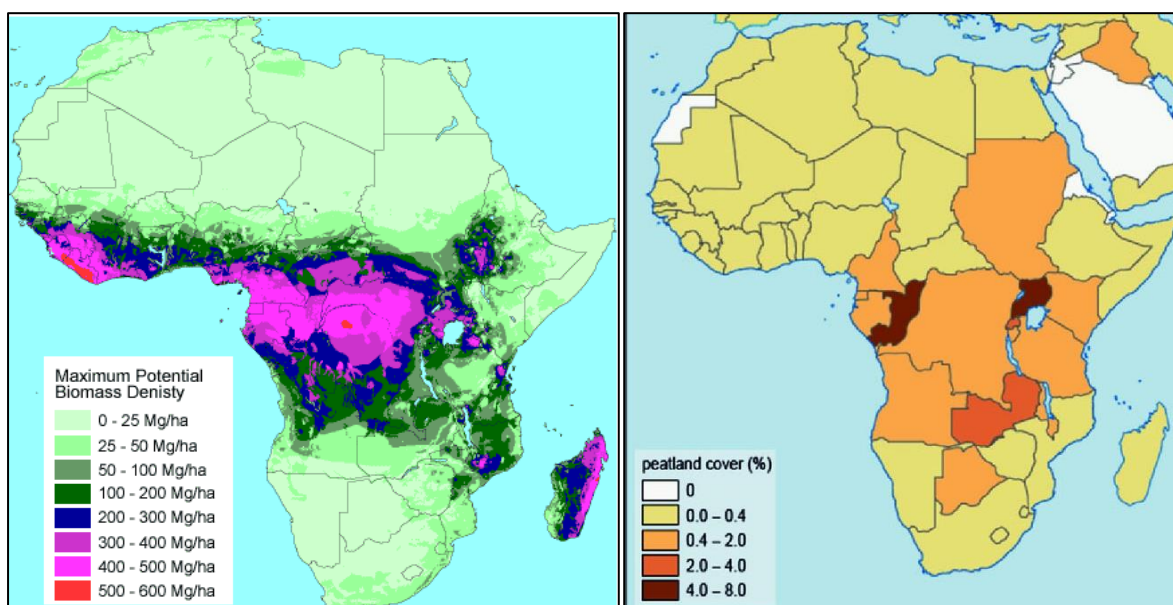
<sup>17</sup> Tanzania is transitioning country between EAPP and SAPP. In this study TZ is member state of EAPP

<sup>18</sup> Libya belongs to NAPP and EAPP. In this study LY is member of NAPP.

### 3.2.1 Local resource availability (biomass/biogas, peat and coal)

The potential of local resources such as biomass, peat and coal, varies significantly across countries. Some regions, such as CAPP, or large individual countries, like Democratic Republic of the Congo, have access to all resources, while in other countries, such as Somalia and Egypt, those resources are scarce. A summary of availability of these resources is presented in Figure 6**Error! Reference source not found.** Among the three analysed power pools, CAPP is most resource abundant and closely followed by southern regions of EAPP. NAPP and northern regions of EAPP are exposed to resource scarcity. The opposite is true for oil and gas rich regions, especially in NAPP where two of the largest African gas and oil deposits are located. In this study resource availability is used for estimating the local fuel prices (e.g. in biomass abundant countries a fingerprint representing local production was assigned, in countries where biomass availability is scarce a fingerprint representing import was assigned).

**Figure 6** Availability of other major resources, biomass<sup>19</sup> (left) and peat<sup>20</sup> (right).



Sources: (Brown, Gaston, and Daniels, 1996), (Grundling and Grootjans, 2018).

### 3.3 Hourly load profiles

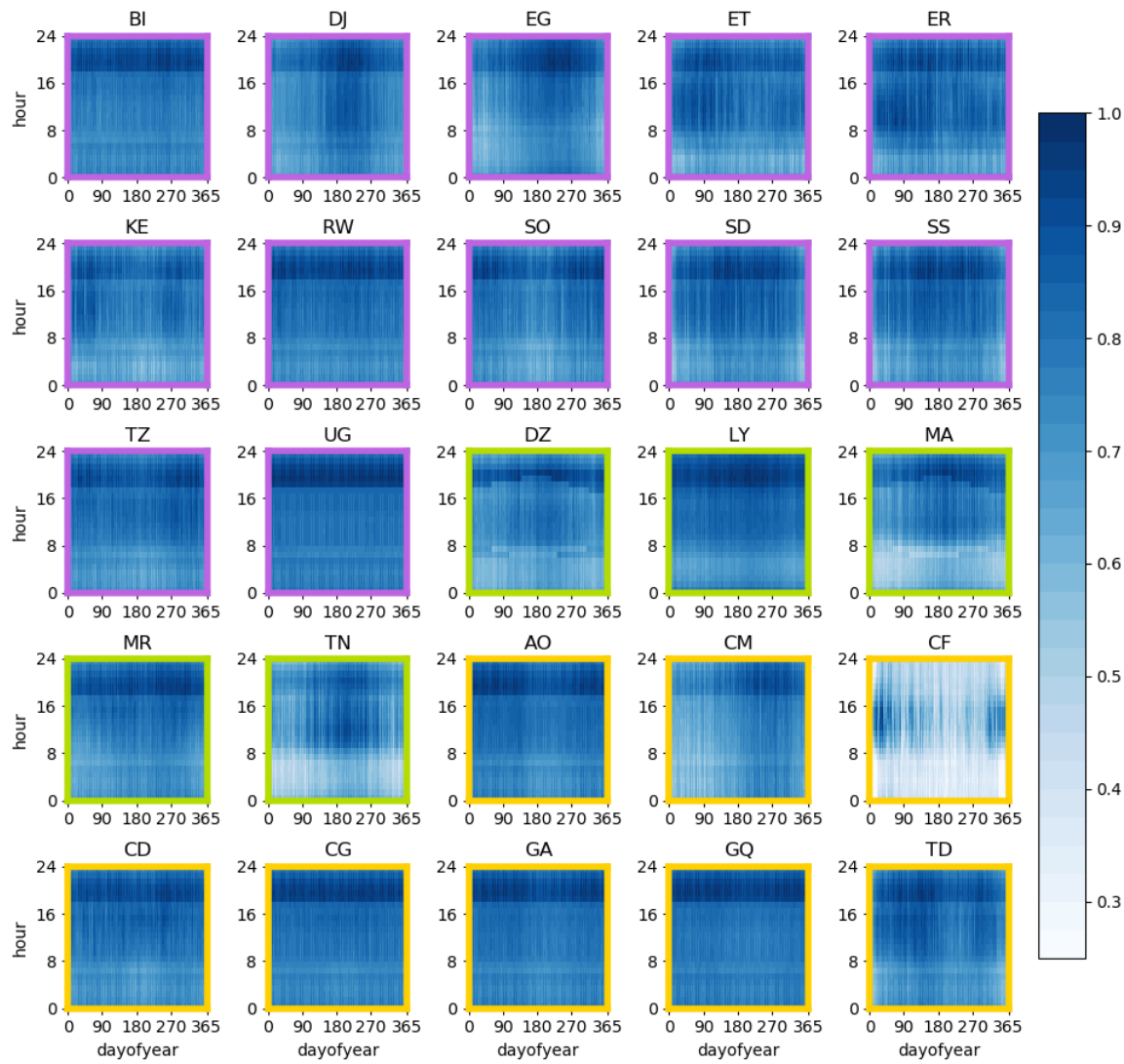
Due to the lack of data for most African countries, hourly demand profiles are estimated based on available historical data, as proposed by (De Felice et al., 2018). Demand profiles in most CAPP and EAPP member states are based on the profile of Ghana (provided by IRENA), while the demand profiles of NAPP member states are modelled individually, as provided in the BETTER<sup>21</sup> project. A heatmap of normalized demand distributions in individual zones is presented in Figure 7. Relatively flat demand profiles are observed for Uganda, Rwanda, Mauritania, Gabon, Equatorial Guinea, Congo and Democratic Republic of Congo and Burundi.

<sup>19</sup> Biomass availability as computed by (Brown, Gaston, and Daniels, 1996)

<sup>20</sup> Peatlands of Africa as shown in (Grundling and Grootjans, 2018)

<sup>21</sup> Deliverable 3.2.1 "Demand Development Scenarios": <https://www.ec-better.eu/pages/better-project>

**Figure 7** Electricity demand distributions in the three power pools.



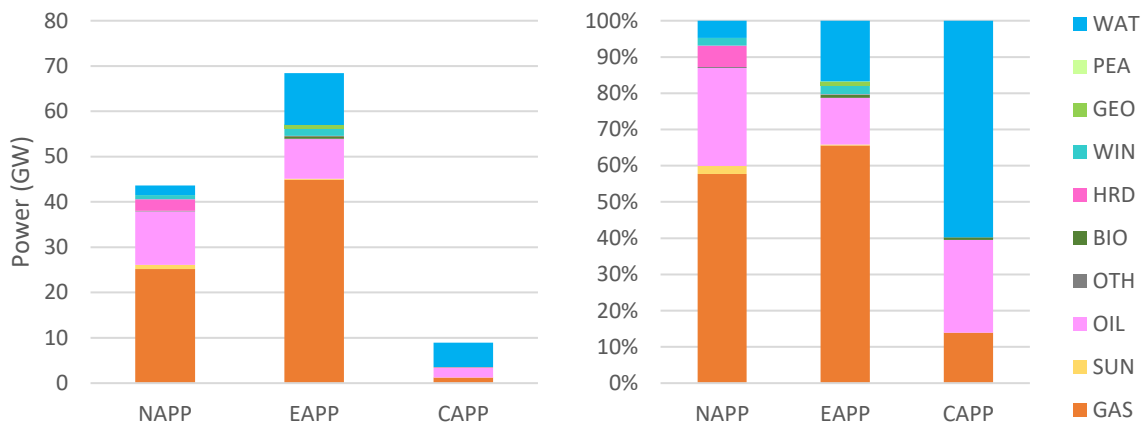
Source: JRC, 2020

Values are given as percentage of hourly peak load. Purple, green and yellow zones belong respectively to EAPP, NAPP and CAPP.

### 3.4 Supply

On the supply side the capacity mix varies significantly among the power pools, as shown in Figure 8. Capacity-wise, EAPP is the largest, followed by NAPP. They are both mostly dominated by fossil fuels, especially oil and gas, whose combined capacity sums up to more than 78% and 92% respectively. CAPP, on the other hand, is the smallest power pool and it mostly relies on hydro and oil. EAPP is particularly interesting due to the most diversified capacity mix. CAPP heavily relies on RES whose total capacity sums up to more than 60%. A detailed table of installed capacities per country and power pool is presented in Table 4.

**Figure 8** Capacity mix in all three power pools.



Source: JRC, 2020

WAT: hydro, PEA: peat, GEO: geothermal, WIN: onshore wind, HRD: hard coal, BIO: biomass, OIL: fuel oil, SUN: solar, OTH: other sources, GAS: natural gas. Total installed capacity used in Reference and Interconnected scenarios (more detailed scenario definitions are provided in Section 4) is presented on the left. Share of individual fuel types is shown on the right.

**Table 4** Installed capacity in each of the analysed countries within the three power pools.

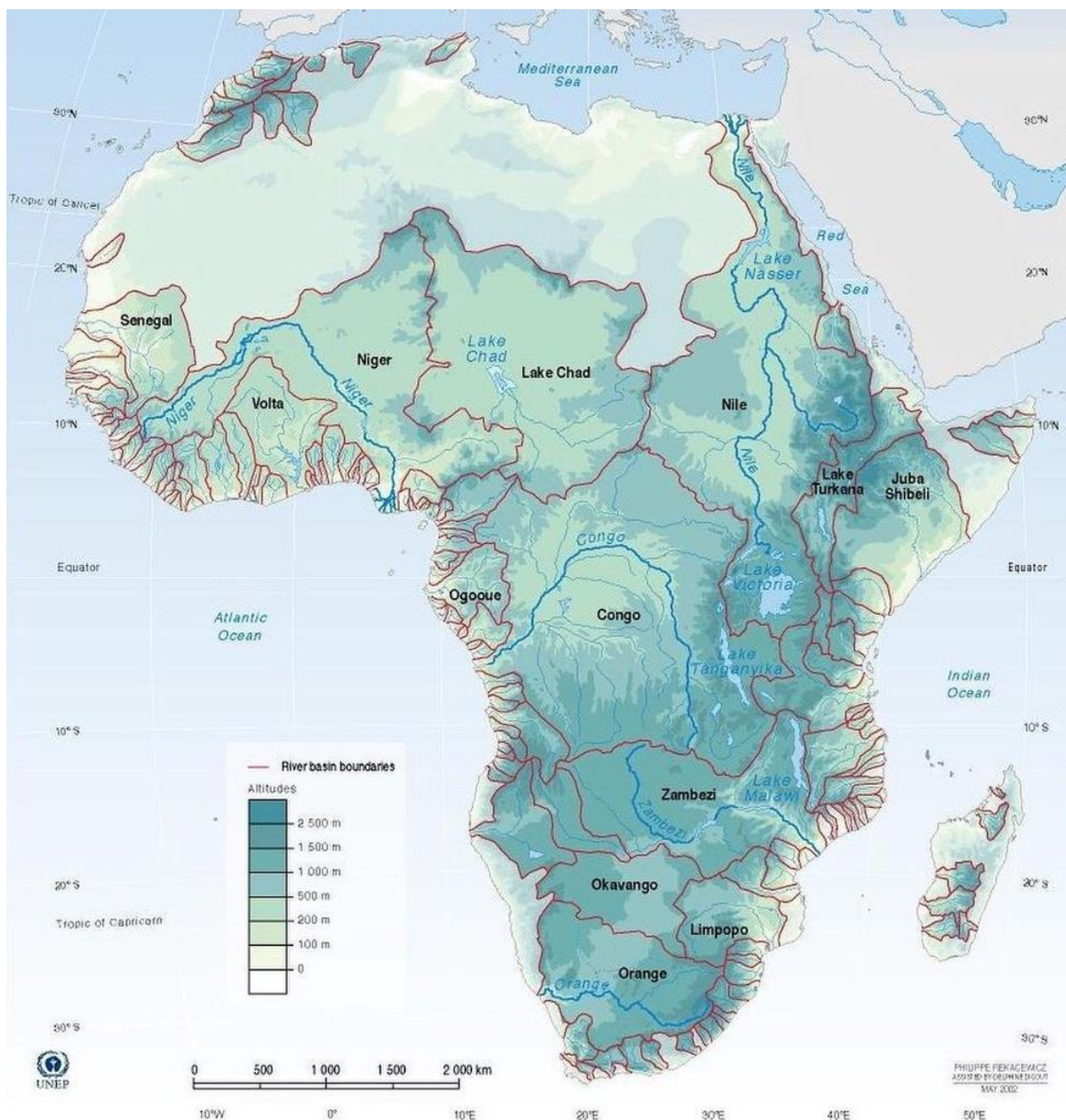
Power Pool	Zone	SUN	BIO	GAS	GEO	HRD	OIL	PEA	WAT	WIN
CAPP	AO		51	591			1 087		1 374	
	CD								2 561	
	CF						5.1		18	
	CG		8.5	352			70		194	
	CM						302		743	
	GA			92			204		286	
EAPP	GQ			146			37		120	
	TD	0.0					185			
	BI						5.5		26	
	DJ						85			
	EG	52	67	40 955			2 659		2 842	883
	ER						175			
NAPP	ET	0.2	120		8.5		154		4 073	324
	KE	55	28	0.2	617		976		961	5.4
	RW	12		30			57	15	141	
	SD	0.1	244				2 137		1 731	
	SO		0.8				101			
	SS	18					32		5	
	TZ	0.0	48	997		16	402		566	
	UG	20	63				274		730	
	DZ	315		16 881			1 455		237	
	LY			4 364			5 161			
	MA	360		856		2 575	2 344		1 534	626
	MR	15					345			30
	TN			3 077			1 983	49	208	

Source: JRC, 2020

### 3.5 Hydropower units

The major African river basins are presented in Figure 9. Hydro units are the dominant technology in the equatorial region. The main reason for such a high hydro availability comes from the Congo river (second largest river in the world with average annual discharge rate of 41 200 m<sup>3</sup>/s<sup>22</sup>) and the Nile river (longest African river with average annual discharge rate of 2 830 m<sup>3</sup>/s) as well as the great lakes, whose total hydro potential is estimated to around 549 218 GWh<sup>23</sup>. Hydro potential in the NAPP is limited, with a total installed power capacity of 1820 MW, of which more than 85% is located in Morocco alone. The total usable hydro capacity in countries such as Tunisia and Algeria are limited to a fraction of the maximum installed power, with CF below 10% and 8%, respectively. This is mainly due to water shortages, water leakages, and the multiple purposes of the water reservoirs (drinking water, power generation and irrigation).

**Figure 9** Major African river basins.



Source: (Wolf et al., 1999)

<sup>22</sup> River discharge - <https://web.archive.org/web/20040814072422/http://home.comcast.net/~igpl/Rivers.html>

<sup>23</sup> Estimated by the World Bank, IEA, World Energy Outlook, Hydropower & Dams World Atlas 2016: <https://www.andritz.com/hydro-en/hydropower-news/hydropower-africa/east-africa>

Statistical data for different power pools and river basins are presented in Table 5. Hydro dams across all three power pools have an average commissioning year ranging from 1969 in NAPP up to 1990 in EAPP. The average start date of operation across all three power pools is 1982. The highest installed power is EAPP (Shebelli and Juba Basin) while the largest reservoirs in terms of volume and area are in EAPP (Nile Basin). On average, the smallest reservoirs by volume are located in CAPP and the Congo river basin. Out of 25 countries, 19 have local hydro capability. The largest total hydro capacity is in Ethiopia (4 074 MW), followed by Egypt (2 842 MW) and the Democratic Republic of the Congo (2 561 MW).

**Table 5** Statistical data for different power pools and major river basins.

Power Pool / Basin	Start Date	Height (m)	Power (MW)		Volume (mil m³)		Area (m²)	
			Average	Total	Average	Total	Average	Total
<b>CAPP</b>	<b>1976</b>	36	177	5 311	510	11 220	40	1 092
Central West Coast	1983	31	137	1 229	567	2 837	80	639
Congo River Basin	1974	36	226	2 707	75	671	23	252
South West Coast	1974	42	153	1 375	964	7 712	25	201
<b>EAPP</b>	<b>1990</b>	38	179	11 077	8 900	249 212	221	9 048
Central West Coast	1987	5	13	26	-	-	2	2
East Central Coast	1986	33	69	1 383	594	6 530	48	771
Nile Basin	1990	28	202	6 266	17 973	215 671	481	7 689
Rift Valley	1991	155	106	106	1 645	1 645	26	26
Shebelli & Juba Basin	2000	84	412	3 296	6 342	25 367	80	560
<b>NAPP</b>	<b>1969</b>	76	67	2 062	667	13 330	16	462
Mediterranean Coast	1964	56	22	310	341	2 388	9	103
North West Coast	1971	93	103	1 752	842	10 942	21	359
<b>TOTAL</b>		1982	47	18 450	3 911	273 763	110	10 601

Source: JRC, 2020

In the scope of this study, attention has been given to hydro power plants because of their importance in both wet and dry regions. For each hydro unit, characteristics such as head, storage capacity and area have been cross-checked using several sources such as S&P Global Platts<sup>24</sup>, Harvard<sup>25</sup>, EnergyData<sup>26</sup>, WRI<sup>27</sup> and PowerAfrica<sup>28</sup>. A visual summary of the three main HDAM parameters (nominal head, storage capacity and installed power) is presented in Figure 10. Five of the seven largest units are located in EAPP, while the rest of the units is scattered across all three power pools. For the sake of consistency and due to lack of detailed data regarding the technical and operational parameters of individual units, a typical unit approach is adopted, in which all units sharing the same fuel and technology are assumed to have equal operational parameters. The technical parameters of hydro units used within this study are presented in Table 15 and provided in the annex 2. It is important to note that HDAM units with 10 752.9 MW (of which 1 293.2 MW is located in CAPP, 8 363.0 MW is located in EAPP and 1 096.7 MW is located in NAPP) across all three power pools, represent majority of the total installed hydropower capacity. The total non-dispatchable HROR capacity across all three power pools sums up to 7 696.9 MW (of which 4 017.7 MW is located in CAPP, 2 713.8 MW is located in EAPP and 965.4 MW is located in NAPP). However, the share of installed hydro capacities in individual power pools differs substantially. In CAPP HROR units represent 75 %, in EAPP 75 % of units are HDAM, while in NAPP distribution of HDAM and HROR units is around 50 % (slightly in favour of HDAM units).

<sup>24</sup> <https://www.spglobal.com/platts/en/products-services/electric-power/world-electric-power-plants-database>

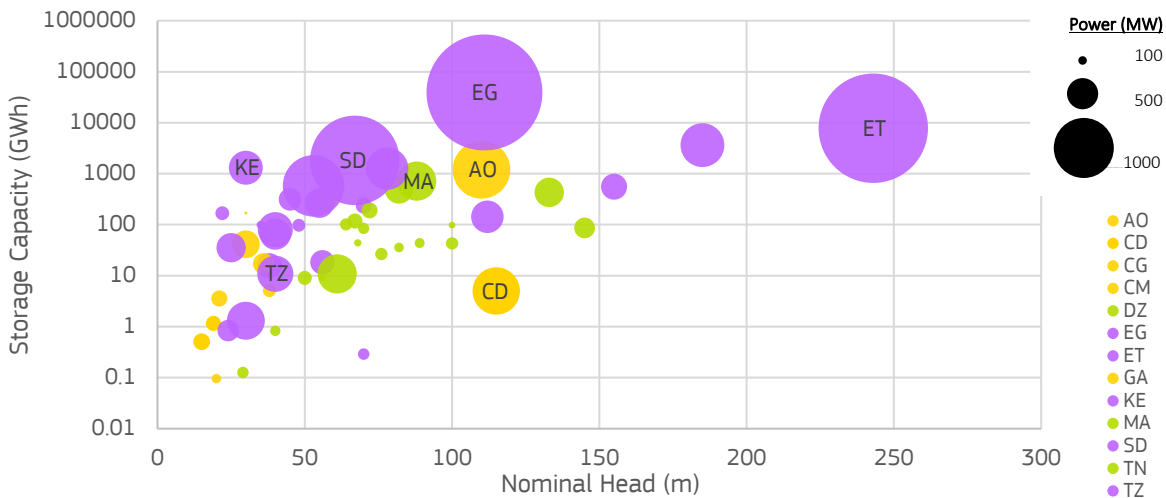
<sup>25</sup> [http://worldmap.harvard.edu/data/geonode:africa\\_power\\_plants\\_gd4](http://worldmap.harvard.edu/data/geonode:africa_power_plants_gd4)

<sup>26</sup> <https://energydata.info/en/dataset/powerstations>

<sup>27</sup> <http://datasets.wri.org/dataset/globalpowerplantdatabase>

<sup>28</sup> <http://powerafrica.opendataforafrica.org/>

**Figure 10** Semi logarithmic three parameter diagram of HDAM units in the proposed power pools.



Source: JRC, 2020

Bubble size indicates the installed capacities, while colour code indicates the power pool (yellow for CAPP, pink for EAPP and green for NAPP).

### 3.5.1 Evapotranspiration

In Africa significant amounts of water are consumed by hydropower units due to evapotranspiration. The methods for calculating evapotranspiration from meteorological data require various climatological and physical inputs. Some of the data are measured directly in weather stations. Other parameters are related to commonly measured data and can be derived with the help of direct or empirical relationships. In this study, evapotranspiration is calculated following (Hargreaves and Samani, 1982), who estimate the daily evapotranspiration from the elevation in meters and the maximum and minimum daily temperatures. The elevation data have been obtained from the TerrainBase (TBASE) dataset<sup>29</sup> from the National Center for Atmospheric Research (NCAR), the temperature data are derived from the ECMWF ERA-INTERIM reanalysis (Dee et al., 2011). The Hargreaves-Samani formula is applied for each reservoir where the nearest grid point for the elevation and temperature data sets are known.

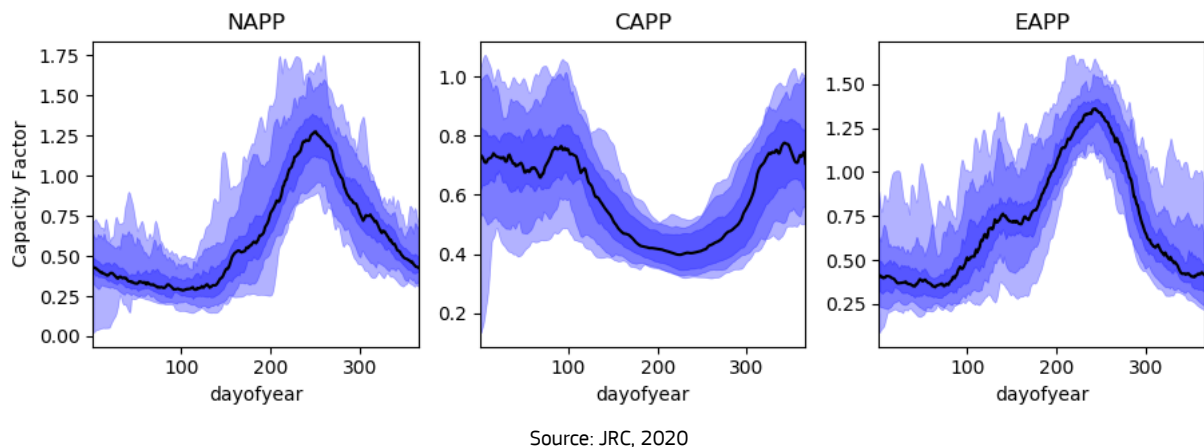
### 3.5.2 Inflows

Considering the importance of hydro-power generation in the CAPP and EAPP area, the definition of realistic inflows is fundamental. However, river discharge observations as well as proper and useful statistics that can be used for a simulation on daily or hourly scale are very limited. For this reason, LISFLOOD, a hydrological rainfall-runoff model operated by the JRC, has been used to generate the required data consistently and at high-resolution for a long time period. LISFLOOD is capable of simulating the hydrological conditions with a resolution of 10 by 10 km for the period 1980-2018. These data are assigned to each hydro power plant using the nearest grid point from its geographical coordinates.

The inflow time-series are calibrated by using the annual generation data produced by the International Hydropower Association for the year 2015 (IHA, 2016), following the methodology described in chapter 2.2.1. The historical (1980 - 2018) annual AF and scaled Inflows in different power pools used are presented in Figure 11. A detailed Inflow breakdown of all HDAM units is provided in the Annex 5 (from Figure 45 to Figure 47).

<sup>29</sup> TBASE - <https://rda.ucar.edu/datasets/ds759.2/>

**Figure 11** Historical time series of AF and scaled Inflows for one year with the 0th, 5th, 25th, 50th (black line), 75th, 95th and 100th percentiles.



### 3.6 Thermal units

A complete list of thermal power plants in the three power pools is obtained from several open sources, such as Harvard, EnergyData, WRI and PowerAfrica and numerous regional, local and annual TSO and electric utility reports.

The total installed capacity of thermal units across all three power pools amounts to more than 80% of total installed capacity. Gas, with total of 68 GW, is the dominant technology, followed by 20 GW of oil derivatives such as LFO, diesel, crude oil or gasoline, and 3 GW of hard coal units. The combined capacity of other thermal units amounts to less than 2 GW. Because of the limited data availability at the power plant level, the units are clustered by technology and fuel, following the methodology proposed in (Pavičević et al., 2019). A short summary of technical and economical parameters of typical thermal units is presented in Table 16, located in Annex 3.

### 3.7 Grid infrastructure

This work considers the existing, short-term (until 2025 and used in the Connected scenario) and long-term (until 2060 as used in the TEMBA scenarios) grid infrastructure projects. The existing grid infrastructure in sub-Saharan countries is currently relatively weak. Countries such as Central African Republic and South Sudan experience system-wide outages for up to 10 hours per day (Central African Republic, 2014). A better situation is observed in NAPP, where more than 97% of the population has access to electricity and national grids are modernized. NAPP is also the most interconnected power pool, followed by EAPP, where Eritrea and Somalia<sup>30</sup> do not have any cross-border lines, and CAPP where Central African Republic<sup>31</sup>, Chad<sup>32</sup> and most regions inside Democratic Republic of the Congo are isolated. Nevertheless, several interconnection projects such as Kenya-Ethiopia<sup>33</sup>, Tanzania-Uganda<sup>34</sup>, Kenya-Tanzania<sup>35</sup>, Rwanda and Democratic Republic of the Congo<sup>36</sup>, and Equatorial Guinea – Cameroon<sup>37</sup> are already in the later stages of the development. There are significant developments planned until 2025, while large interconnections surrounding the Grand Inga project are planned

<sup>30</sup> Somalia - <https://www.usaid.gov/powerafrica/wherewework/somalia>

<sup>31</sup> Central African Republic and Democratic Republic of the Congo project - [https://www.afdb.org/fileadmin/uploads/afdb/Documents/Project-and-Operations/CAR-DRC\\_-\\_Project\\_to\\_Interconnect\\_the\\_Power\\_Grids\\_of\\_the\\_Central\\_African\\_Republic\\_and\\_the\\_Democratic\\_Republic\\_of\\_Congo\\_from\\_the\\_Boali\\_Hydro-Power\\_System%20%93Phase\\_1\\_-\\_Project\\_Appraisal\\_Report\\_.pdf](https://www.afdb.org/fileadmin/uploads/afdb/Documents/Project-and-Operations/CAR-DRC_-_Project_to_Interconnect_the_Power_Grids_of_the_Central_African_Republic_and_the_Democratic_Republic_of_Congo_from_the_Boali_Hydro-Power_System%20%93Phase_1_-_Project_Appraisal_Report_.pdf)

<sup>32</sup> Chad – Cameroon - <http://documents.worldbank.org/curated/en/890241579640031323/text/Concept-Project-Information-Document-Integrated-Safeguards-Data-Sheet-Cameroon-Chad-Power-Interconnection-Project-P168185.txt>

<sup>33</sup> Kenya – Ethiopia - <https://allafrica.com/stories/201910010643.html>

<sup>34</sup> The roadmap to a fully integrated and operational East African Power Pool - [https://www2.deloitte.com/content/dam/Deloitte/ke/Documents/energy-resources/ER\\_Power%20TL.pdf](https://www2.deloitte.com/content/dam/Deloitte/ke/Documents/energy-resources/ER_Power%20TL.pdf)

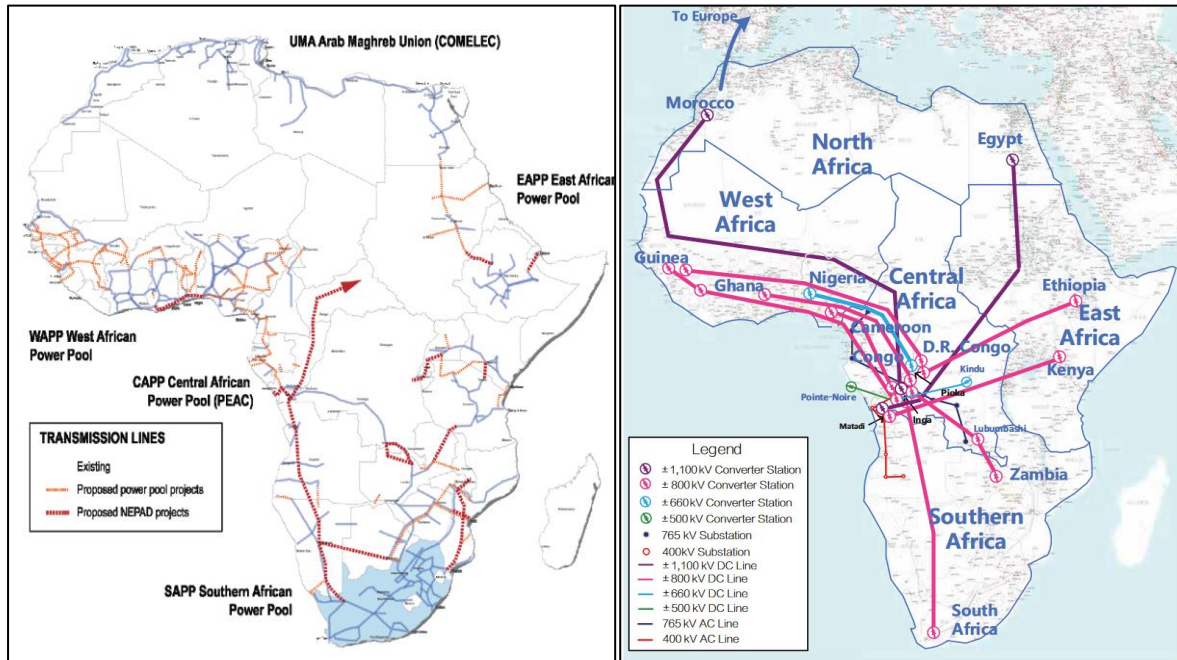
<sup>35</sup> Tanzania – Kenya - <https://www.theeastfrican.co.ke/business/Tanzania-Kenya-joint-electricity-project/2560-4974190-iuw57/index.html> and [https://www.usaid.gov/sites/default/files/documents/1860/PA\\_Transmission\\_Roadmap\\_508.pdf](https://www.usaid.gov/sites/default/files/documents/1860/PA_Transmission_Roadmap_508.pdf)

<sup>36</sup> Rwanda and Democratic Republic of the Congo - <https://www.nilebasindiscourse.org/images/downloads/The-NELSPower-Interconnection-Projects-Fact-Sheet.pdf>

<sup>37</sup> Equatorial Guinea – Cameroon - <https://es.wikipedia.org/wiki/Segeza>

for the period between 2030 and 2060. A summary of short and long-term cross-border projects is presented in Figure 12.

**Figure 12** A map of existing and short-term African interconnection projects (left) and long-term projects scheduled for period 2030 - 2060



Source: Global Energy Interconnection Development and Cooperation Organization (<https://www.gei-journal.com/en/contents/102/912.html>)

NTC capacities in the analysed power pools are presented in Source: JRC, 2020

**Figure 13.** In this analysis, the availability of NTC capacities remains constant throughout the year (because of the lack of data, seasonal variabilities are not considered in this study). It is worthwhile to note that historical NTCs from 2017 are limited compared to the planned ones. Thus, this analysis investigates both options as boundary conditions. In post 2030 scenarios, NTC data is limited, thus for AC interconnections the NTC capacity in MW is approximated by the Power-Voltage-Distance table presented in Table 6.

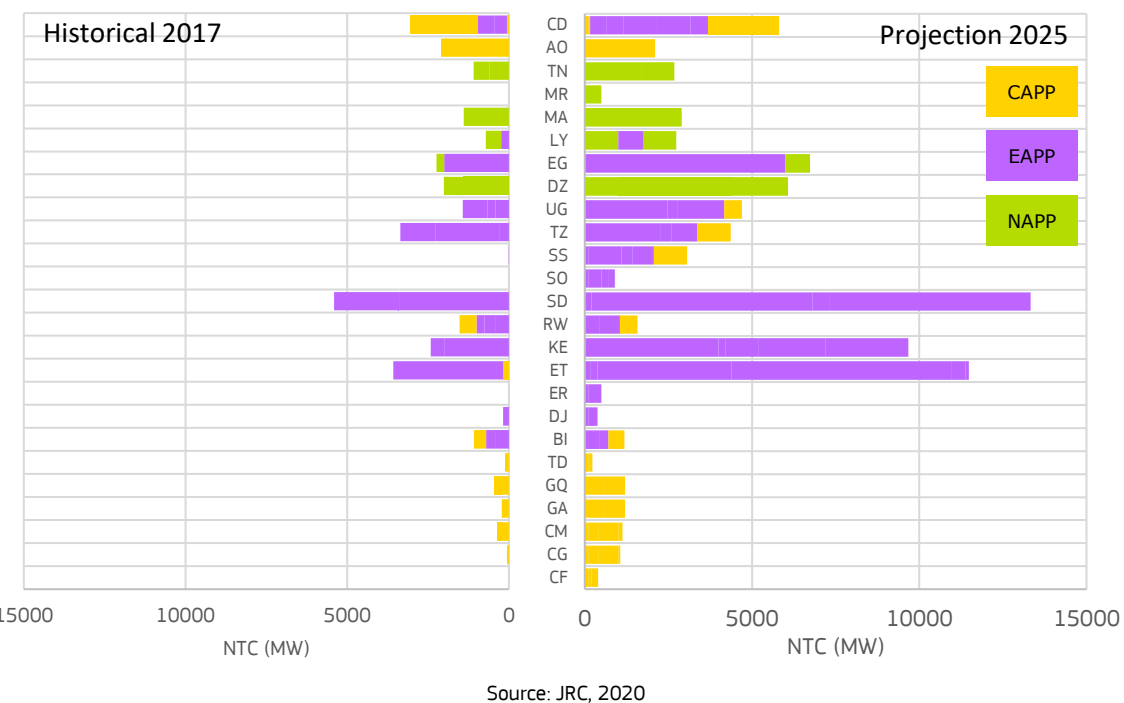
**Table 6** Power-voltage-distance approximation table<sup>38</sup>

Voltage [kV]	Power [MW]	Distance [km]					
		50	100	200	400	800	1600
66	66	22	11	6	3	1	1
	132	120	60	30	15	8	4
	220	400	200	100	50	25	13
	400	1 500	750	375	188	94	47
	765	728	2 864	1 432	716	358	179
	800	6 279	3 140	1 570	785	392	196
	1 000	9 914	4 957	2 478	1 239	620	310

Source: JRC, 2020

<sup>38</sup> <http://www.iitk.ac.in/npsc/Papers/NPSC1998/p2.pdf>

**Figure 13** Cross border transfer capacities.



Source: JRC, 2020

Left diagram represents historical NTC's from 2017. Right diagram represents all projects planned for the near future.

## 4 Scenarios

In order to evaluate the potential flexibility originating from the water-energy nexus in the considered African power pools, two scenarios are defined. The reference scenario refers to the historical data from 2015. The Connected scenario analyses the impact of fully developed grid as planned for year 2025. In addition, special attention is paid to the capacity of the system to accommodate increased shares of VRES from the NAPP and hydro generation from CAPP and EAPP. In total 38 weather years representing different historic inflows as computed by LISFLOOD model for the period from 1980 till 2018 are considered. Summary of scenario definitions is presented in Table 7. More detailed scenario descriptions are provided in the following chapters.

**Table 7** Summary of scenario definitions

Scenarios	Weather years	Scenario definition		
		NTC Infrastructure		
		CAPP	EAPP	NAPP
Reference	38	+	+	++
Connected		++	+++	++
Interconnection capacity:		+ Low	++ Medium	+++ High

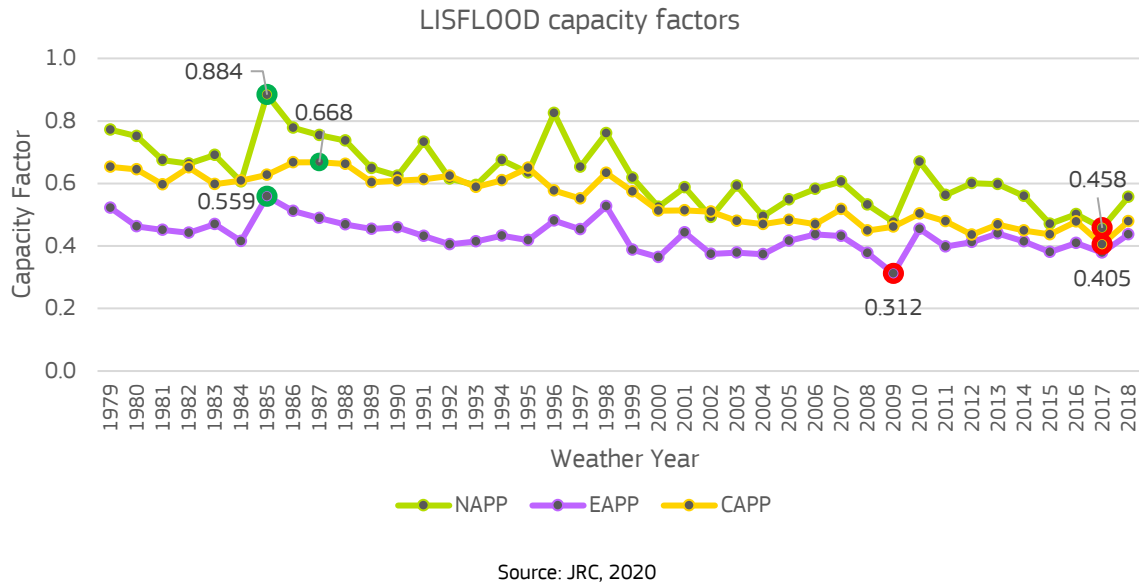
Source: JRC, 2020

### 4.1 Reference scenario

The Reference scenario is the starting point of this analysis and is used for the calibration of the models. The LISFLOOD river discharge rates used for power generation are adjusted to match the historical capacity factors, NTC availability is either limited to match historical cross border flows (where applicable) or allowed at full interconnector capacity. Outage factors are also adjusted to limit the generation of certain technology-fuel combinations which would otherwise results in unrealistic over/under-generation, such as cheap GEO and BIO units or expensive oil in well interconnected countries. Furthermore, 28 additional subcases representing historical weather years as computed by LISFLOOD from 1980 until 2018 are investigated. A more detailed representation of the historical CF in each of the three power pools as computed by the LISFLOOD model is provided in Figure 14. It is worth noting that:

- Overall, the three power pools are dominated hydro-thermal units, with negligible wind, solar and geothermal capacity. In some cases (Somalia, Eritrea, Djibouti and Libya), hydro potential remains limited and there is no hydro capacity installed.
- Among the three power pools, only NAPP is fully interconnected. Somalia in EAPP and Central African Republic in the CAPP do not have any cross-border transmission infrastructure. New transmission lines for those countries are either planned or under development.
- The driest weather year according to LISFLOOD is 2017 for CAPP and NAPP and 2009 for EAPP. The wettest year is 1985 for EAPP and NAPP and 1987 for CAPP. Special attention in this study is given to extreme weather years, namely 2017 (dry) and 1985 (wet).
- Total VRES penetration across all three power pools varies between 17.5% in extremely dry year and 22.7% in extremely wet year.

**Figure 14** Historical CF for each power pool as computed by LISFLOOD model.



Largest CF are computed in the 1980's while lowest from 2010 onward. Green circles stand for extremely wet and red circles stand for extremely dry years. Capacity factors in this diagram are computed for the system configuration as it was in 2017. Labels on the x-axis do not represent historical CF but rather indicate the hydrological weather conditions computed by LISFLOOD for those particular weather years.

## 4.2 Connected scenario

In the Connected scenario, all parameters from the Reference scenario are kept equal, except the NTC capacities. This scenario is a hypothetical scenario where, instead of investing in new generation capacities, all power pools become well interconnected (as proposed by multiple interconnection studies such as African Energy Atlas (Cross-border Information, 2020) and hydro development in the Congo river (Global Energy Interconnection Development and Cooperation Organization, 2020) among others). In this scenario, cross-border flows are expected to increase and the prices of electricity across the three power pools are expected to decrease, along with the locational spread. Total VRES penetration across all three power pools in the Connected scenario is slightly higher when compared to the Reference scenario and varies between 17.9% in extremely dry year and 22.9% in extremely wet year.

## 5 Results and discussion of the Reference and Connected scenarios

A summary of important results such as total system costs and average generation costs are presented in Table 8. For this study, a “per typical unit” formulation was used, in which a technology is clustered into  $n$  identical units, which are constrained by their minimum part-load, maximum ramping rates and minimum up/down times. The resulting total number of units in Reference and Connected scenarios was reduced from 816 historical units to 183 typical units.

**Table 8** Minimum (Min), average (Avg) and maximum (Max) costs from all three scenarios

Scenarios	Weather years	Dispa-SET clusters (total number of units)	Total system cost [billion EUR]	Average generation cost [EUR/MWh]
<b>Reference</b>	Min		12.52	29.65
	Avg	183 (816)	13.27	31.42
	Max		13.90	32.93
<b>Connected</b>	Min		12.19	28.87
	Avg	183 (816)	12.86	30.47
	Max		13.38	31.69

Source: JRC, 2020

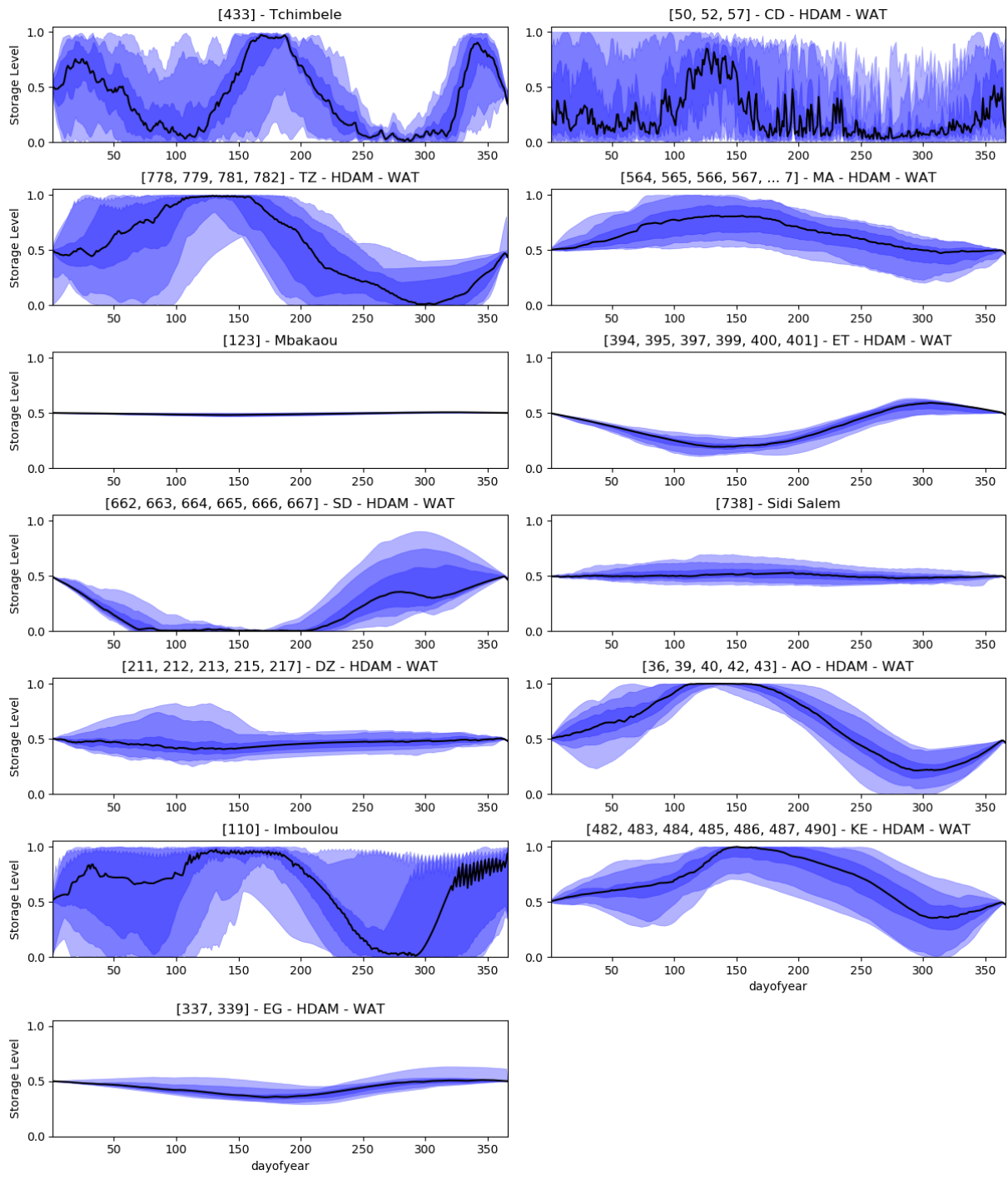
### 5.1 Storage levels computed by Dispa-SET MTS

The Dispa-SET MTS model has been used to compute the reservoir levels for each of the 38 climate years. Although the Reference scenario is based on the historical generation data for 2015, in this study 38 historical inflow profiles are considered in order to assess the impact of the climate variability (i.e. availability of water resources) on the analysed power system.

Reservoir levels of all 13 HDAM power plant clusters has been simulated using the modelling framework (described in Section 2.1), applying the proposed methods (described in 2.2), and using the power plant characteristics (Sections 3.4 and 3.5).

The storage levels provided as output of the Dispa-SET MTS model are shown in Figure 15.

**Figure 15** Reservoir levels in major HDAM units for one year as computed by the Dispa-SET MTS model..



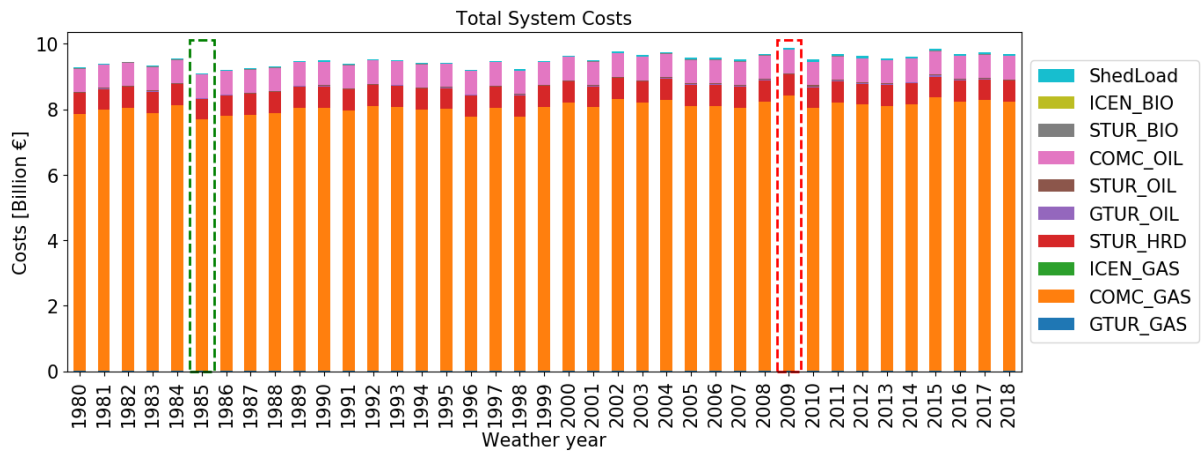
Source: JRC, 2020

The 0th, 5th, 25th, 50th (black line), 75th, 95th and 100th percentiles are presented. They highlight computed reservoir levels for weather years being closest to the proposed percentiles. Reservoir levels of all other weather years are contained inside the highlighted area. Numbers in the headings indicate the indexes of the clustered units inside the Dispa-SET database. In total 13 HDAM clusters, sharing similar techno-economical parameters, were identified.

## 5.2 Total system costs

A detailed cost breakdown is presented in Figure 16. As expected, increased availability of zero marginal cost units (units powered by VRES HDAM's and CSP's) positively impacts the total system costs. This difference is clearly visible between the two extreme weather years, 1985 (9.084 billion €) and 2009 (9.874 billion €). The main reason is the increased / decreased share of zero marginal cost units, especially HROR and HDAM. Furthermore, well interlinked parts of the analysed systems do enable even higher integration of VRES, which significantly increases the energy flows from VRES-abundant to VRES-scarce regions where lack of total installed capacity also causes implementation of load shedding. This can also be observed in hourly shadow prices across the power pools.

**Figure 16** Costs breakdown for all 38 weather years in Reference scenario



Source: JRC, 2020

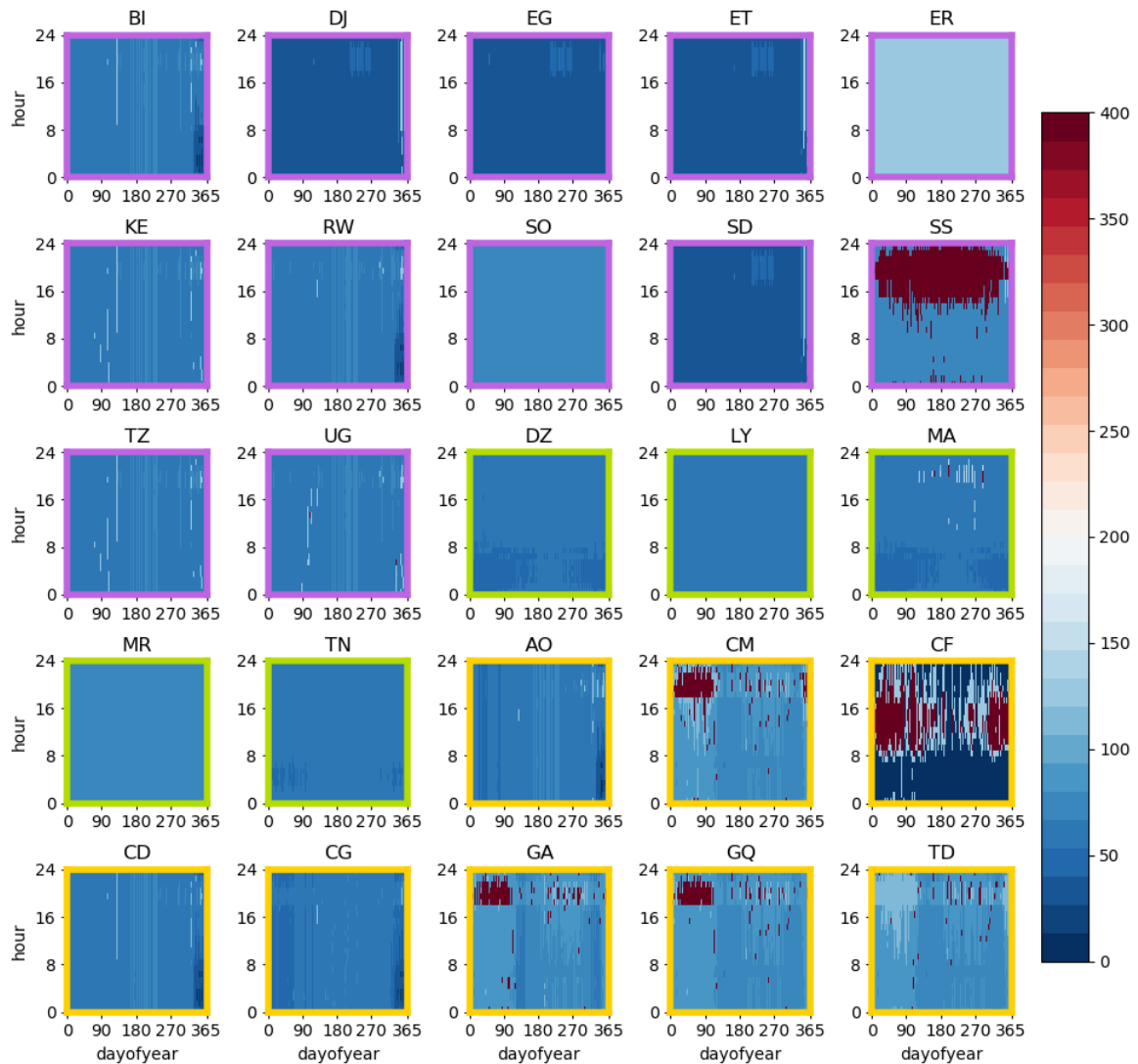
Variable fuel costs are presented per fuel and per technology type and other costs represent shed load. Weather year highlighted with the green box indicates the cheapest (unusually wet) year. Weather year highlighted with the red box indicates the year with the most expensive (unusually dry) system costs.

## 5.3 Shadow prices

### 5.3.1 Reference scenario

In this study, shadow prices are used to evaluate the clearing prices on the wholesale electricity market. Well interconnected power pools are expected to have a more uniform price range and reduced load shedding needs. A summary of hourly shadow prices for an average weather year (1999) is presented in Figure 17. Extremely wet (1985) and dry (2009) years are presented in Figure 48 and Figure 49 (Annex 6). Countries with no interconnections (such as Central African Republic, CF or Somalia, SO), limited interconnections (e.g. South Sudan, SS, and Gabon, GA), or countries bordering other power pools not considered in this study (e.g. Cameroon, CM) are more subject to load shedding. A more uniform shadow price distribution is observed in other, well interconnected countries (Morocco, MA; Algeria, DZ; Tunis, TN; and Libya, LY in NAPP, Egypt, EG; and Sudan, SD; as well as Kenya, KE; Tanzania, TZ; Burundi, BI; Uganda, UG; and Rwanda, RW; in EAPP, and Democratic Republic of Congo, CD; and Angola, AO; in CAPP).

**Figure 17** Heat map of computed shadow prices from the Reference scenario with hourly scale in each of the 25 countries.



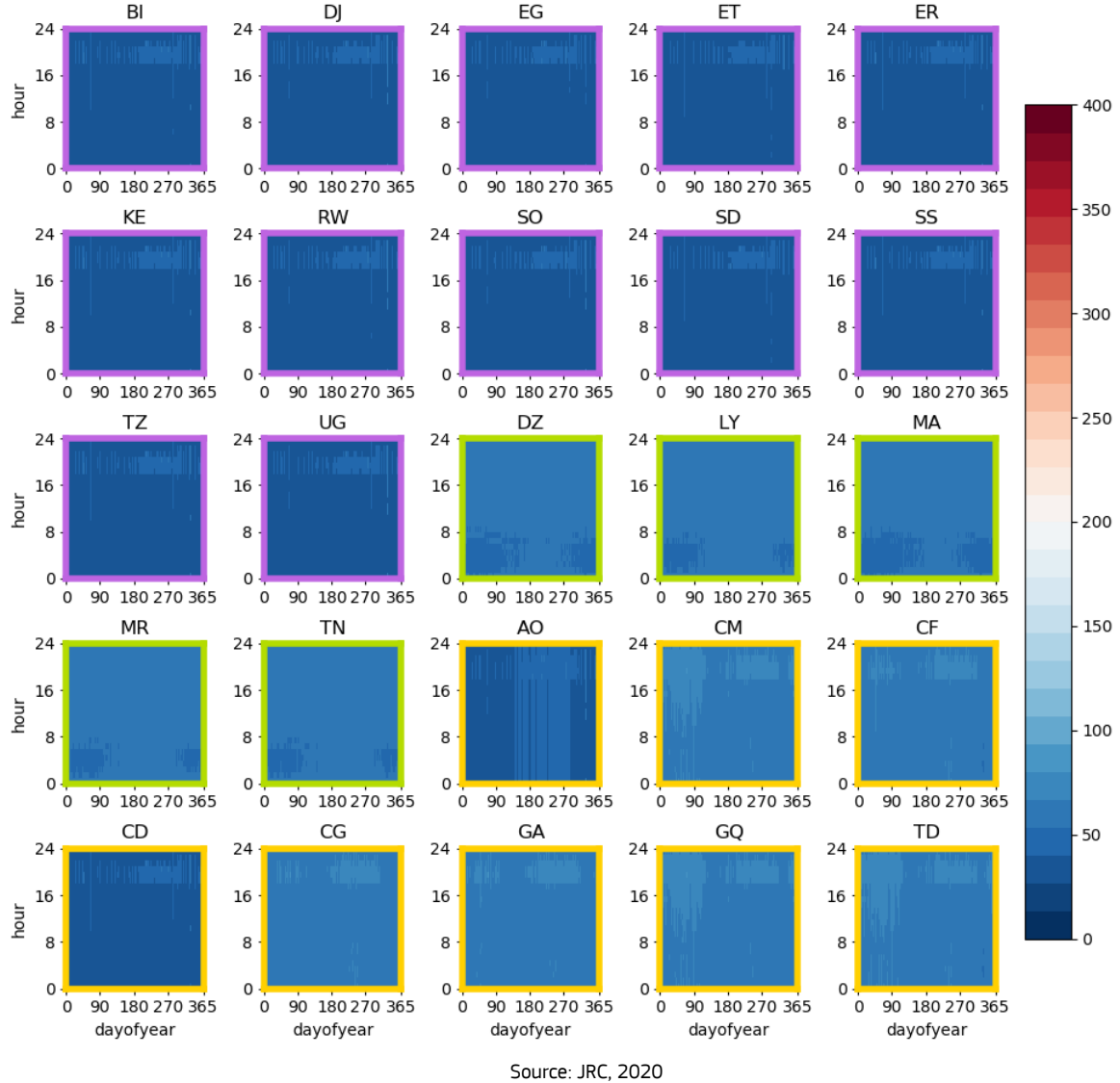
Source: JRC, 2020

Values on the legend indicate shadow prices in EUR/MWh, blue colours represent variable dispatch costs, red stands for shed load. Purple zones belong to EAPP, green zones belong to NAPP and yellow zones belong to CAPP.

### 5.3.2 Connected scenario

Contrary to the Reference scenario, shadow prices in the Connected scenario are, due to increased cross-border line capacities, more uniform across the continent. This increased regional and intercontinental interconnectivity results in fewer load shedding hours and lower average price of electricity in general. Shadow prices for an average weather year (1999) are presented in Figure 18. Extremely wet (1985) and dry (2009) years are presented in Figure 50 and Figure 51 (Annex 6). In this scenario, three large clusters of price convergence are identified.

**Figure 18** Heat map of computed shadow prices from Connected scenario with hourly scale in each of the 25 countries.



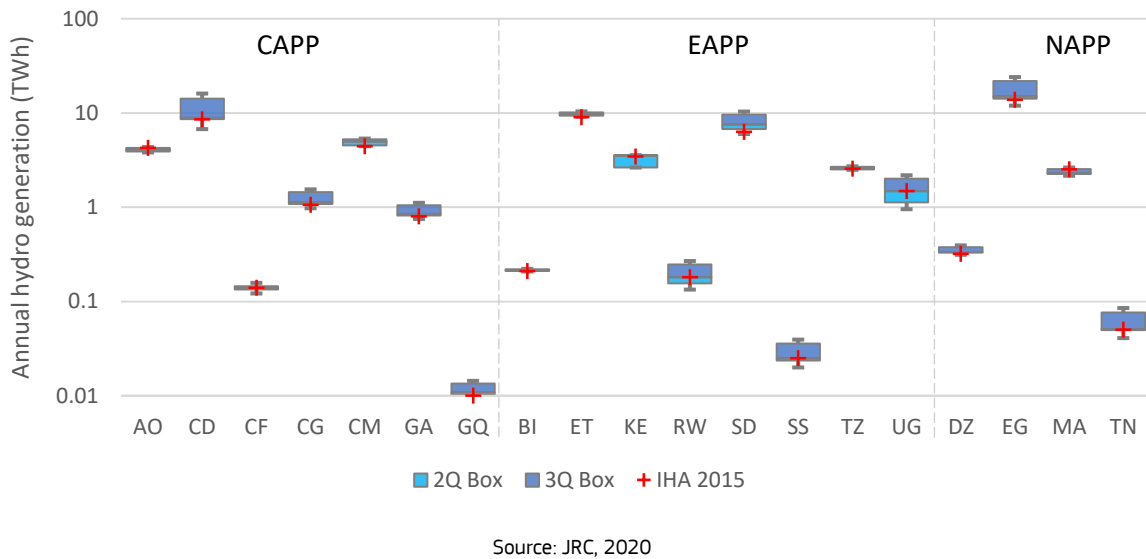
Source: JRC, 2020

Values on the legend indicate shadow prices in EUR/MWh, blue colours represent variable dispatch costs, red stands for shed load. Purple zones belong to EAPP, green zones belong to NAPP and yellow zones belong to CAPP.

#### 5.4 Electricity generation

The Dispa-SET UCM and MTS models are used to simulate the 38 considered weather years. The energy output of hydro units is presented in Figure 19. Due to data availability, the model was calibrated to match historical outputs for the year 2015. That particular year was an extremely dry year across the three power pools, resulting in relatively low hydro generation when compared to the average hydro potential. The model was, however, successfully calibrated and the hydro generation in all countries was within an acceptable error margin. It is important to note that hydro generation can vary significantly between different years and power pools. Overall, NAPP has the most stable hydro generation, mostly because of its large reservoirs with relatively stable inflows. On the contrary, EAPP has the most unpredictable hydro patterns, which is due to the predominance of HROR units.

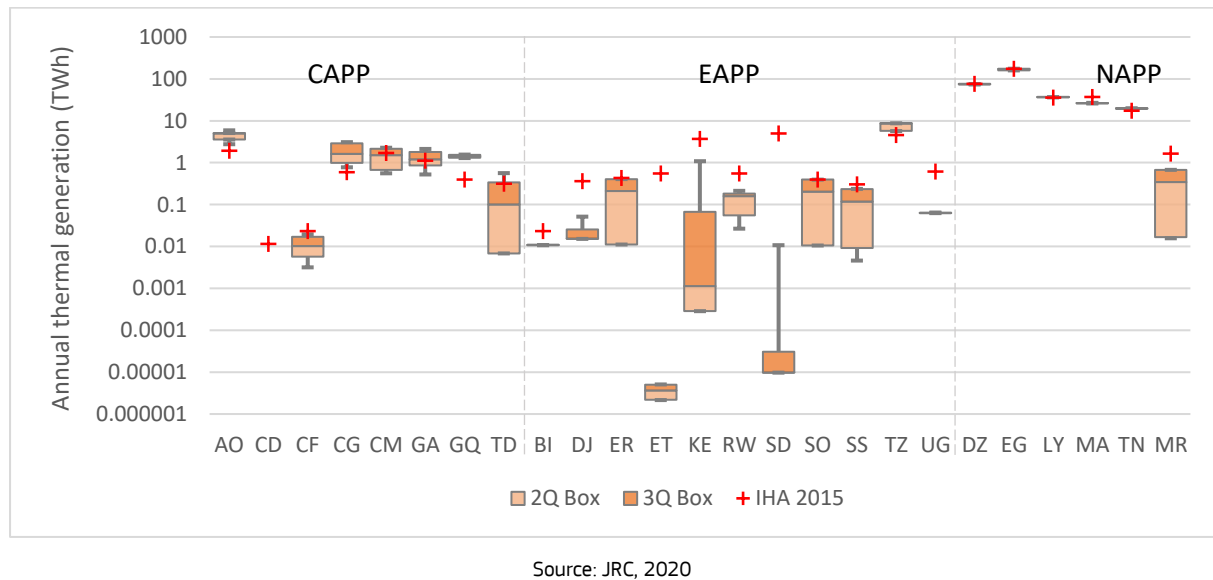
**Figure 19** Simulated annual hydro-power generation in the three power pools.



Red cross indicates the historical flows for the year 2015 as reported in IHA annual report 2016 (IHA, 2016). In this analysis only weather years from the Reference scenario are included.

The energy output of thermal units is presented in Figure 20. Because of the limited data availability, deviations between historical and simulated thermal generation are present, especially in countries belonging to the EAPP. The main reasons are the outages of the local generation fleet and the limited usage of the NTCs. In practice, local dispatch is influenced by power plants and interconnection lines outages (e.g. due to political decisions, extreme weather conditions or inappropriate infrastructure), which could not be taken into account. The present analysis demonstrates that the historical dispatch is sub-optimal, especially in the countries with the lowest GDP per capita.

**Figure 20** Simulated annual thermal-power generation in the three power pools.

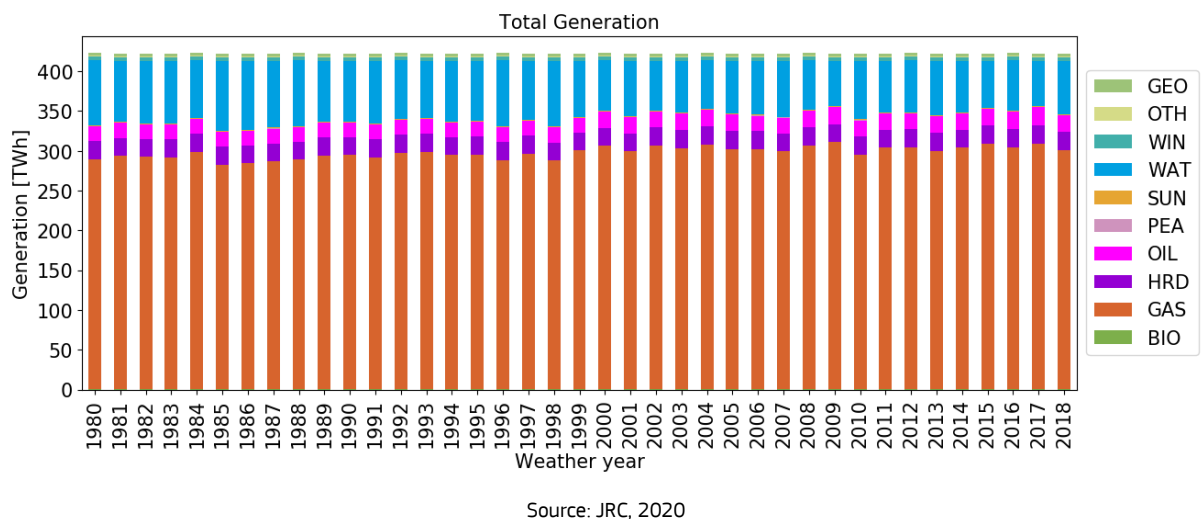


Red cross indicates the historical generation for the year 2015 as reported by AFREC-Energy (AFREC Energy, 2016). In this analysis only weather years from the Reference scenario are included

### 5.4.1 Reference scenario

The total energy generated across all power pools for each fuel type (the acronyms can be found in the nomenclature) and each weather year are presented in Figure 21. The most important sources are natural gas (GAS) and hydro power (WAT). Both show some variability (up to 35 TWh) due to the meteorological factor. Overall, oil derivatives (OIL) are the third most used source of electricity generation, followed by coal and smaller shares of other renewable and non-renewable sources. A more detailed generation breakdown in individual power pools is presented in Figure 52 (Annex 6).

**Figure 21** Total annual generation in the Reference scenario and all 38 weather years.



Source: JRC, 2020

### 5.4.2 Connected scenario

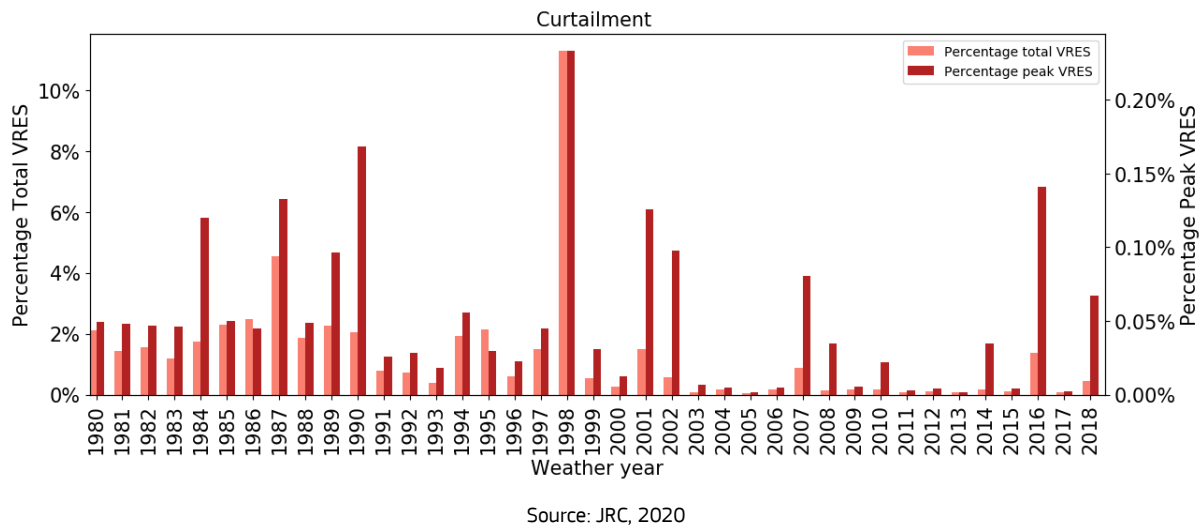
When compared to the Reference scenario, higher cross border interconnectivity allows up to 5 % higher utilization of hydro generation. Consequently, this results in a reduced oil generation and slightly higher use of base load units such as coal generation. Shares of other renewable and non-renewable sources remain on the same level as in Reference scenario. A more detailed generation breakdown in individual power pools is presented in Figure 53 (Annex 7).

## 5.5 Curtailment and spillage

In the current system configuration, a fraction of the total VRES production needs to be curtailed or spilled, in case of HROR units (the reservoirs are quite big, on average 500–3000 hours of storage). Across the three power pools yearly curtailment and spillage reach a maximum of 11% of VRES generation. Maximum hourly curtailment, expressed as a percentage of the peak VRES generation, also reaches a maximum value of 11%. This is mostly observed in isolated countries with no cross-border interconnections and limited flexibility resources such as Central African Republic in CAPP and South Sudan in EAPP. Total annual and peak curtailment in terms of total installed VRES capacity are presented in Figure 22. A more detailed curtailment breakdown is available in Figure 55 (Annex 8).

In the Connected scenario, no curtailment or spillage are obtained, which highlights the importance of increased cross border line capacity to allow the system to fully utilize all VRES and hydro potential.

**Figure 22** Total annual and maximum aggregated hourly curtailment as percentage of total and peak generation from VRES in the Reference scenario and all 38 cases.



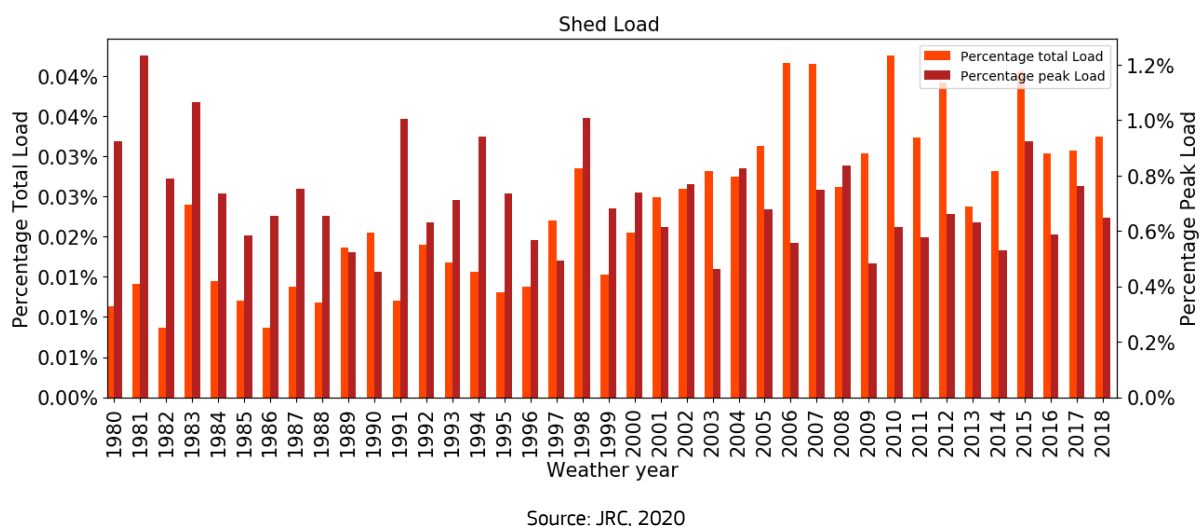
Source: JRC, 2020

## 5.6 Load shedding

### 5.6.1 Reference scenario

Lack of adequate power infrastructure leads to unreliable grid operation in several African countries. The Central African Republic and South Sudan, two isolated countries still recovering from the ongoing civil unrests and recent wars, experience system outages for more than 10 hours per day on average (Central African Republic, 2014). In this analysis, the highest load shedding was observed in the CAPP and EAPP zones. No outages are recorded in NAPP, mostly due to relatively stable overall energy system and good cross border interconnections, as well as relatively small share of VRES and hydro generation and high backup generation capacity. The total annual and peak load shedding in terms of total demand across all power pools are shown in Figure 23. A more detailed breakdown of load shedding values is available in Figure 57

**Figure 23** Total annual and maximum hourly shed load in Reference scenario as a percentage of total and peak load.

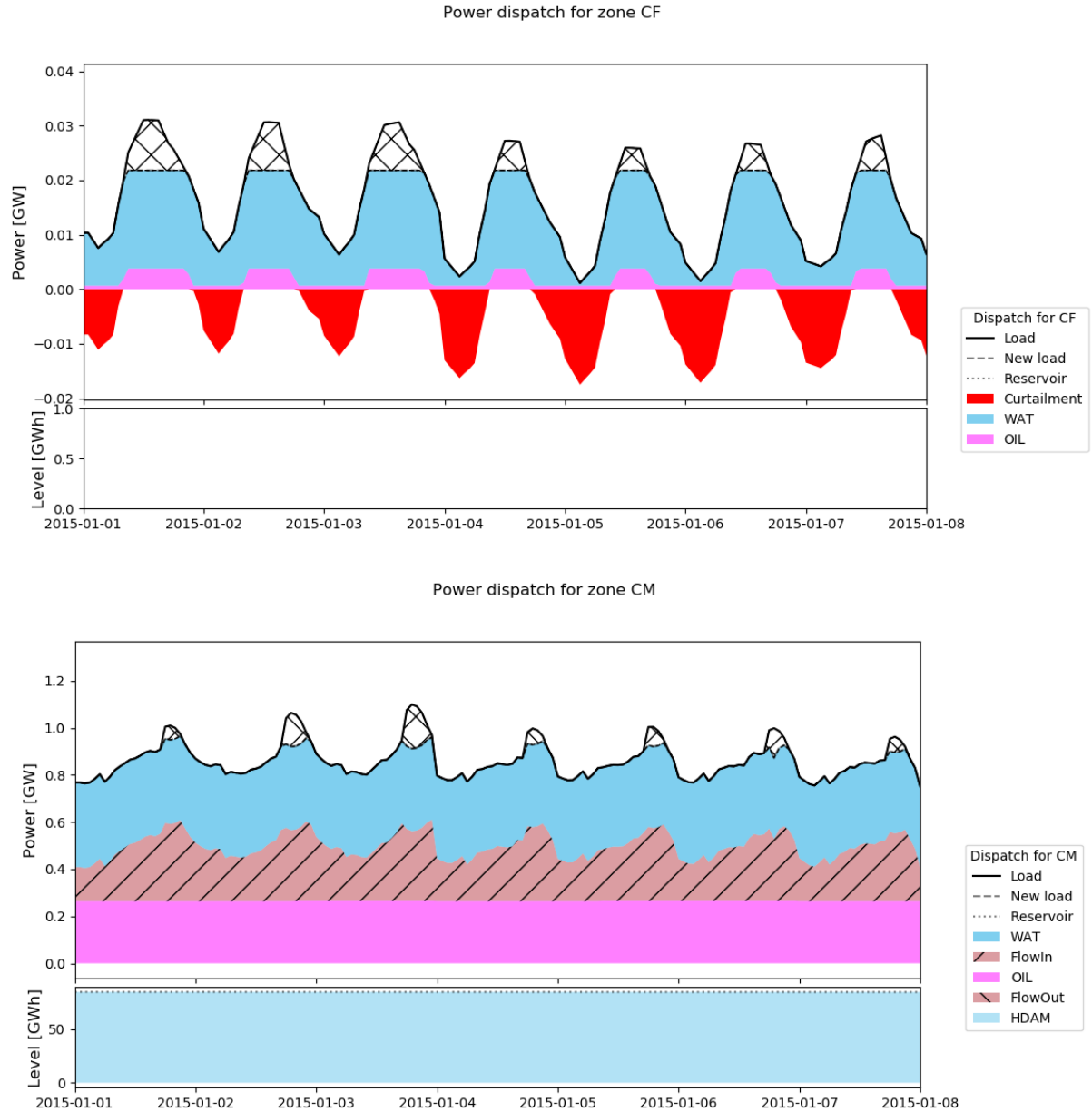


Source: JRC, 2020

An example of two countries where the mismatch between available generation capacity and the local demand are clearly visible, especially during the evening hours, is presented in Figure 24. Although the total installed capacity in the Central African Republic is higher than the peak demand, this local demand cannot be entirely

covered at all times since a large portion (more than 90%) of the local generation relies on inflexible HROR units. In countries such as Cameroon, load shedding is necessary for two reasons. First, the total installed local generation capacity is below the peak load. Second, it has interconnections with countries such as Nigeria, which are not included in the model and cannot be accurately modelled.

**Figure 24** Dispatch plot for the Central African Republic, CF (top), and Cameroon, CM (bottom) for the first week of January.



Source: JRC, 2020

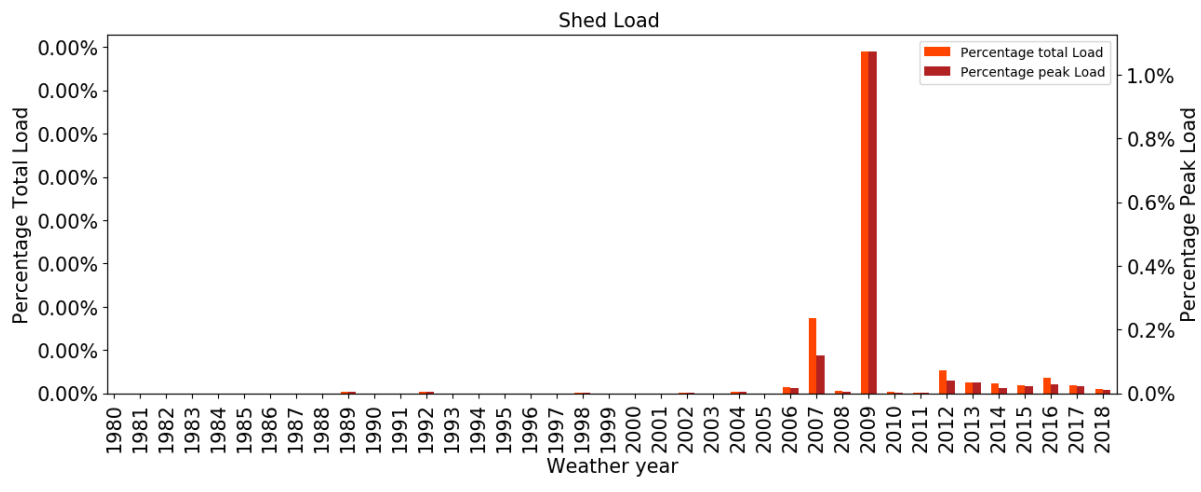
On the top diagram mismatch between available generation capacity and local demand is observed (hatched area), especially in the night hours. On the bottom diagram lack of total installed capacity does not allow covering of the peak demands, despite the full utilization of the NTC.

Finally, it is worth mentioning that the total average shed load across the three power pools remains limited (less than 1%) and is most likely lower than the actual values (for which no harmonized data are available). This is explained by the lack of accurate input regarding the outages of power generation units and interconnection lines. Nevertheless, load shedding in specific countries indicates that the existing power generation and grid infrastructure is not adequate with regard to the local power demand.

## 5.6.2 Connected scenario

Load shedding in the Connected scenario is almost negligible. The highest value (1.05%) can only be observed during the extremely dry weather year (2009). In all other weather years, peak shed load is always below 0.1% of the total load. Total annual and peak load shedding across all power pools are shown in Figure 25. These results clearly indicate that additional interconnection capacities have the potential to drastically increase the adequacy of the African power system and reduce the amount of load not served.

**Figure 25** Total annual and maximum hourly shed load in the Connected scenario as a percentage of total and peak load.

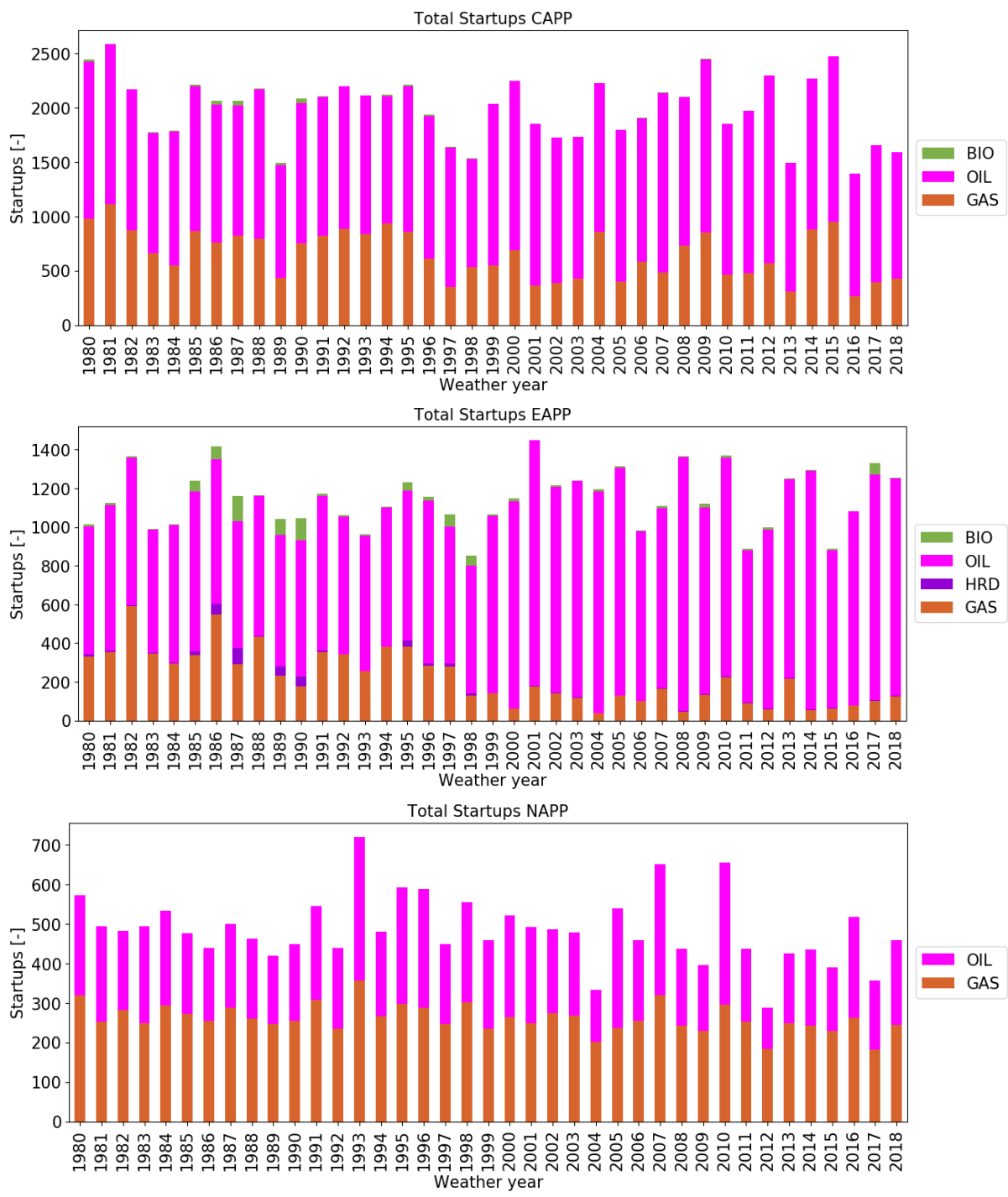


Source: JRC, 2020

## 5.7 Start-ups

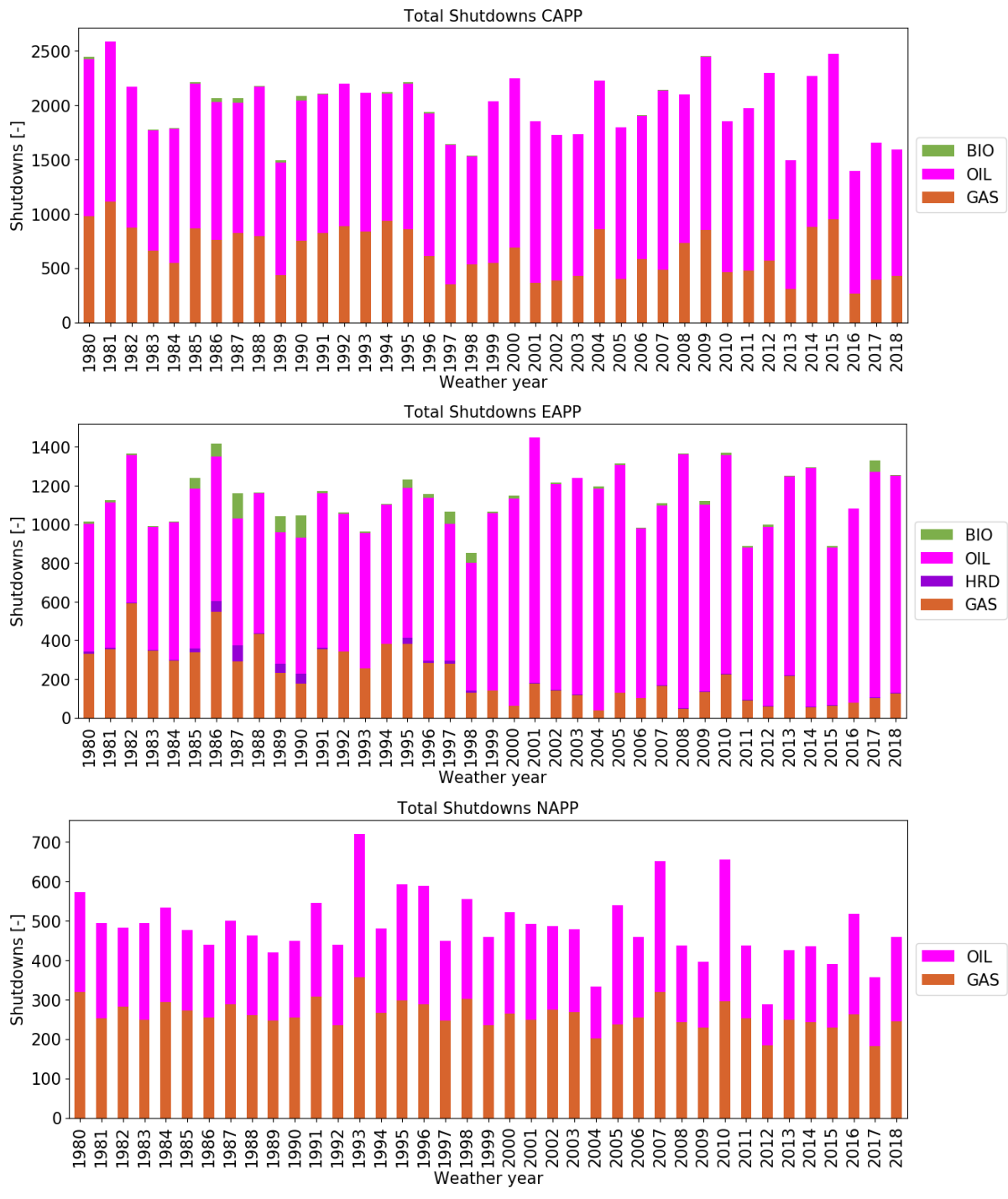
An analysis carried out at the individual power plant level shows the units which are meant for covering the base load: in NAPP and EAPP these are mostly gas and coal-fired power plants, while in CAPP they also include oil fired power plants). The units used for peaking and balancing are mostly oil-fired, and can be detected e.g. by the number of start-ups, as indicated in Figure 26, and by the number of shut-downs, as indicated in Figure 27. The yearly number of start-ups, and shutdowns of all units, most of which are also influenced by the water availability in the system gives an idea of the number of cycles of each thermal unit which consequently would affect the pollutant emissions. The impact of water availability on the power system can be seen in the annual generation costs which decrease as the water availability increase in the system. Specifically, the cost rises in the unusually dry weather years compared to the cost in the unusually wet weather years. Although the unusually wet year has lower average electricity cost compared to the average and unusually dry weather year, it may have a negative impact in other sectors different from the power sector due to floods or channel flow limitations. The increase of annual generation costs for dry hydrological years, which may be exacerbated with extreme weather conditions, encourages the use of renewable resources to offset such increase. The total start-ups and shut-downs are higher for the dry and average weather years than for the wet one because thermal units are committed less often in the latter ones, thus reducing their number of cycles. However, there is a negative correlation for the two types of thermal generators (oil and gas) when it comes to the number of start-ups and/or shut-downs. In other words, the number of cycles of oil fired units decreases in an unusually wet weather years; however, an opposite effect can be observed for gas fired units. This could have an impact on the pollutant emissions since they are strongly related to the number of start-ups and shutdowns of thermal generators.

**Figure 26** Number of start-ups in individual power pools as computed for different availability of water resources.



Source: JRC, 2020

**Figure 27** Number of shut-downs in individual power pools as computed for different availability of water resources.



Source: JRC, 2020

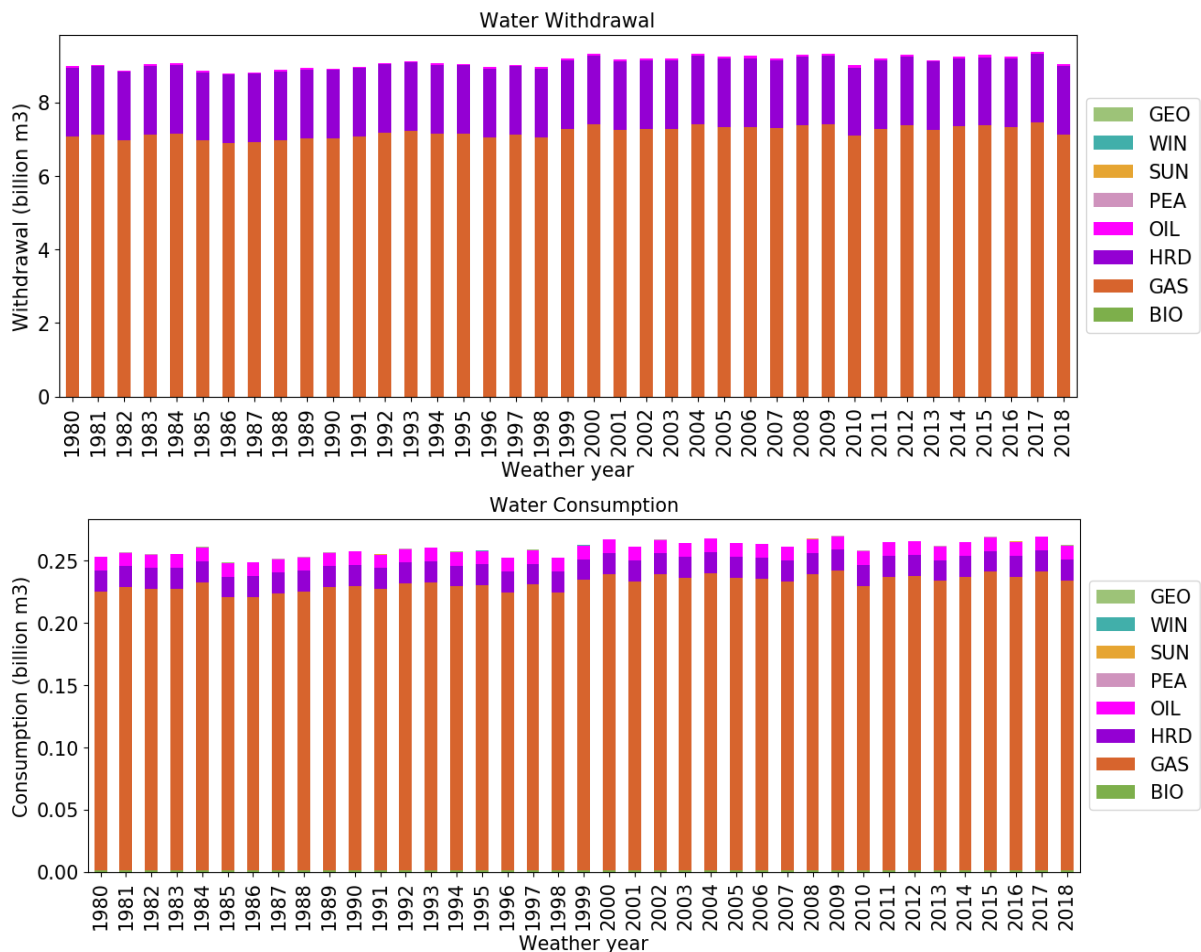
## 5.8 Water stress and water value

### 5.8.1 Reference scenario

According to the methodology discussed in section 2.3.5, freshwater withdrawn and consumed are analysed for the 38 climate years. These indicators are presented in Figure 28. Water consumption for energy needs is inversely proportional to water availability in hydro power plants: when more energy is generated by the hydro units, less water is consumed or withdrawn by thermal units. This can clearly be seen for the year 1985 (wet year), where the water consumption and withdrawals are the lowest, while in year 2009 (dry year) they are at the highest levels. A more detailed representation of the water indicators in individual power pools is shown in Figure 60 and Figure 63 located in Annex 10. Water withdrawal is predominant in gas fired power plants, averaging 7.2 billion m<sup>3</sup> per year, followed by coal fired units, averaging 1.2 billion m<sup>3</sup> per year.

The power pool with the largest water withdrawal is NAPP, amounting to more than 90%, followed by EAPP and CAPP. The highest impact on water withdrawal can be observed in CAPP, where the difference between wet and dry years is around 35%.

**Figure 28** Water withdrawal and water consumption indicators in the Reference scenario

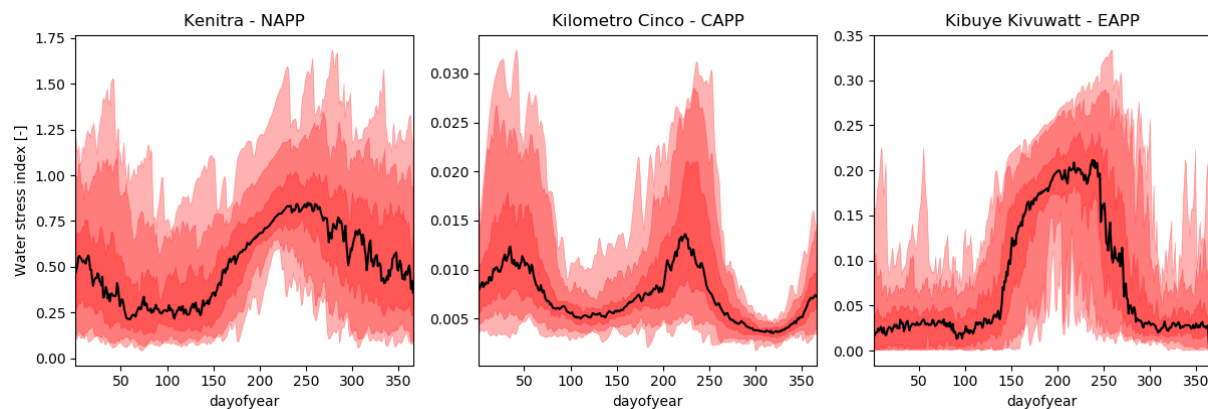


Source: JRC, 2020

In the same manner as for water withdrawal, water consumption is dominated by gas fired units, averaging 0.23 billion m<sup>3</sup>, followed by coal and oil-fired units, averaging 0.11 and 0.09 billion m<sup>3</sup>. Difference between individual power pools is significant. The water consumption in both EAPP and NAPP is on similar levels, averaging around 0.13 and 0.12 billion m<sup>3</sup>, respectively. The water consumption in CAPP is significantly lower, with an average of 0.06 billion m<sup>3</sup>.

The impact of water availability on the operation of individual thermal power plants using fresh water for cooling is analysed in Figure 29. Because of limited data availability, this analysis could not be carried out for all units of the considered power systems. Instead one representative individual unit per power pool has been selected and is analysed in detail. It appears clearly that water scarcity in NAPP is problematic, especially during the dry seasons. For example, hourly water stress index in Kenitra, a gas power plant located in Algeria, was higher than 1, meaning that power plant is using more water than available according to the LISFLOOD model, for 25% of the analysed weather years. This can result in excessive thermal pollution in the river, or to the necessity to operate the power plant at reduced capacity during the dry season. The situation is less sensitive in the two other pools, with average water stress indexes always below 1. This is explained by more favourable cooling conditions (power plants are located close to the large rivers and lakes) and/or relatively small total installed capacity.

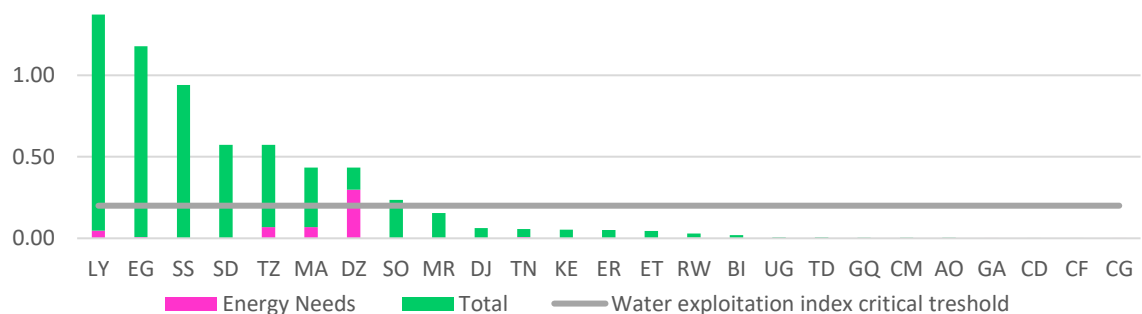
**Figure 29** Hourly water stress index for thermal power generation in individual countries. The 0th, 5th, 25th, 50th (black line), 75th, 95th and 100th percentiles are presented. They highlight water stress in years closest to the proposed percentiles.



Source: JRC, 2020

In the analysed weather years, countries with limited water availability (Libya, Egypt, South Sudan, Sudan, Tanzania, Morocco, Algeria and Somalia) have units characterized by high water stress index, meaning that for the large portion of the year water withdrawal and consumption is on the upper limit of the water availability. At the country level, this is captured by the water exploitation index, presented in Figure 30. Countries with high water potential (Democratic Republic of the Congo and Congo) have the lowest water exploitation index. Water exploitation index in NAPP is however always above the critical threshold as defined in (Adamovic et al., 2019). The water exploitation index for energy purposes above the proposed threshold is only observed in Algeria.

**Figure 30** Water exploitation index for energy and total needs inspired by (Adamovic et al., 2019)



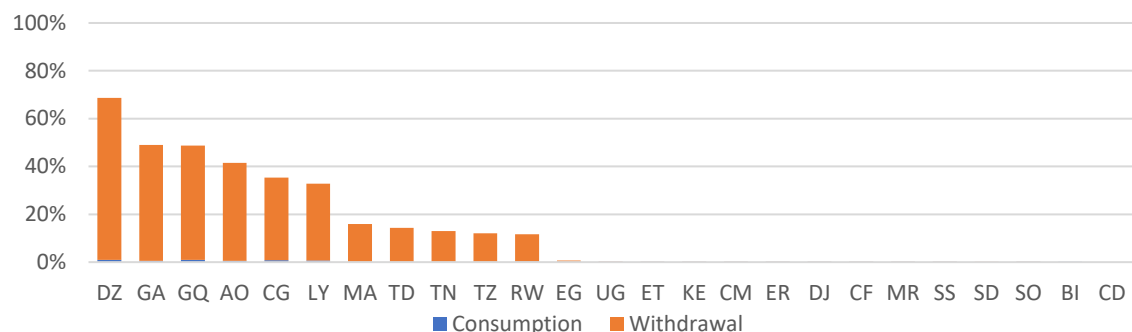
Source: Aquastat<sup>39</sup> (total fresh water availability) and Water for Africa<sup>40</sup> data (total water consumption) and simulations (water consumption for energy sector needs)

<sup>39</sup> <https://www.greenfacts.org/en/water-resources/figtableboxes/3.htm>

<sup>40</sup> <https://water-for-africa.org/en/water-consumption/articles/water-consumption-in-africa.html>

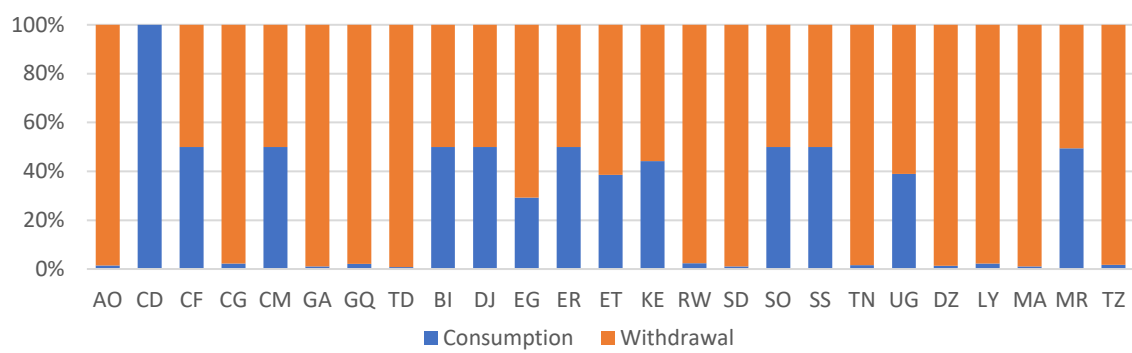
Furthermore, water consumption and water withdrawal for power generation purposes as a share of total water needs are presented in Figure 31. In countries where industry is the largest water consumer (in this case countries with large oil and gas refineries such as Algeria, Libya and Equatorial Guinea and strong mining industry such as Angola and Tanzania) and/or countries where water availability is rather low (Chad), the share of water for energy purposes is relatively high. A more detailed representation of water withdrawal and water consumption for cooling needs in individual countries is presented in Figure 32 and Figure 33. It appears that water consumption remains marginal compared to withdrawals in the most vulnerable countries.

**Figure 31** Water for energy needs as share of total water needs across all analysed countries as computed by Dispa-SET.



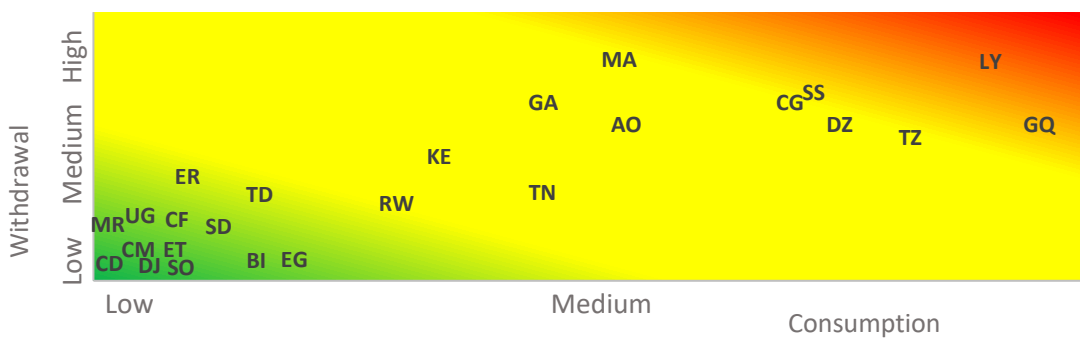
Source: JRC, 2020

**Figure 32** Share of water consumption and water withdrawal as total water needs for energy production



Source: JRC, 2020

**Figure 33** Water stress index heatmap in terms of water withdrawal and water consumption.



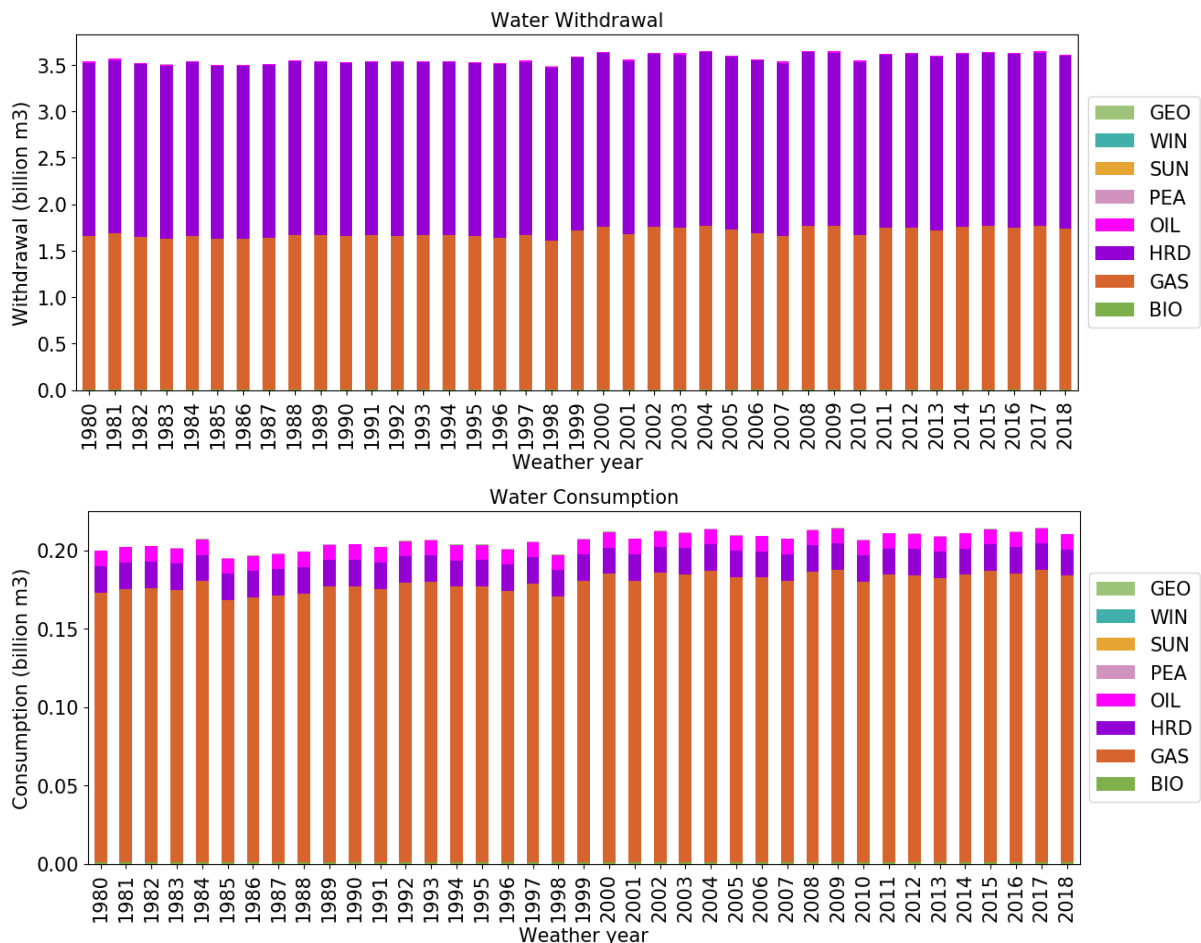
Source: JRC, 2020

Upper right indicates high water stress, while lower left indicates low water stress index.

## 5.8.2 Connected scenario

In the Connected scenario, increased cross-border interconnectivity results in a 47% decrease in water withdrawal when compared to the Reference scenario. The average total water withdrawn for the three power pools amounts to 3.5 billion m<sup>3</sup>, reducing the average total annual water consumption by 0.05 billion m<sup>3</sup> per year. Both water indicators in Connected scenario are presented in Figure 34. A more detailed representation in individual power pools is presented in Figure 61 and Figure 64, located in the Annex 10 of this study. It is worthwhile mentioning that even a small increase in intra-regional cross border interconnectivity significantly impacts the water stress indicators across the continent. The highest benefit is observed in NAPP where coal units are used more, and gas units significantly less than in the Reference scenario.

**Figure 34** Water withdrawal and water consumption indicators in Connected scenario

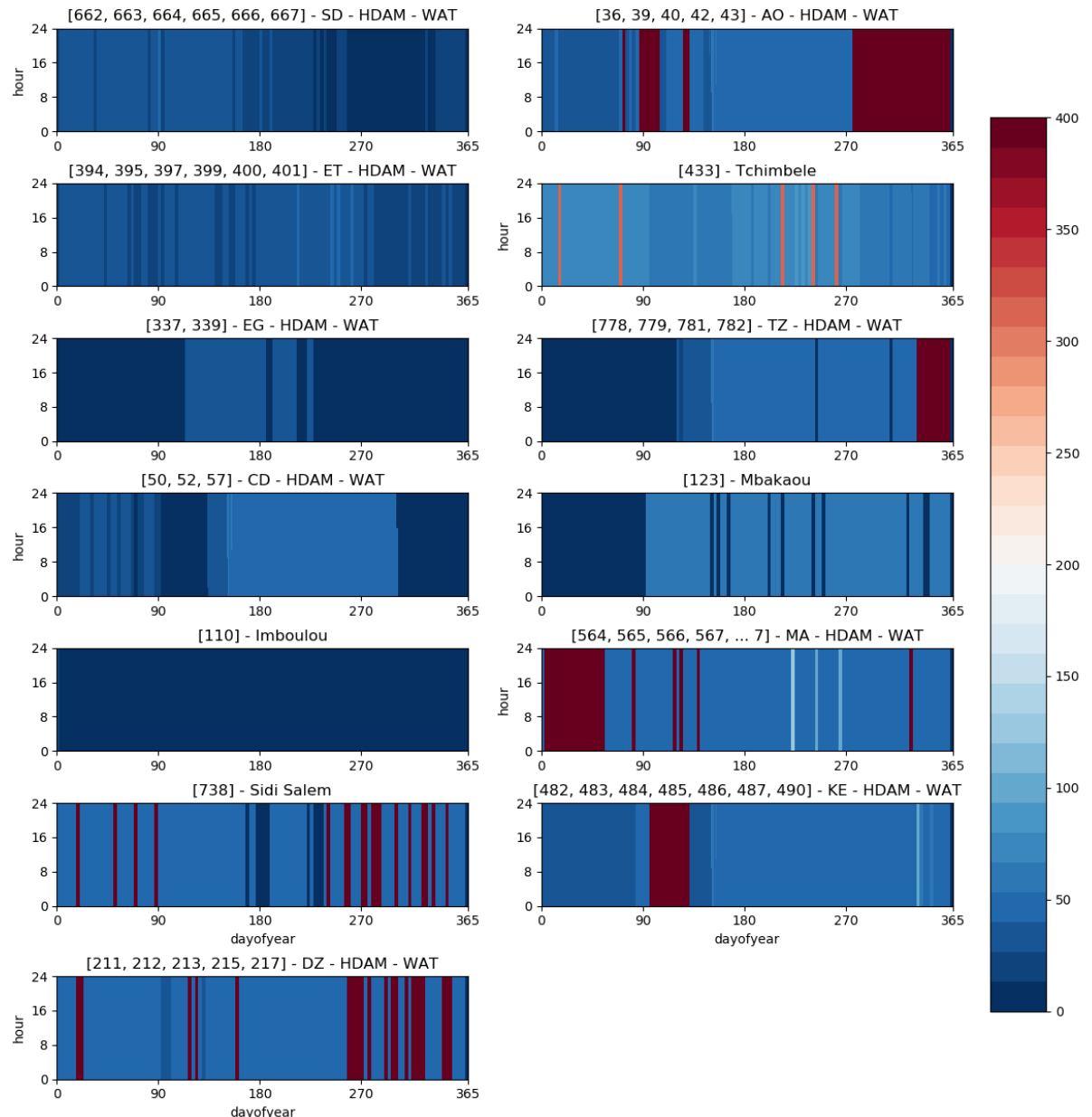


Source: JRC, 2020

## 5.9 Water values

The daily water values for each catchment and for each of the two extreme weather years in the Reference scenario (dark red indicates high water values close to 400 €/MWh whereas dark blue indicates low water values close to 0) are shown in Figure 35 and Figure 36. In the dry scenario, water values are kept high regardless of the catchment. In the wet year, average water values are usually below 50 €/MWh, but only in the catchment located in the CAPP, where the precipitations (and thus the inflows) are usually higher. In wintertime, high water values are computed in the wet scenario, but there is a clear difference with respect to the summer, wherein the water values attain their minimum. The apparent discontinuous character of the water values is due to the fact that its value is equal to the variable cost of the marginal unit during the considered period. Higher variability may be observed if different variable costs were used throughout the year if these costs were disaggregated at the power plant level.

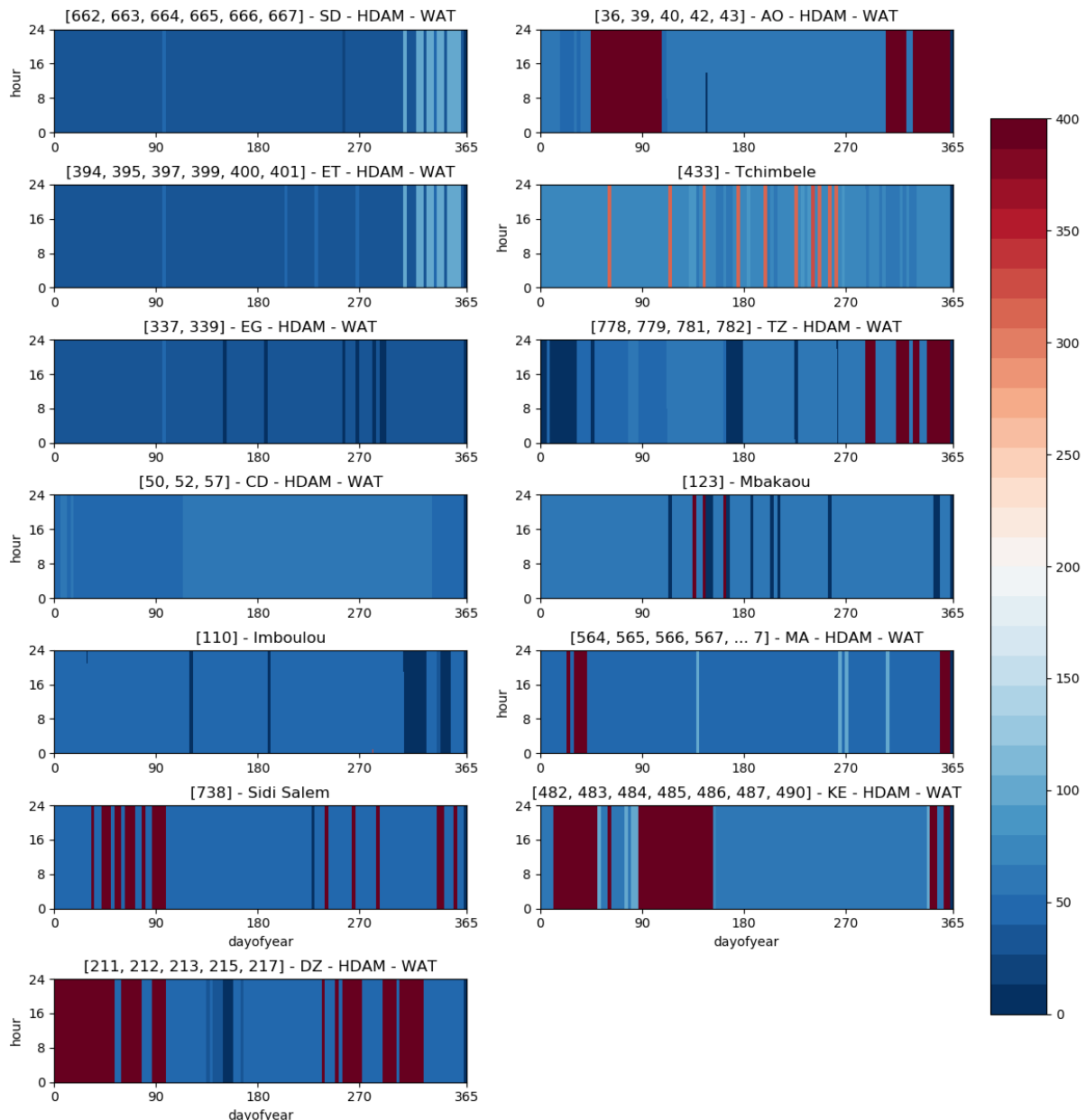
**Figure 35** Water values in Reference scenario for the extremely dry year (2009)



Source: JRC, 2020

Numbers in the headings indicate the indexes of the clustered units inside the Dispa-SET database. Water values are computed for 13 HDAM clusters, sharing similar techno-economical parameters.

**Figure 36** Water values in Reference scenario for the extremely wet year (1985)



Source: JRC, 2020

Numbers in the headings indicate the indexes of the clustered units inside the Dispa-SET database. Water values are computed for 13 HDAM clusters, sharing similar techno-economical parameters.

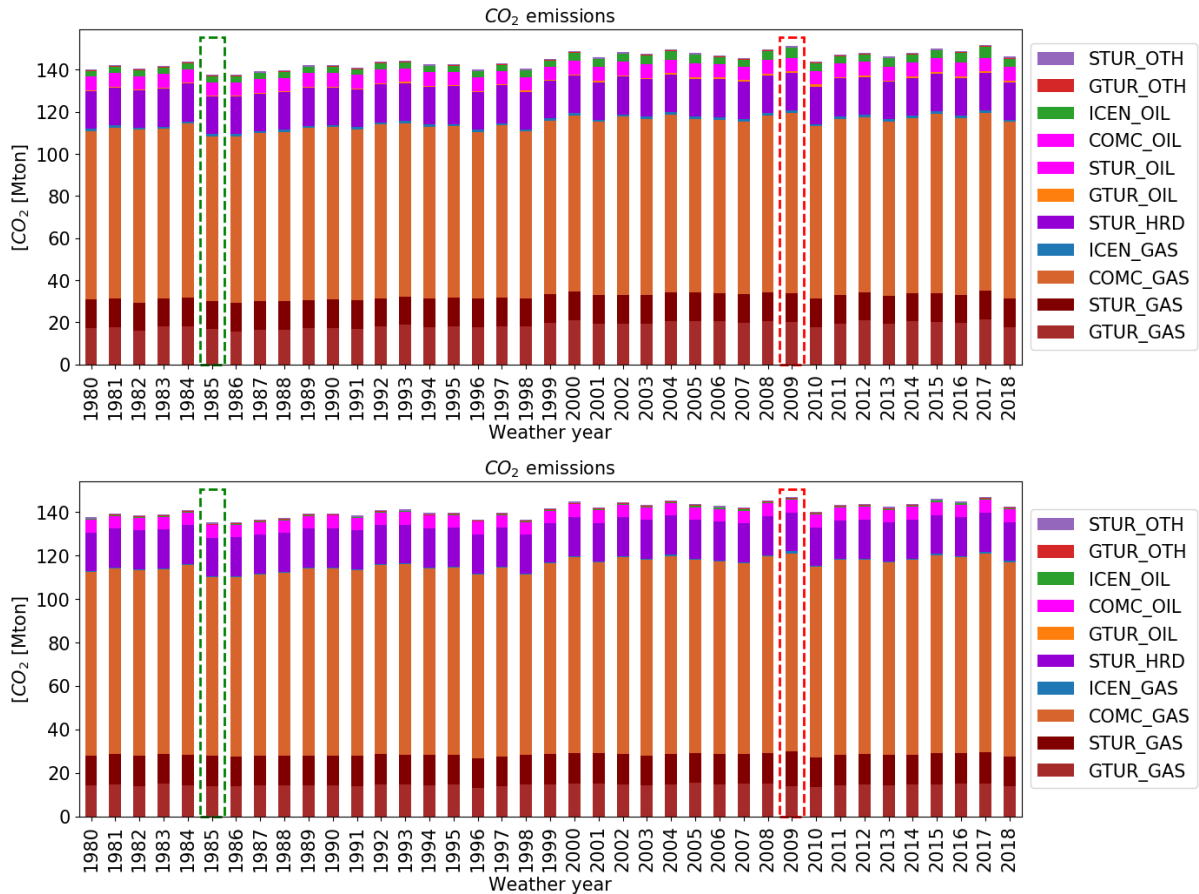
By comparing the wet year to the dry year, results indicate that the average water value increases by 39.8 % to 85.42 EUR/MWh, depending on the selected zone. This variability is indicating the strong influence of climate conditions on the use of water for power generation purposes.

## 5.10 CO<sub>2</sub> emissions

A summary of operational carbon emissions from all thermal units is finally presented in Figure 37 for both scenarios and each of the 38 weather years. There is a clear downwards trend in carbon emissions in years with particularly long wet seasons (year 1985) and full grid availability. Nevertheless, water availability still contributes more to the total carbon emissions. The NAPP pool is the most dependent on fossil fuels, and its total emissions amount to more than 70% of total emissions from the three power pools. 87.2% of total

emissions in reference scenarios come from gas units. Despite the oil abundance and availability in Saharan countries, relatively high oil prices almost entirely prevent the dispatch of oil-fired units.

**Figure 37** Summary of carbon emissions grouped per fuel and per technology type in Reference (top) and Connected (bottom) scenarios and all weather years.



Source: JRC, 2020

## 6 Long-term simulations: soft linking with TEMBA

Another objective of this study is to assess the flexibility potential in future energy system characterized by relatively high penetration of variable renewable energy. To that aim, a long-term energy planning model (TEMBA) is first run until year 2045 and beyond with a certain target for CO<sub>2</sub> emissions (Ref scenario). The simulated energy system is then used as input for the high time-resolution Dispa-SET model, which allows capturing the effects of VRES generation.

The selected long-term objectives include an energy related CO<sub>2</sub> emission reduction target. More details regarding the inputs and constraints of the simulated TEMBA-Reference scenario are available in (Pappis et al., 2019). Uni-directional soft-linking between TEMBA model and the Dispa-SET model is achieved through several intersecting variables:

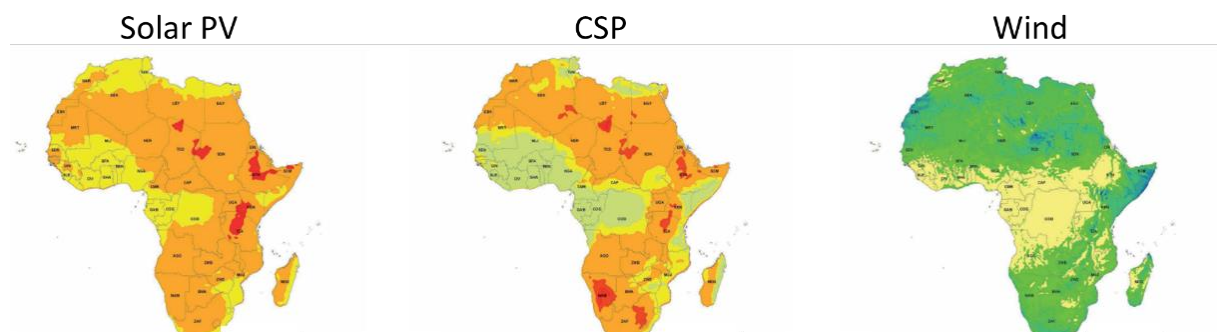
- Total annual demands per country: power and water
- Total installed capacities per country: RES, Conventional, hydro and CSP units

These variables are processed within a “translation model” to generate formatted Dispa-SET inputs, such as scaled time series for all types of demands or realistic power plant fleet according to the projected capacities. Other parameters such as river inflows are assumed unchanged from their historically computed values from the LISFLOOD model. Re-forecasting of AF due to technological advancements, climate change or wake effects are out of scope for this work. Nevertheless, total PV, wind and CSP potentials in different zones were assessed and AF curves were scaled accordingly.

### 6.1 PV, Wind and CSP

Although, VRES potential across Africa is one of the largest in the world, the current deployment remains limited. Total installed VRES (excluding hydro) capacity is 4 GW across the three power pools, which represents only 3.68% of the total installed capacity. A graphical summary of the overall VRES potential is presented in Figure 38. Supplementary tables containing detailed data about the total usable VRES potential is provided in Table 17 and Table 18, located in Annex 4. Wind CF are based on the normalized power curves proposed by King et al., while PV and CSP are estimated according to an IEA methodology (IEA, 2010).

**Figure 38** Overall resource potential for PV, CSP and wind technologies.



Source: figure taken from (Hermann, Miketa, and Fichaux, 2014). Potentials are calculated based on solar irradiation and average wind speed. Dark orange and red areas indicate best suited locations for solar energy systems while dark green and blue areas are best suited for wind systems. A more detailed VRES potential is provided in **Table 17** and **Table 18**, located in Annex 4.

### 6.2 TEMBA Scenarios

In this section, the three scenarios developed by (Pappis et al., 2019; Taliotis et al., 2016) for the future developments of the African energy system are considered. Each scenario is internally consistent, but they differ across several dimensions. These dimensions form part of the scenario space and are exogenous assumptions provided to the model:

- Fuel demand, where both the absolute magnitude and the mix of fuels differ;
- The CO<sub>2</sub> mitigation level, ranging from no mitigation target to carbon emission caps that are consistent with the 2.0 °C and the more stringent 1.5 °C targets;

- The development of technology, and in particular the availability of CCS (Carbon Capture and Storage);
- The adoption of climate friendly energy policies.

All other assumptions presented earlier remain constant across the scenarios. In the Ref scenario, the aim is to extrapolate a business-as-usual African energy policy. The two mitigation scenarios ( $2.0^{\circ}\text{C}$  and  $1.5^{\circ}\text{C}$ ) are developed to compare the future energy mix, power generation investments, water withdrawal and system costs with the Ref scenario. A summary of the proposed scenario definitions is presented in Table 9.

**Table 9** Scenario definitions and demand, infrastructure, and technology availability hypothesis.

Scenario definition									
Definitions		Demand	Infrastructure		Supply				
Scenarios	Years considered	Electricity	NTC	Gas/oil - pipeline	Hydro	Solar	Wind	Biofuels	
<b>Ref</b>	2025	+++	+++	+++	+	+	+	+	+++
<b>2.0 °C</b>	2035	+++	+++	++	+	++	++	++	++
<b>1.5 °C</b>	2045	+++	+++	+	+	++	++	++	++

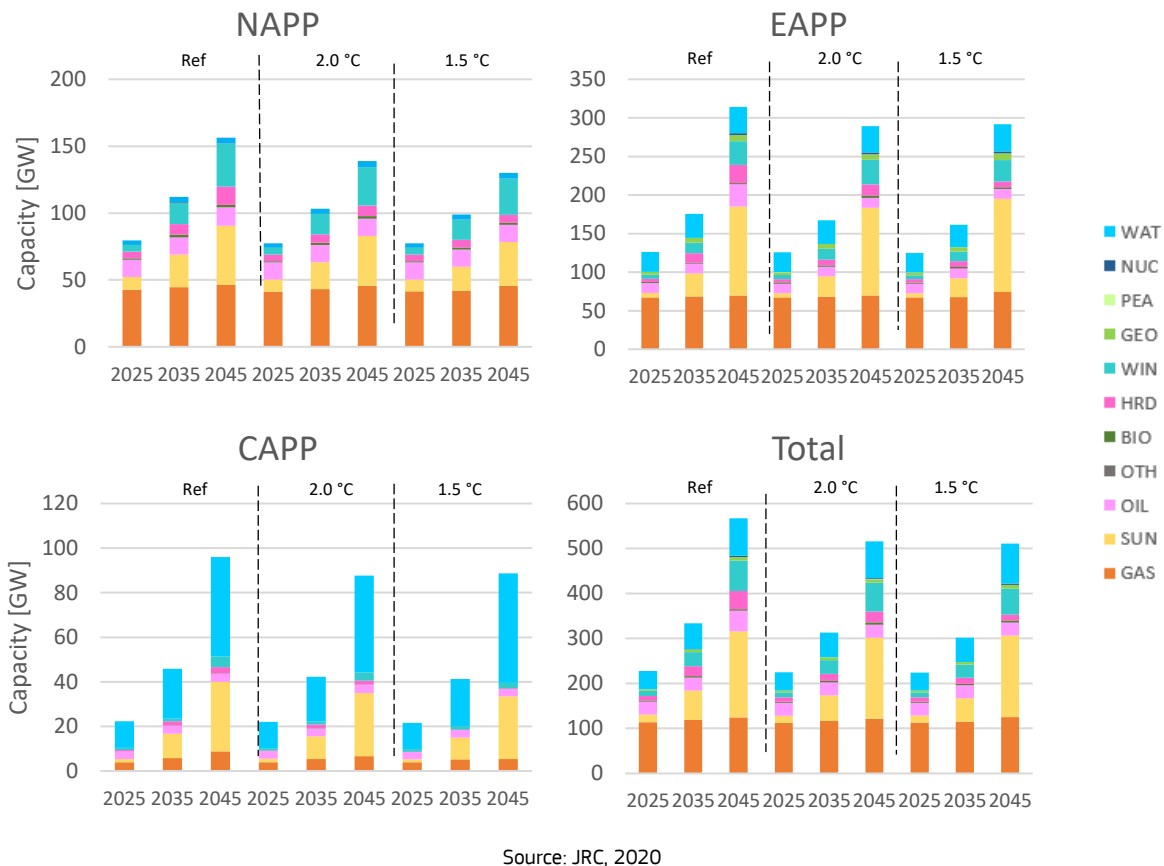
+ Low    ++ Medium    +++ High

Source: JRC, 2020

### 6.3 Power supply

The total installed capacities as computed by TEMBA in each scenario are presented in Figure 39. Total installed capacities and capacity mix in different power pools are slightly different between the three scenarios. In the  $1.5^{\circ}\text{C}$  scenario the highest additions are observed for solar and wind. In contrast to  $2.0^{\circ}\text{C}$  scenario, coal is entirely avoided partly substituted by slightly higher gas and oil additions. The annual VRES capacity factors, especially for wind, are based on the potential locations (i.e. new power stations are firstly built in areas with the highest potential, afterwards, if the total installed capacity is higher than the available potential, sites with lower potential are selected and new capacity factor is calculated based on the weighted average method). Assumptions regarding selection of the cooling technologies are explained in Table 2.

**Figure 39** Total installed capacity and total installed capacity in individual power pools for the three TEMBA scenarios.



Source: JRC, 2020

### 6.3.1 NTC

Long term cross border interconnection projections, after 2025, are taken from (Global Energy Interconnection Development and Cooperation Organization, 2020). They are divided in three main power transmission schemes by 2030, 2040 and 2050. All these schemes are focused around the 35 GW Grand Inga project located close to the mouth of the Congo River. The main considered projects are:

— 2030

- Democratic Republic of the Congo – Republic of Congo ±500 kV DC with total capacity of 3 GW
- Republic of Congo – Angola 400kV AC with total capacity of 2 GW, 3 countries
- Democratic Republic of the Congo – Republic of Congo 765 kV AC transmission project
- Democratic Republic of the Congo – Guinea 800 kV DC with total capacity of 8 GW
- Democratic Republic of the Congo – Zambia 800 kV DC with total capacity of 8 GW
- Democratic Republic of the Congo – Nigeria 660 kV DC with total capacity of 4 GW
- Ethiopia – South Africa 800 kV DC with total capacity of 8 GW
- Cameroon – Nigeria 660 kV DC with total capacity of 8 GW

— 2040

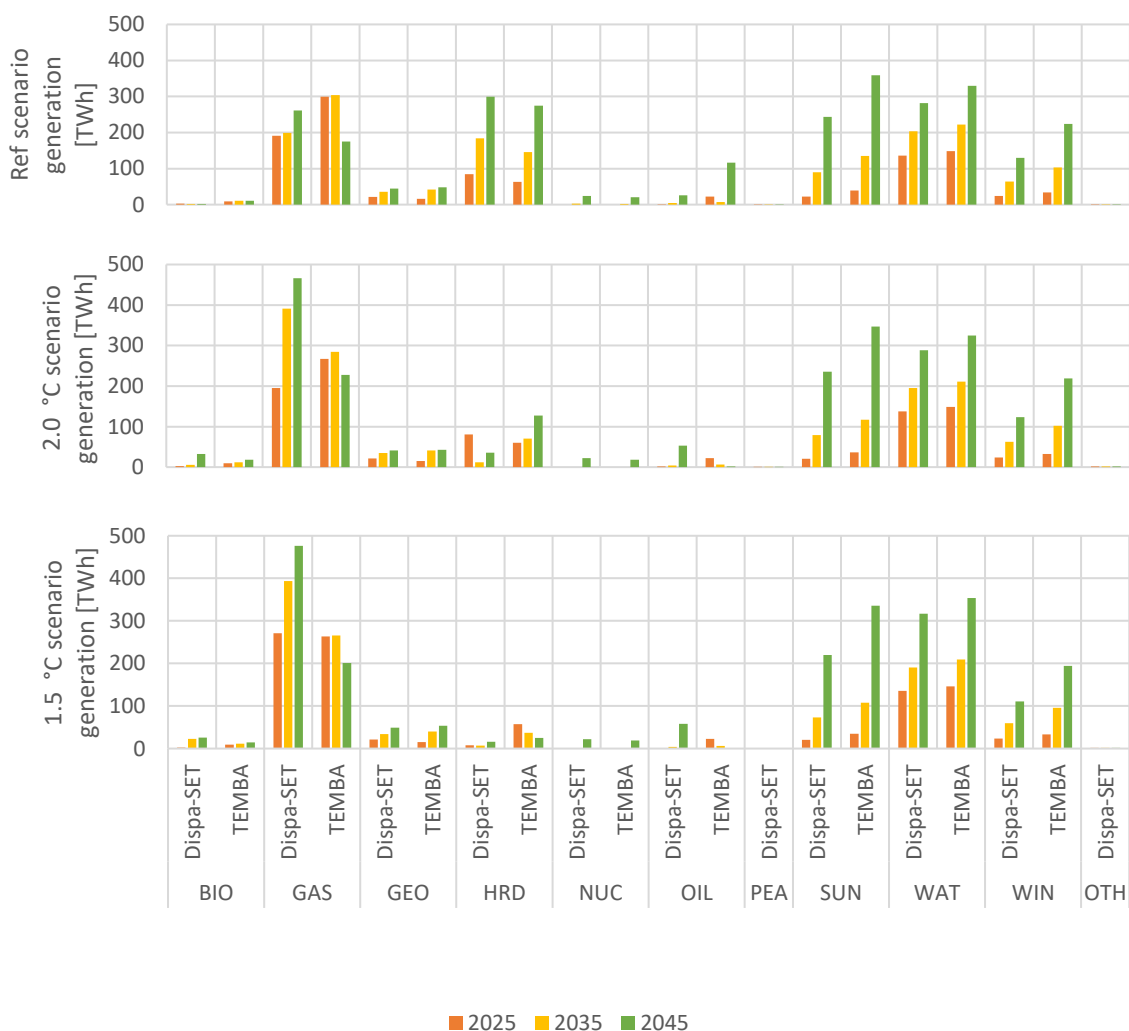
- Democratic Republic of the Congo – Nigeria 800 kV DC with total capacity of 8 GW
- Democratic Republic of the Congo – Ghana 800 kV DC with total capacity of 8 GW
- Morocco – Egypt – 1000 kV AC Corridor, 5 countries
- Sudan – South Africa – 765/500 kV Corridor, 13 countries
- Congo – Chad – 765 kV Corridor, 7 countries

## 6.4 Results and discussion from TEMBA scenarios

### 6.4.1 Generation

Despite the large VRES capacity increase in the three TEMBA scenarios, gas and hydro power remain the predominant sources of electricity. New hydro power capacity additions are identical across the three scenarios. The main difference is the utilization of low carbon technologies: gas and biomass are more utilized in both (2.0 °C and 1.5 °C) carbon-constrained scenarios, thereby replacing coal generation. These two scenarios involve a higher utilization of oil capacities, mainly to cover the peak in regions with low cross-border interconnection capacities. Overall, coal is the third most used source of electricity in the Ref scenario. In the two carbon constrained scenarios overall, solar is the third most used source of electricity generation, followed by wind and smaller shares of other renewable and non-renewable sources. The main difference between the two carbon constrained scenarios is that the shift from coal to gas occurs earlier in the 1.5 °C scenario. The total energy generated across the three power pools is broken down by fuel type and is presented in Figure 40 for each model. In all scenarios, TEMBA overestimates the generation from VRES and underestimates the fossil fuel generation, in particularly gas. This is especially pronounced in the VRES dominant years (2035 onwards) where gas units utilisation between both models varies by 33% to 58% depending on the scenario. This can be attributed to the lower time resolution in TEMBA, which does not allow to fully capture the daily, weekly and seasonal variabilities of renewables. A more detailed generation breakdown (computed by the Dispa-SET model) in individual power pools is presented in Figure 54, located in Annex 6.

**Figure 40** Comparison of total annual generation between Dispa-SET and TEMBA models.

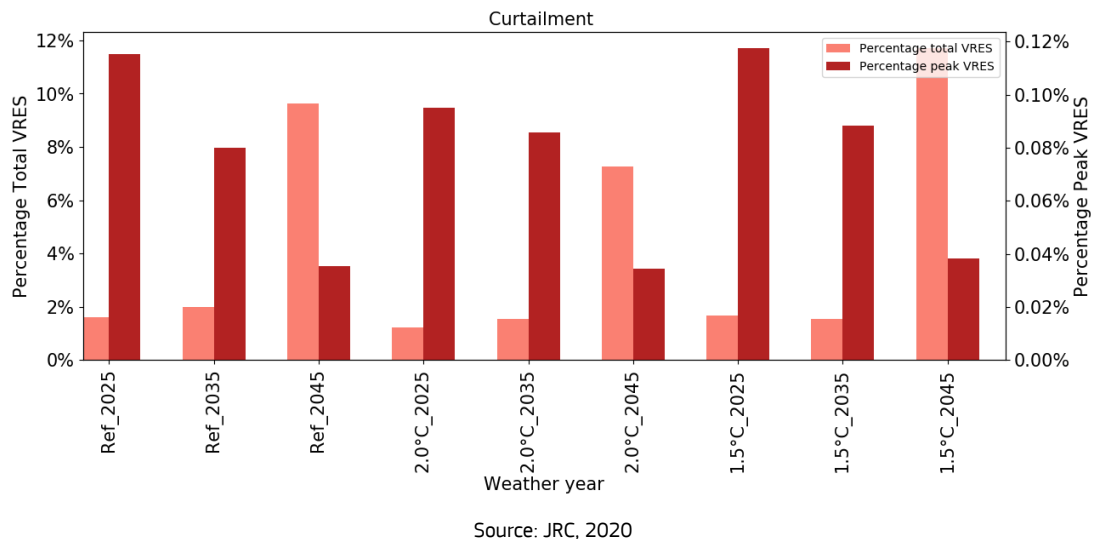


Source: JRC, 2020

## 6.4.2 Curtailment

This analysis shows that, in the three system configurations, a certain fraction of the total VRES production needs to be curtailed. For each power pool, the total curtailed VRES generation (depending on the scenario) is almost entirely related to HROR, and to a smaller extent to wind and sun) is always below 12%. Maximum hourly curtailment, expressed as a percentage of the peak VRES generation, in the two carbon-constrained scenarios is always higher when compared to the Ref scenario. This curtailment is mostly observed in isolated countries with limited cross border interconnections and limited flexibility resources such as the Central African Republic in CAPP and Somalia in EAPP. The total annual and peak curtailment normalized by the VRES generation and are presented in Figure 41. A more detailed curtailment breakdown for each of the three power pools is presented in Figure 56 (Annex 8). It is important to note that increased cross border capacity allows the system to absorb significant amounts of VRES and hydro. Curtailment however remains higher than 10% in 2025 in all three scenarios.

**Figure 41** Total annual and maximum aggregated hourly curtailment as percentage of total and peak VRES generation

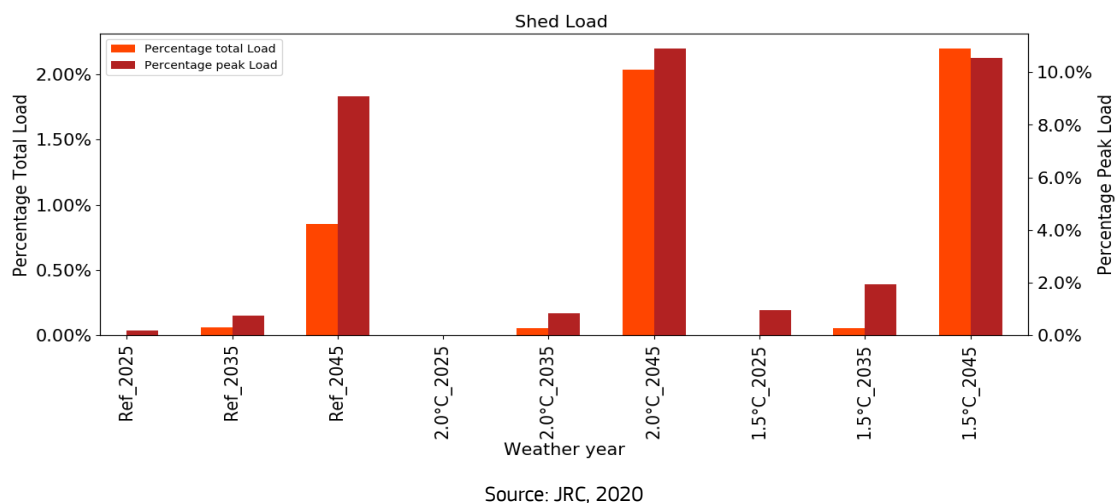


Source: JRC, 2020

## 6.4.3 Load shedding

The highest load shedding is observed in CAPP and EAPP. No capacity deficit is noted in NAPP, mostly due to good cross border interconnections, relatively small share of VRES and hydro generation and high backup generation capacity. Total annual and peak load shedding normalized by the total and peak demand are shown in Figure 42.

**Figure 42** Total annual and maximum hourly shed load in TEMBA scenarios as a percentage of total and peak load



Source: JRC, 2020

More detailed load shedding diagrams for individual power pools are presented in Figure 59 (Annex 9). It is worth mentioning that total annual shed load across the three power pools by year 2025 is small, less than 0.1% which is explained by a better overall interconnectivity when compared to the Reference and Connected scenarios. Nevertheless, load shedding in 2045 is significant, especially in isolated countries or countries bordering the two other African power pools (not analysed within this study). In order to unlock the full utilization of available VRES capacities, more flexibility in form of daily or seasonal storage or flexibility from other sectors such as heating and cooling, gas and transportation, would be needed.

#### 6.4.4 Fresh water withdrawal and consumption

Water stress indicators computed by the two models are presented in Figure 43. Water withdrawal in the TEMBA scenarios is higher because of a higher utilization of coal units, with higher water withdrawal factors when compared to the gas units. In the two alternative scenarios ( $2.0^{\circ}\text{C}$  and  $1.5^{\circ}\text{C}$ ) water consumption is higher in the Dispa-SET model, mainly due to reduced VRES availability and thus increased need for backup gas capacity, when compared to the TEMBA model.

**Figure 43** Comparison of water withdrawal (top) and water consumption (bottom) indicators from power sector only between Dispa-SET and TEMBA models



Source: JRC, 2020

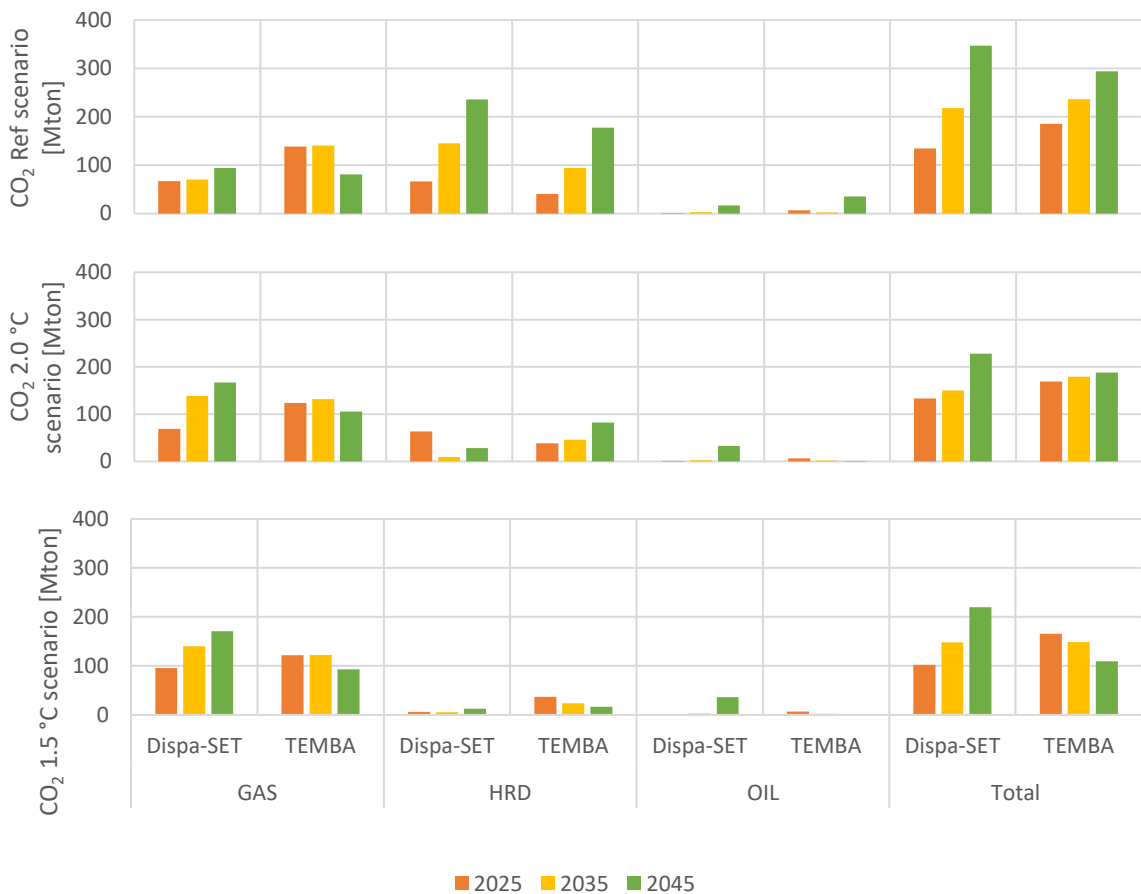
Dispa-SET results indicate that water withdrawal in the Ref scenario increases by a factor of 2 by 2025, 6 by 2035, and 10 by 2045. This is explained by the preferred use of coal units with once-through cooling systems. In the two carbon constrained scenarios, water withdrawn also increases, but in a smaller extent than in the Ref scenario. The most efficient scenario in terms of water withdrawal is  $1.5^{\circ}\text{C}$  scenario where total annual

water withdrawn by 2045 is only 1.8 times higher than the one computed for 2015 system. The highest water withdrawal is relative to coal-fired power plants, followed by gas and oil-fired units. A significant increase in water consumption is observed for each scenario. Nevertheless, in the worst-case scenario ( $2.0^{\circ}\text{C}$  and  $1.5^{\circ}\text{C}$  scenarios) water consumption only increases by a factor of 2 by the year 2045. A more detailed representation of the water indicators in individual power pools is shown in Figure 62 and Figure 65 (Annex 8). Contrary to water withdrawal, water consumption is dominated by gas fired units, followed by coal and oil-fired units.

#### 6.4.5 CO<sub>2</sub> emissions

A summary of operational carbon emissions from all thermal units is finally presented in Figure 66 (Annex 11) for the three scenarios and the three case studies. There is a clear upward trend in carbon emissions in the upcoming years in each scenario. Nevertheless, they remain within the  $2.0^{\circ}\text{C}$  and  $1.5^{\circ}\text{C}$  targets. According to these scenarios, in the upcoming 20 years, NAPP will still largely rely on fossil fuels. Among the three analysed power pools, CAPP can be considered the cleanest since almost 85% of local electricity generation comes from renewables, mostly hydro. The total emissions from NAPP sum up to more than 70% of total emissions from the three power pools. 87.2% of total emissions in Ref scenario come from coal units. Despite oil abundance across all Saharan countries, the relatively high oil price almost entirely prevents the dispatch of oil units. Oil units are however still used in the two carbon-constrained scenarios because of their slightly lower carbon intensity (0.627 t/MWh) in comparison to coal (0.788 t/MWh). Comparison of CO<sub>2</sub> emissions between Dispa-SET and TEMBA models is presented in Figure 44. The difference between the two models can be explained by the different time resolution of the two models.

**Figure 44** Comparison of carbon emissions between Dispa-SET and TEMBA models



Source: JRC, 2020

#### **6.4.6 Adequacy of the TEMBA system**

Overall, the proposed TEMBA systems across the three scenarios are sub optimal with respect to the metrics used for assessing the system adequacy. Despite large capacity additions, load shedding is still necessary in the three scenarios, especially for the years 2035 and 2045. In the three scenarios on average 11% in 2025, 9% in 2035 and 3.5% in 2045 of VRES need to be curtailed, which indicates a lack of system flexibility. The main reason for lower curtailment in the latter years is the deployment of the power grid across the three power pools.

The energy system proposed by TEMBA for the years after 2050 and for the three scenarios did not result in feasible solutions, and large amounts of lost load were computed. For the three years up until 2045 several bottlenecks are identified:

- The lack of additional inter regional flexibility is the main reason for load shedding in isolated countries.
- The lack of flexible units such as HDAM and HPHS in poorly connected countries such as the Central African Republic and Chad also leads to load shedding.
- Intracontinental transmission lines, in particular between the Democratic Republic of the Congo and both Egypt and Morocco would enable more VRES flows from the north to the south, and hydro flows from the south to the north. This would significantly reduce the total VRES curtailment and water spillage currently present in the system.

The lack of adequacy stated in the energy system simulated in TEMBA is explained by the limitations of long-term planning models, which, for computational efficiency reasons, cannot simulate the evolution with a one-hour time resolution. In TEMBA, the time resolution is four time slices (two slices representing different seasons and two time slices representing the time of the day), which is insufficient to capture extreme weather events or temporal variations in the demand and VRE profiles. This demonstrates the pertinence of the soft-linking approach, in which the low-temporal resolution projections of a multi-sectoral long-term planning model are complemented by a power system model. Although not implemented in this work, feedback loops from the power system model to the long-term planning can usefully complement the analysis and help improve the adequacy of the proposed future energy system.

Besides, results such as water withdrawal, water consumption and CO<sub>2</sub> emissions, computed within this study, could not be replicated, and follow different trends than ones proposed by the TEMBA. For example, water consumption in TEMBA 2.0 °C and 1.5 °C scenarios is following a decreasing trend, whereas in Dispa-SET the situation is reversed. Same trends are observed for water withdrawals in all power pools. Some differences are also stated in the power-sector CO<sub>2</sub> emissions, which are on average 15 % in 2025, 17 % in 2035 and 25 % in 2045 % lower in the TEMBA model. This difference is also explained by the different time resolution of the two models.

## 7 Conclusions

This study provides an open modelling framework and input dataset for the analysis of the water-power nexus in three of the five African power pools. It considers both the current (or near-future) situation and long-term scenarios constrained by climate-related CO<sub>2</sub> limitations.

In the Reference scenario, capacity additions varying between 573–589 GW are anticipated by year 2045, for an overall demand which is expected to grow by 16 % by 2025, 89 % by 2035 and 216 % by 2045. To ensure the adequacy of this system, it is of primary importance to increase the transfer capacities between countries. Results indicate that load shedding and curtailment can be significantly reduced by a higher degree of interconnection, both in the current and in the future (long-term) scenarios. The existing grid configuration, where several countries are isolated and do not share any cross-border lines with the neighbours, is not adequate and load shedding is necessary, especially in the Central African Republic and South Sudan, where a lack of generation capacity is stated.

The simulations highlight the dependence of the power sector on the availability of freshwater resources in the three power pools. Variations between wet and dry years significantly impact the final energy mix: the share of electricity coming from hydro units can vary up to 5.2%. Consequently, they also impact the total operational costs: the difference between the wet and dry seasons is around 1.4 billion EUR, or 3.28 EUR/MWh. CO<sub>2</sub> emissions vary by around 15 million tons per year between wet and dry years. It is important to note that the impact of the power fleet on the water sector is mainly related to water withdrawals, water consumption remaining marginal in the most vulnerable countries. This is due to the large share of once-through cooling systems in NAPP, whose main effect is to increase the water temperature, but do not limit the quantity of water available for other usages.

A highly interconnected grid reduces water consumption by 50% in NAPP and 2% in EAPP. Withdrawals are reduced by 50% across the three power pools when compared to the existing system configuration. Interconnections also influences the average price of electricity, which is 2.7% lower in extremely wet, and 3.9% lower in extremely dry seasons. Furthermore, a well interconnected grid also reduces the need for VRES curtailment and water spillage in HROR and HDAM units, allowing higher integration from renewable sources, as well as reduced needs for load shedding, which are only observed in extremely dry seasons.

The analysis further shows that simultaneous system integration and new VRES capacity additions can reduce the potential carbon emissions by more than 32% compared to the reference scenario. Congestion in the proposed interconnection lines might cause serious VRES curtailment by limiting the energy flows from southern (hydro-abundant) countries, and energy flows from the northern (VRES-abundant) countries. As the primary energy generation from thermal units in future low carbon scenarios is significantly lower, lack of flexibility and load shifting resources can lead to curtailment in time periods with high availability and load shedding in time periods with low renewable availability. Despite this, excess capacity in NAPP combined with a well-developed transmission network is sufficient to cover all potential mismatches between the supply and demand in EAPP and CAPP.

From a methodological point of view, the results suggest that long term planning models such as TEMBA – OSeMOSYS can usefully be complemented by a more detailed dispatch model to ensure the feasibility of the proposed scenarios. Further steps of this work include a bi-directional soft linking between the two models, which would provide a more insightful global economic optimum for the analysed power pools.

Finally, it is worthwhile to note that in order to ensure transparency and reproducibility of the work, all the proposed models, methods, and data are released under open licenses and can be freely downloaded from the JRC Data Catalogue<sup>41</sup>.

---

<sup>41</sup> JRC Data Catalogue <https://data.jrc.ec.europa.eu/collection/id-00134>, as well as [https://github.com/energy-modelling-toolkit/Dispa-SET\\_\(model\\_code\)](https://github.com/energy-modelling-toolkit/Dispa-SET_(model_code)), and <https://zenodo.org/deposit/3839756> (databases).

## 8 References

- Adamovic, M., I. Hidalgo Gonzalez, G. Bidoglio, and S. Peteves, 'Water - Energy Nexus in Europe', *Publications Office of the European Union*, 2019.
- AFREC Energy, *African Energy Statistics 2015 Edition*, African Union, Addis Ababa, 2016.
- African Development Bank Group, *African Economic Outlook 2019*, Outlook, African Development Bank Group, Cote d'Ivoire, 2019.
- Brown, S., G. Gaston, and R.C. Daniels, 'Tropical Africa: Land Use, Biomass, and Carbon Estimates for 1980', 1996.
- Burek, P.A., J. Van der Knijff, and A. De Roo, 'LISFLOOD - Distributed Water Balance and Flood Simulation Model - Revised User Manual 2013', *Scientific and Technical Research Reports*, 2013.
- Carrion, M., and J.M. Arroyo, 'A Computationally Efficient Mixed-Integer Linear Formulation for the Thermal Unit Commitment Problem', *IEEE Transactions on Power Systems*, Vol. 21, No. 3, August 2006, pp. 1371–1378.
- Central African Republic, 'Expression of Interest by the Central African Republic to CIF/SREP Program', 2014.
- Cross-border Information, 'African Energy Atlas 2020/2021', *Africa-Energy*, 2020.
- De Felice, M., I. Gonzalez Aparicio, T. Huld, S. Busch, and I. Hidalgo Gonzalez, 'Analysis of the Water-Power Nexus in the West African Power Pool', *Publications Office of the European Union*, 2018.
- Dee, D.P., S.M. Uppala, A.J. Simmons, P. Berrisford, P. Poli, S. Kobayashi, U. Andrae, et al., 'The ERA-Interim Reanalysis: Configuration and Performance of the Data Assimilation System', *Quarterly Journal of the Royal Meteorological Society*, Vol. 137, No. 656, April 2011, pp. 553–597.
- ECOWAS, *Update of the ECOWAS Revised Master Plan for the Generation and Transmission of Electrical Energy: Final Report Volume 1: Study Data*, Economic Community of West African States, 2011.
- European Commission, 'Towards a Comprehensive Strategy with Africa - 52020JC0004', European Commission, March 9, 2020.
- European Investment Bank, *EIB Project Carbon Footprint Methodologies: Methodologies for the Assessment of Project GHG Emissions and Emission Variations*, European Investment Bank, 2018.
- Fernandez Blanco Carramolino, R., K. Kavvadias, M. Adamovic, B. Bisselink, A. de Roo, and I. Hidalgo Gonzalez, 'The Water-Power Nexus of the Iberian Peninsula Power System', *Publications Office of the European Union*, 2017, p. 93.
- Fernández-Blanco, R., K. Kavvadias, and I. Hidalgo González, 'Quantifying the Water-Power Linkage on Hydrothermal Power Systems: A Greek Case Study', *Applied Energy*, Vol. 203, October 1, 2017, pp. 240–253.
- Global Energy Interconnection Development and Cooperation Organization, *Research on Hydropower Development and Delivery in Congo River*, Springer Singapore, Singapore, 2020.
- Gonzalez Aparicio, I., T. Huld, F. Careri, F. Monforti, and A. Zucker, 'EMHIRES DatasetPart II: Solar Power Generation - European Meteorological Derived High Resolution RES Generation Time Series for Present and Future Scenarios.Part II: PV Generation Using the PVGIS Model', *European Commission*, 2017.
- Gonzalez Aparicio, I., A. Zucker, F. Careri, F. Monforti, and J. Badger, 'EMHIRES Dataset Part I: Wind Power Generation - European Meteorological Derived High Resolution RES Generation Time Series for Present and Future Scenarios', *European Commission*, 2016.
- Grundling, P.-L., and A.P. Grootjans, 'Peatlands of Africa', in C.M. Finlayson, G.R. Milton, R.C. Prentice, and N.C. Davidson (eds.), *The Wetland Book*, Springer Netherlands, Dordrecht, 2018, pp. 1413–1422.
- Hargreaves, G., and Z. Samani, 'Estimating Potential Evapotranspiration', *Journal of the Irrigation and Drainage Division*, Vol. 108, No. 3, 1982, pp. 225–230.
- Hermann, S., A. Miketa, and N. Fichaux, *Estimating the Renewable Energy Potential in Africa*, IRENA-KTH Working Paper, International Renewable Energy Agency, Abu Dhabi, 2014.

- IEA, *Technology Roadmap - Concentrating Solar Power*, IEA, Paris, 2010.
- , *World Energy Outlook 2019*, IEA, Paris, 2020.
- IHA, *Hydropower Status Report - 2016*, International Hydropower Association, London, 2016.
- International Energy Agency, *Energy Access Outlook 2017: From Poverty to Prosperity*, OECD, 2017.
- Keramidas, K., A. Diaz Vazquez, M. Weitzel, T. Vandyck, M. Tamba, S. Tchung-Ming, A. Soria Ramirez, et al., 'Global Energy and Climate Outlook 2019: Electrification for the Low-Carbon Transition', *Publications Office of the European Union*, Vol. EUR 30053 EN, 2020.
- Macknick, J., R. Newmark, G. Heath, and K.C. Hallett, 'Operational Water Consumption and Withdrawal Factors for Electricity Generating Technologies: A Review of Existing Literature', *Environmental Research Letters*, Vol. 7, No. 4, December 2012, p. 045802.
- Medinilla, A., B. Byieres, and K. Karaki, *Discussion Paper NO. 244 - African Power Pools: REGIONALENERGY, NATIONAL POWER*, Discussion Paper, ECDPM, 2019.
- Pappis, I., M. Howells, V. Sridharan, W. Usher, A. Shivakumar, F. Gardumi, and E. Ramos, 'Energy Projections for African Countries', *Publications Office of the European Union*, 2019.
- Pavičević, M., K. Kavvadias, T. Pukšec, and S. Quoilin, 'Comparison of Different Model Formulations for Modelling Future Power Systems with High Shares of Renewables – The Dispa-SET Balkans Model', *Applied Energy*, Vol. 252, October 2019, p. 113425.
- Taliotis, C., A. Shivakumar, E. Ramos, M. Howells, D. Mentis, V. Sridharan, O. Broad, and L. Mofor, 'An Indicative Analysis of Investment Opportunities in the African Electricity Supply Sector — Using TEMBA (The Electricity Model Base for Africa)', *Energy for Sustainable Development*, Vol. 31, April 2016, pp. 50–66.
- The World Bank, *Thirsty Energy: Securing Energy in a Water-Constrained World*, World Bank, Washington DC, 2014.
- Wolf, A.T., J.A. Natharius, J.J. Danielson, B.S. Ward, and J.K. Pender, 'International River Basins of the World', *International Journal of Water Resources Development*, Vol. 15, No. 4, December 1999, pp. 387–427.

## **List of abbreviations and definitions**

AO	Angola
BI	Burundi
CAPP	Central African Power Pool
CD	Democratic Republic of the Congo
CF	Central African Republic
CG	Congo
CM	Cameroon
	Dispa-SET unit commitment and optimal dispatch model
	Dispa-SET MTS Dispa-SET's mid-term scheduling module
	Dispa-SET UCM Dispa-SET's unit commitment module
DJ	Djibouti
DZ	Algeria
EAPP	Eastern African Power Pool
EG	Egypt
ER	Eritrea
ET	Ethiopia
GA	Gabon
KE	Kenya
KUL	Katholieke Universiteit Leuven
	LISFLOOD rainfall-runoff hydrological model
LY	Libya
MA	Morocco
MR	Mauritania
NAPP	North Africa Power Pool
NTC	Net transfer capacity
OSeMOSYS	Open Source Energy Modeling System
QE	Equatorial Guinea
RES	Renewable energy sources
RW	Rwanda
SD	Sudan
SO	Somalia
SS	South Sudan
TD	Chad
TEMBA	The Electricity Model Base for Africa
TN	Tunisia
TZ	Tanzania
UG	Uganda
VRES	Variable renewable energy sources
WEFE	Water-energy-food-ecosystems

## List of figures

<b>Figure 1</b> Organization of African power pools .....	4
<b>Figure 2</b> Relational block-diagram between models and various data sources used within this study.....	7
<b>Figure 3</b> Flowchart for generating availability factors time series for run-of-river (HROR) and scaled inflows time series for hydro dams (HDAM) units.....	9
<b>Figure 4</b> Fuel price estimation based on three fingerprint types: geography, fuel production and availability. ....	11
<b>Figure 5</b> Fuel prices in different zones. Variability is based on the proposed price modification fingerprints.	13
<b>Figure 6</b> Availability of other major resources, biomass (left) and peat (right). ....	14
<b>Figure 7</b> Electricity demand distributions in the three power pools.....	15
<b>Figure 8</b> Capacity mix in all three power pools. ....	16
<b>Figure 9</b> Major African river basins.....	17
<b>Figure 10</b> Semi logarithmic three parameter diagram of HDAM units in the proposed power pools. ....	19
<b>Figure 11</b> Historical time series of AF and scaled Inflows for one year with the 0th, 5th, 25th, 50th (black line), 75th, 95th and 100th percentiles. ....	20
<b>Figure 12</b> A map of existing and short-term African interconnection projects (left) and long-term projects scheduled for period 2030 - 2060.....	21
<b>Figure 13</b> Cross border transfer capacities. ....	22
<b>Figure 14</b> Historical CF for each power pool as computed by LISFLOOD model.....	24
<b>Figure 15</b> Reservoir levels in major HDAM units for one year as computed by the Dispa-SET MTS model.. .	26
<b>Figure 16</b> Costs breakdown for all 38 weather years in Reference scenario .....	27
<b>Figure 17</b> Heat map of computed shadow prices from the Reference scenario with hourly scale in each of the 25 countries. ....	28
<b>Figure 18</b> Heat map of computed shadow prices from Connected scenario with hourly scale in each of the 25 countries.....	29
<b>Figure 19</b> Simulated annual hydro-power generation in the three power pools.....	30
<b>Figure 20</b> Simulated annual thermal-power generation in the three power pools. ....	30
<b>Figure 21</b> Total annual generation in the Reference scenario and all 38 weather years. ....	31
<b>Figure 22</b> Total annual and maximum aggregated hourly curtailment as percentage of total and peak generation from VRES in the Reference scenario and all 38 cases. ....	32
<b>Figure 23</b> Total annual and maximum hourly shed load in Reference scenario as a percentage of total and peak load. ....	32
<b>Figure 24</b> Dispatch plot for the Central African Republic, CF (top), and Cameroon, CM (bottom) for the first week of January. ....	33
<b>Figure 25</b> Total annual and maximum hourly shed load in the Connected scenario as a percentage of total and peak load. ....	34
<b>Figure 26</b> Number of start-ups in individual power pools as computed for different availability of water resources. ....	35
<b>Figure 27</b> Number of shut-downs in individual power pools as computed for different availability of water resources. ....	36

<b>Figure 28</b> Water withdrawal and water consumption indicators in the Reference scenario .....	37
<b>Figure 29</b> Hourly water stress index for thermal power generation in individual countries. The 0th, 5th, 25th, 50th (black line), 75th, 95th and 100th percentiles are presented. They highlight water stress in years closest to the proposed percentiles. ....	38
<b>Figure 30</b> Water exploitation index for energy and total needs inspired by (Adamovic et al., 2019).....	38
<b>Figure 31</b> Water for energy needs as share of total water needs across all analysed countries as computed by Dispa-SET. ....	39
<b>Figure 32</b> Share of water consumption and water withdrawal as total water needs for energy production	39
<b>Figure 33</b> Water stress index heatmap in terms of water withdrawal and water consumption.....	39
<b>Figure 34</b> Water withdrawal and water consumption indicators in Connected scenario .....	40
<b>Figure 35</b> Water values in Reference scenario for the extremely dry year (2009) .....	41
<b>Figure 36</b> Water values in Reference scenario for the extremely wet year (1985) .....	42
<b>Figure 37</b> Summary of carbon emissions grouped per fuel and per technology type in Reference (top) and Connected (bottom) scenarios and all weather years.....	43
<b>Figure 38</b> Overall resource potential for PV, CSP and wind technologies. ....	44
<b>Figure 39</b> Total installed capacity and total installed capacity in individual power pools for the three TEMBA scenarios. ....	46
<b>Figure 40</b> Comparison of total annual generation between Dispa-SET and TEMBA models.....	47
<b>Figure 41</b> Total annual and maximum aggregated hourly curtailment as percentage of total and peak VRES generation .....	48
<b>Figure 42</b> Total annual and maximum hourly shed load in TEMBA scenarios as a percentage of total and peak load .....	48
<b>Figure 43</b> Comparison of water withdrawal (top) and water consumption (bottom) indicators from power sector only between Dispa-SET and TEMBA models.....	49
<b>Figure 44</b> Comparison of carbon emissions between Dispa-SET and TEMBA models .....	50
<b>Figure 45</b> Historical time series of Inflows in major HDAM units located in CAPP for one year. ....	68
<b>Figure 46</b> Historical time series of Inflows in major HDAM units located in EAPP for one year. ....	69
<b>Figure 47</b> Historical time series of Inflows in major HDAM units located in NAPP for one year .....	70
<b>Figure 48</b> Heatmap of shadow prices in individual countries for the driest year (2009) in Reference scenario .....	71
<b>Figure 49</b> Heatmap of shadow prices in individual countries for the wettest year (1985) in Reference scenario .....	72
<b>Figure 50</b> Heatmap of shadow prices in individual countries for the driest year (2009) in Connected scenario .....	73
<b>Figure 51</b> Heatmap of shadow prices in individual countries for the wettest year (1985) in Connected scenario .....	74
<b>Figure 52</b> Generation breakdown for individual power pools in Reference scenario .....	75
<b>Figure 53</b> Generation breakdown for individual power pools in Connected scenario .....	76
<b>Figure 54</b> Generation breakdown for individual power pools in TEMBA scenarios .....	77
<b>Figure 55</b> VRES curtailment for individual power pools and different weather years in Reference scenario	78

<b>Figure 56</b> VRES curtailment for individual power pools and different weather years in TEMBA scenarios ..	79
<b>Figure 57</b> Load shedding for Reference scenario.....	80
<b>Figure 58</b> Load shedding for Connected scenario .....	81
<b>Figure 59</b> Load shedding for TEMBA scenarios .....	82
<b>Figure 60</b> Water Withdrawal for Reference scenario.....	83
<b>Figure 61</b> Water Withdrawal for Connected scenario .....	84
<b>Figure 62</b> Water Withdrawal for TEMBA scenarios .....	85
<b>Figure 63</b> Water Consumption for Reference scenario .....	86
<b>Figure 64</b> Water Consumption for Connected scenario .....	87
<b>Figure 65</b> Water Consumption for TEMBA scenarios .....	88
<b>Figure 66</b> Summary of carbon emissions grouped per fuel and per technology type in TEMBA scenarios ..	89

## List of tables

<b>Table 1</b> Statistics for the three power pools .....	5
<b>Table 2</b> Selection algorithm for cooling systems and different fuel and technology combinations .....	12
<b>Table 3</b> African power pools and participating member states. ....	13
<b>Table 4</b> Installed capacity in each of the analysed countries within the three power pools. ....	16
<b>Table 5</b> Statistical data for different power pools and major river basins. ....	18
<b>Table 6</b> Power-voltage-distance approximation table .....	21
<b>Table 7</b> Summary of scenario definitions .....	23
<b>Table 8</b> Minimum (Min), average (Avg) and maximum (Max) costs from all three scenarios .....	25
<b>Table 9</b> Scenario definitions and demand, infrastructure, and technology availability hypothesis. ....	45
<b>Table 10</b> Estimation of coal prices.....	60
<b>Table 11</b> Estimation of gas prices .....	61
<b>Table 12</b> Estimation of oil prices.....	62
<b>Table 13</b> Estimation of biomass and peat prices .....	63
<b>Table 14</b> Detailed statistics on hydro capacity in different power pools, basins and countries .....	64
<b>Table 15</b> Technical and cost parameters of hydro units.....	65
<b>Table 16</b> Technical and costs parameters for typical power generation units .....	65
<b>Table 17</b> Areas associated with different suitability classes (Wind). Areas restricted to 10-200 km around urban centres. Wind (Potential Categories): Yearly Wind Speed Average [m/s] .....	66
<b>Table 18</b> Areas associated with different suitability classes (PV). PV (Potential Categories) Global Horizontal Irradiation [kWh/m <sup>2</sup> /year) .....	67

## Annexes

### Annex 1. Fuel price estimation

#### A1.1 Coal

**Table 10** Estimation of coal prices

Country	Port	Destination	Port distance km	Shipping and port charges		Total €/tonne	Total transport costs €/GJ	Coal Price €/MWh
				€/GJ	€/tonne			
<b>AO</b>	Luanda	Luanda	0	0.74	0	0.74	0.74	12.49
<b>BI</b>	Dar es-Salaam	Bujumbura	1508	0.84	80	3.57	22.67	
<b>CD</b>	Matadi	Kinshasa	360	0.74	19	1.39	14.83	
<b>CF</b>	Douala	Bangui	1427	0.84	76	3.42	22.14	
<b>CG</b>	Pointe-Noire	Pointe-Noire	0	0.74	0	0.74	12.49	
<b>CM</b>	Douala	Douala	0	0.74	0	0.74	12.49	
<b>DJ</b>	Djibouti	Djibouti	0	0.74	0	0.74	12.49	
<b>DZ</b>	Algiers	Algiers	0	0.74	0	0.74	12.49	
<b>EG</b>	Cairo	Cairo	0	0.74	0	0.74	12.49	
<b>ER</b>	Massawa	Massawa	0	0.74	0	0.74	12.49	
<b>ET</b>	Djibouti	Dire Dawa	324	0.84	17	1.43	14.96	
<b>GA</b>	Libreville	Libreville	0	0.74	0	0.74	12.49	
<b>GQ</b>	Bata	Bata	0	0.74	0	0.74	12.49	
<b>KE</b>	Mombasa	Mombasa	0	0.74	0	0.74	12.49	
<b>LY</b>	Tripoli	Tripoli	0	0.74	0	0.74	12.49	
<b>MA</b>	Rabat	Rabat	0	0.74	0	0.74	12.49	
<b>MR</b>	Nouakchott	Nouakchott	0	0.74	0	0.74	12.49	
<b>RW</b>	Mombasa	Kigali	1464	0.84	78	3.49	22.38	
<b>SD</b>	Port Sudan	Port Sudan	0	0.74	0	0.74	12.49	
<b>SO</b>	Mogadishu	Mogadishu	0	0.74	0	0.74	12.49	
<b>SS</b>	Mombasa	Juba	1617	0.84	86	3.76	23.38	
<b>TD</b>	Port Harcourt	N'Djamena	1570	0.84	83	3.68	23.07	
<b>TN</b>	Tunis	Tunis	0	0.74	0	0.74	12.49	
<b>TZ</b>	Dar es-Salaam	Dar es-Salaam	0	0.74	0	0.74	12.49	
<b>UG</b>	Mombasa	Kampala	1146	0.84	61	2.91	20.31	

Trucking costs are set to 0.053 €/tonne/km while port charges for none-port countries is set to 0.1 €/GJ, average wholesale price was 80 €/tonne, 1 tonne of coal = 29.31 GJ

Source: JRC, 2020

## A1.2 Gas

**Table 11** Estimation of gas prices

Country	LNG Terminal	Local Production	Pipeline	Import	Transport		Total
						€/MMBtu	€/MWh
<b>AO</b>	Soyo	Yes	No	No		0	19.55
<b>BI</b>		No	No	Yes		6.44	44.01
<b>CD</b>		Yes	No	No		0	19.55
<b>CF</b>		No	No	Yes		6.44	44.01
<b>CG</b>		Yes	No	No		0	19.55
<b>CM</b>		Yes	No	No		0	19.55
<b>DJ</b>		No	No	Yes		3.68	33.52
<b>DZ</b>	Arzew	Yes	No	No		0	19.55
<b>EG</b>	Damietta	Yes	No	No		0	19.55
<b>ER</b>		No	No	Yes		3.68	33.52
<b>ET</b>		Yes	No	No		0	19.55
<b>GA</b>		Yes	No	No		0	19.55
<b>GQ</b>		Yes	No	No		0	19.55
<b>KE</b>		No	No	Yes		3.68	33.52
<b>LY</b>		Yes	No	No		0	19.55
<b>MA</b>		No	Yes	Yes		1.5	25.24
<b>MR</b>		No	No	Yes		6.44	44.01
<b>RW</b>		Yes	No	No		0	19.55
<b>SD</b>		No	No	Yes		3.68	33.52
<b>SO</b>		No	No	Yes		3.68	33.52
<b>SS</b>		No	No	Yes		6.44	44.01
<b>TD</b>	Boni Island	No	No	Yes		6.44	44.01
<b>TN</b>		Yes	No	No		0	19.55
<b>TZ</b>		Yes	No	No		0	19.55
<b>UG</b>		No	No	Yes		6.44	44.01

Average price of gas on US and EU stock exchange was 2.75-5.55 €/Mbtu respectively, pipeline costs are estimated to 1.5 €/MMBtu, liquification costs in range from 3.68-6.44 €/MMBtu, distribution costs are estimated to 0.46 €/GJ, 1 MMBtu = 1.055056 GJ

Source: JRC, 2020

### A1.3. Oil

**Table 12** Estimation of oil prices

Country	Local Production	Pipeline	Import	Transport	Total cost
				and distribution	
				€/GJ	€/MWh
<b>AO</b>	Yes	No	No	0.46	29.80
<b>BI</b>	No	No	Yes	7.00	53.33
<b>CD</b>	Yes	No	No	0.46	29.80
<b>CF</b>	No	No	Yes	7.00	53.33
<b>CG</b>	Yes	No	No	0.46	29.80
<b>CM</b>	Yes	No	No	0.46	29.80
<b>DJ</b>	No	No	Yes	7.00	53.33
<b>DZ</b>	Yes	No	No	0.46	29.80
<b>EG</b>	Yes	No	No	0.46	29.80
<b>ER</b>	No	No	Yes	7.00	53.33
<b>ET</b>	No	No	Yes	7.00	53.33
<b>GA</b>	Yes	No	No	0.46	29.80
<b>GQ</b>	Yes	No	No	0.46	29.80
<b>KE</b>	No	No	Yes	7.00	53.33
<b>LY</b>	Yes	No	No	0.46	29.80
<b>MA</b>	No	No	Yes	7.00	53.33
<b>MR</b>	Yes	No	No	0.46	29.80
<b>RW</b>	No	No	Yes	7.00	53.33
<b>SD</b>	Yes	No	No	0.46	29.80
<b>SO</b>	Yes	No	No	0.46	29.80
<b>SS</b>	Yes	No	No	0.46	29.80
<b>TD</b>	No	Yes	Yes	2.91	38.62
<b>TN</b>	Yes	No	No	0.46	29.80
<b>TZ</b>	Yes	No	No	0.46	29.80
<b>UG</b>	No	No	Yes	7.00	53.33

Average crude oil price in 2017 was 47.84 €/Bbl, distribution costs are estimated to 0.46 €/GJ, pipeline costs are estimated to 15 €/Bbl and transport costs are estimated to 40 €/Bbl, 1 Bbl = 6.12 GJ

Source: JRC, 2020

## A1.4 Biomass and peat

**Table 13** Estimation of biomass and peat prices

Country	Biomass €/MWh	Peat €/MWh
<b>AO</b>	10.08	28.08
<b>BI</b>	30.24	9.36
<b>CD</b>	10.08	28.08
<b>CF</b>	10.08	9.36
<b>CG</b>	10.08	9.36
<b>CM</b>	10.08	28.08
<b>DJ</b>	30.24	28.08
<b>DZ</b>	30.24	28.08
<b>EG</b>	30.24	28.08
<b>ER</b>	30.24	28.08
<b>ET</b>	10.08	28.08
<b>GA</b>	10.08	28.08
<b>GQ</b>	10.08	28.08
<b>KE</b>	10.08	9.36
<b>LY</b>	30.24	28.08
<b>MA</b>	30.24	28.08
<b>MR</b>	30.24	28.08
<b>RW</b>	10.08	9.36
<b>SD</b>	30.24	28.08
<b>SO</b>	30.24	28.08
<b>SS</b>	30.24	28.08
<b>TD</b>	30.24	28.08
<b>TN</b>	30.24	28.08
<b>TZ</b>	30.24	28.08
<b>UG</b>	10.08	9.36

Price of biomass in biomass moderate and scarce regions is estimated between 2.8 - 8.4 €/GJ respectively.

Source: JRC, 2020

## Annex 2. Hydro units statistics

**Table 14** Detailed statistics on hydro capacity in different power pools, basins and countries

Pool/Basin/Country	Start date	Head (m)	Power (MW)		Volume (million m³)		Area (km²)	
			Average	Total	Average	Total	Average	Total
<b>CAPP</b>	1976	36	177	5 311	510	11 220	40	1 092
<b>Central West Coast</b>	1983	31	137	1 229	567	2 837	80	639
Cameroon	1968	21	186	743	872	2 617	203	610
Congo	1974	60	79	79	1	1	0	0
Equatorial Guinea	2008	22	120	120			1	1
Gabon	1997	36	96	287	220	220	9	28
<b>Congo River Basin</b>	1974	36	226	2 707	75	671	23	252
Central African Republic	1976	5	18	18	-	-	0	0
Congo	2011	33	128	128	584	584	53	53
Democratic Republic of the Congo	1970	40	256	2 561	11	87	22	199
<b>South West Coast</b>	1974	42	153	1 375	964	7 712	25	201
Angola	1974	42	153	1 375	964	7 712	25	201
<b>EAPP</b>	1990	38	179	11 077	8 900	249 212	221	9 048
<b>Central West Coast</b>	1987	5	13	26	-	-	2	2
Burundi	1987	5	13	26	-	-	2	2
<b>East Central Coast</b>	1986	33	69	1 383	594	6 530	48	771
Kenya	1986	46	96	675	466	2 331	26	154
Rwanda	1991	11	24	142	-	-	1	4
United Republic of Tanzania	1980	39	81	566	700	4 199	88	613
<b>Nile Basin</b>	1990	28	202	6 266	17 973	215 671	481	7 689
Egypt	1976	44	711	2 842	83 500	167 000	2 624	5 248
Ethiopia	1989	32	194	778	420	840	157	472
Kenya	1954	30	180	180	20 000	20 000	1	1
South Sudan	2006	5	5	5				
Sudan	1970	51	289	1 731	4 638	27 830	393	1 967
Uganda	2004	15	49	731	1	1	0	1
<b>Rift Valley</b>	1991	155	106	106	1 645	1 645	26	26
Kenya	1991	155	106	106	1 645	1 645	26	26
<b>Shebelli &amp; Juba Basin</b>	2000	84	412	3 296	6 342	25 367	80	560
Ethiopia	2000	84	412	3 296	6 342	25 367	80	560
<b>NAPP</b>	1969	76	67	2 062	667	13 330	16	462
<b>Mediterranean Coast</b>	1964	56	22	310	341	2 388	9	103
Algeria	1959	62	34	238	222	1 108	5	37
Morocco	1967	64	23	23	725	725	27	27
Tunisia	1966	48	8	50	555	555	13	39
<b>North West Coast</b>	1971	93	103	1 752	842	10 942	21	359
Morocco	1971	93	103	1 752	842	10 942	21	359
<b>Grand Total</b>	1982	47	150	18 450	3 911	273 763	110	10 601

Source: JRC, 2020

### Annex 3. Typical units

**Table 15** Technical and cost parameters of hydro units.

Fuel	Technology	Efficiency	Min Up Time	Min Down Time	Ramp Rate	Start Up Cost	No Load Cost	Ramping Cost	Part Load Min	Start Up Time	CO <sub>2</sub> Intensity
<b>WAT</b>	<b>HDAM</b>	0.80	0	0	0.067	0	0	0	0	0	0
<b>WAT</b>	<b>HROR</b>	1	0	0	0.067	0	0	0	0	0	0

**Table 16** Technical and costs parameters for typical power generation units

Fuel	Technology	Efficiency	Min Up Time	Min Down Time	Ramp Rate	Start Up Cost	No Load Cost	Ramping Cost	Part Load Min	Start Up Time	CO <sub>2</sub> Intensity
<b>BIO</b>	<b>STUR</b>	0.40	4	6	0.020	120	12.5	1.30	0.4	1	0.42
<b>BIO</b>	<b>GTUR</b>	0.33	1	1	0.167	25	2.9	0.25	0.2	0.167	0.32
<b>BIO</b>	<b>COMC</b>	0.51	3	3	0.070	55	2.9	0.25	0.06	1	0.22
<b>BIO</b>	<b>ICEN</b>	0.36	1	1	0.040	24	0	0.63	0.25	1	0.27
<b>GAS</b>	<b>COMC</b>	0.51	3	3	0.070	55	2.9	0.25	0.06	1	0.36
<b>GAS</b>	<b>GTUR</b>	0.33	1	1	0.167	25	2.9	0.25	0.2	0.167	0.68
<b>GAS</b>	<b>STUR</b>	0.37	1	1	0.020	25	2.9	0.25	0.4	0.167	0.53
<b>GAS</b>	<b>ICEN</b>	0.36	0	0	1	0	0	0	0.3	0	0.01
<b>GEO</b>	<b>STUR</b>	0.10	2	2	0.020	0	0	0	0	0	0
<b>HRD</b>	<b>STUR</b>	0.42	6	6	0.040	65	12.5	1.80	0.18	2	0.47
<b>LIG</b>	<b>STUR</b>	0.40	8	8	0.008	65	8	2.20	0.43	7	1.15
<b>OIL</b>	<b>STUR</b>	0.33	5	5	0.020	120	0	1.80	0.4	1	0.73
<b>OIL</b>	<b>GTUR</b>	0.33	0	0	0.167	0	0	0	0.2	0.167	1.08
<b>OTH</b>	<b>STUR</b>	0.33	0	0	0.167	0	0	0	0.2	0.167	0.80

Source: (Pavičević et al., 2019)

#### Annex 4. Renewable capacity factors

##### A.4.1 Wind

**Table 17** Areas associated with different suitability classes (Wind). Areas restricted to 10-200 km around urban centres. Wind (Potential Categories): Yearly Wind Speed Average [m/s]

$PR_{WIN} = 1$		Economically viable area [ $\text{km}^2$ ]						
Power Pool	Zone	5-6 [m/s]	6-7 [m/s]	7-8 [m/s]	8-9 [m/s]	9-10 [m/s]	10-11 [m/s]	$\bar{x}_{WIN}$ [-]
CAPP	<b>AO</b>	5,163						0.149
	<b>CM</b>	23,424	1,133					0.153
	<b>CF</b>	2,013						0.149
	<b>TD</b>	79,055	66,968	23,846	5,407	1,107		0.237
	<b>CG</b>							0
	<b>CD</b>	51,402	2,943					0.154
	<b>GQ</b>							0
	<b>GA</b>							0
EAPP	<b>BI</b>							0
	<b>DJ</b>	8,656	5,108	4,140	98			0.235
	<b>ER</b>	38,524	20,155	6,641	392			0.207
	<b>ET</b>	72,442	72,662	99,912	7,294	321		0.286
	<b>KE</b>	120,110	192,618	78,964	7,375	4,490	1,202	0.261
	<b>RW</b>							0
	<b>SO</b>	27,493	122,616	264,747	153,725	29,664		0.413
	<b>SD</b>	571,245	490,354	154,814	6,242			0.222
	<b>TZ</b>	237,481	107,172	35,021	7,042			0.206
	<b>UG</b>	10,549	5,468	1,312				0.199
NAPP	<b>SS</b>							0.286
	<b>DZ</b>	512,395	169,539	8,449				0.177
	<b>EG</b>	303,703	399,362	31,552				0.215
	<b>LY</b>	26,913	289,631	58,446	836			0.266
	<b>MR</b>	1,551	114,047	66,306	5,994	135		0.309
	<b>MA</b>	139,847	43,254	28,348	13,887	1,363		0.227
	<b>TN</b>	47,780	72,403	12,475				0.227
$x_{WIN,i}$ [-]		0.149	0.251	0.388	0.565	0.762	0.914	

Source: (Hermann, Miketa, and Fichaux, 2014).

#### A4.2 Solar PV

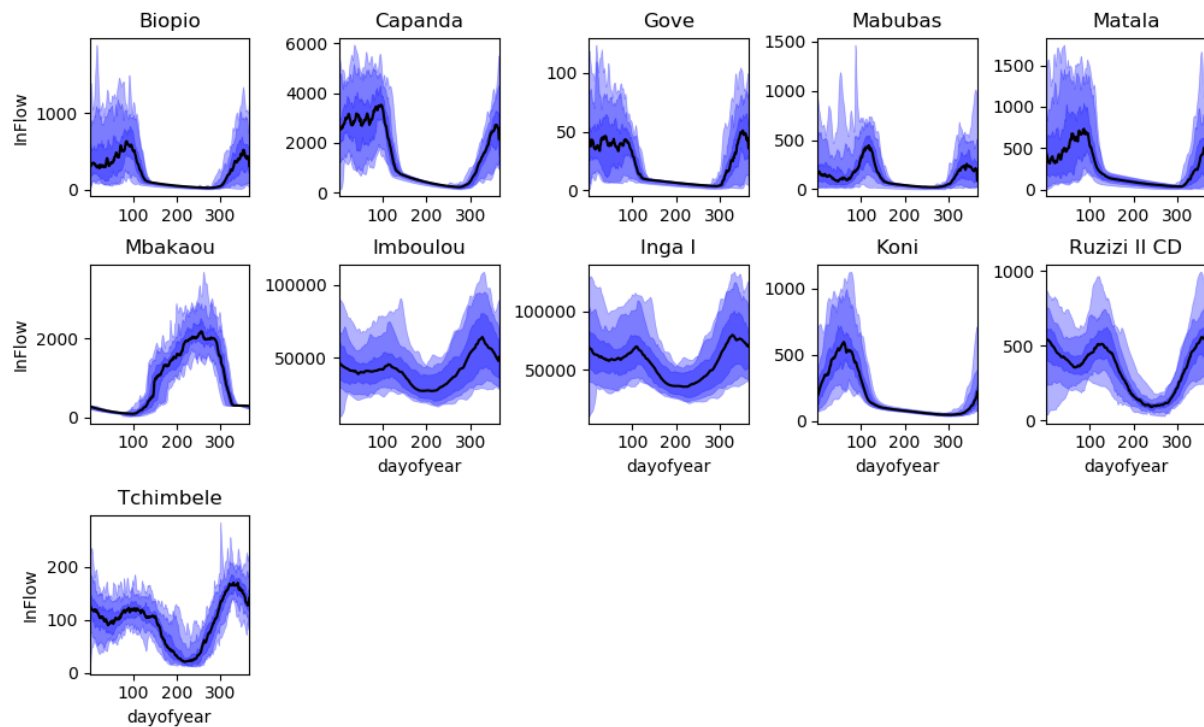
**Table 18** Areas associated with different suitability classes (PV). PV (Potential Categories) Global Horizontal Irradiation [kWh/m<sup>2</sup>/year)

$PR_{SUN} = 0.75$		Economically viable area [km <sup>2</sup> ]			$\bar{x}_{SUN}$ [-]
Power Pool	Zone	1500 – 2000 [kWh/m <sup>2</sup> /a]	2000 – 2500 [kWh/m <sup>2</sup> /a]	2500 – 3000 [kWh/m <sup>2</sup> /a]	
CAPP	<b>A0</b>	70,958	240,784		0.170
	<b>CM</b>	135,617	119,076		0.157
	<b>CF</b>	4,315	114,061		0.178
	<b>TD</b>		233,472		0.180
	<b>CG</b>	193,020	505		0.137
	<b>CD</b>	133,049	404,565		0.169
	<b>GQ</b>	20,159			0.137
	<b>GA</b>	153,793	419		0.137
EAPP	<b>BI</b>		19,737		0.180
	<b>DJ</b>		21,036		0.180
	<b>ER</b>		106,110		0.180
	<b>ET</b>	12,883	588,252	4,216	0.179
	<b>KE</b>	66,369	451,266	7,565	0.175
	<b>RW</b>		19,824		0.180
	<b>SO</b>	155,202	450,114		0.169
	<b>SD</b>	24,504	1,932,441		0.179
NAPP	<b>TZ</b>	5,501	845,122	10,570	0.180
	<b>UG</b>		210,450		0.180
	<b>DZ</b>	570,894	176,064		0.147
	<b>EG</b>	206,412	555,423		0.168
	<b>LY</b>	293,308	82,519		0.146
	<b>MR</b>	53,252	136,134		0.168
	<b>MA</b>	148,136	221,572		0.163
	<b>TN</b>	132,712			0.137

Source: (Hermann, Miketa, and Fichaux, 2014).

## Annex 5. Historical inflows

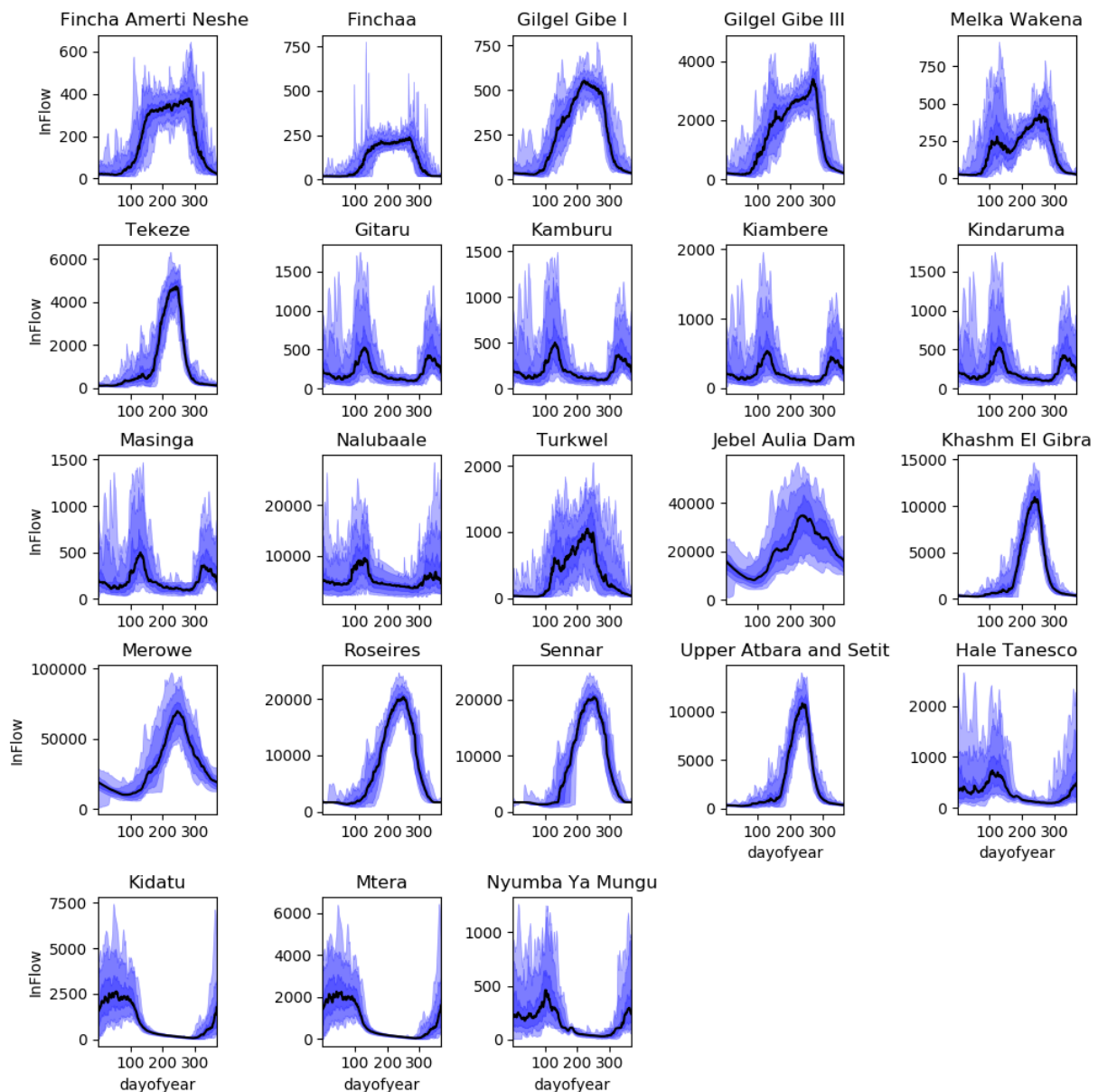
**Figure 45** Historical time series of Inflows in major HDAM units located in CAPP for one year.



Source: JRC, 2020

The 0th, 5th, 25th, 50th (black line), 75th, 95th and 100th percentiles are presented.

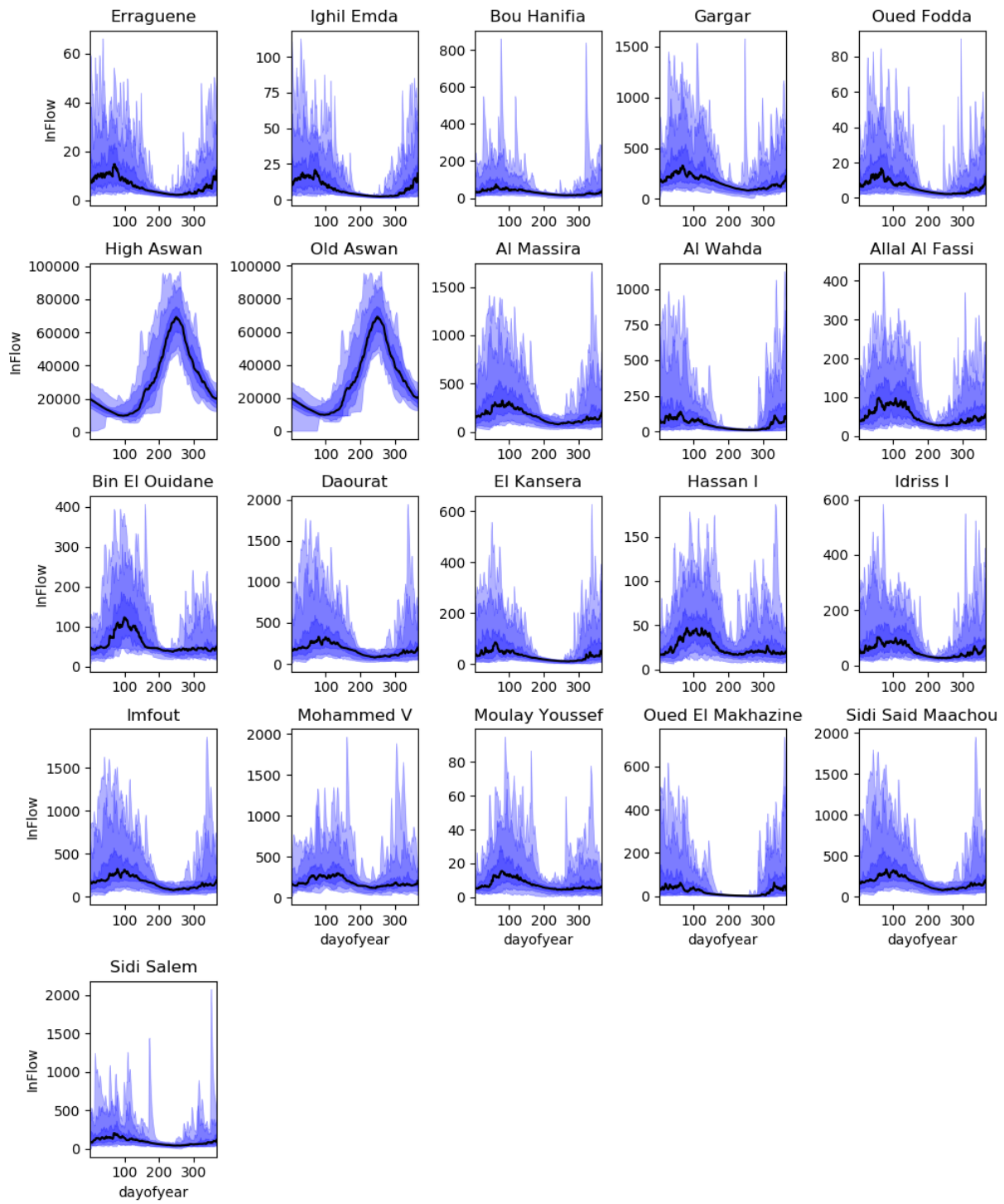
**Figure 46** Historical time series of Inflows in major HDAM units located in EAPP for one year.



Source: JRC, 2020

The 0th, 5th, 25th, 50th (black line), 75th, 95th and 100th percentiles are presented.

**Figure 47** Historical time series of Inflows in major HDAM units located in NAPP for one year



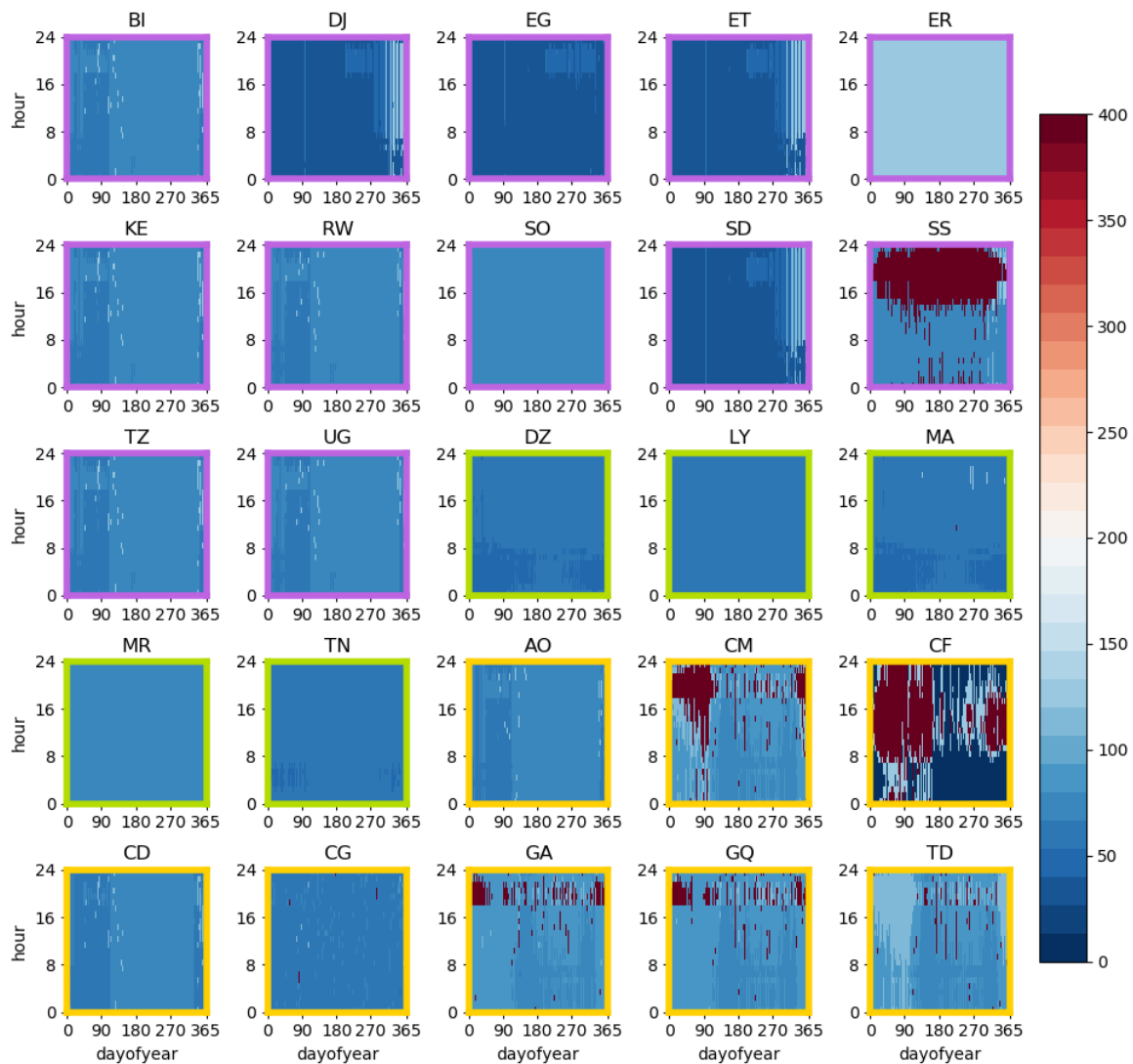
Source: JRC, 2020

The 0th, 5th, 25th, 50th (black line), 75th, 95th and 100th percentiles are presented.

## Annex 6. Shadow prices

### A6.1 Reference scenario

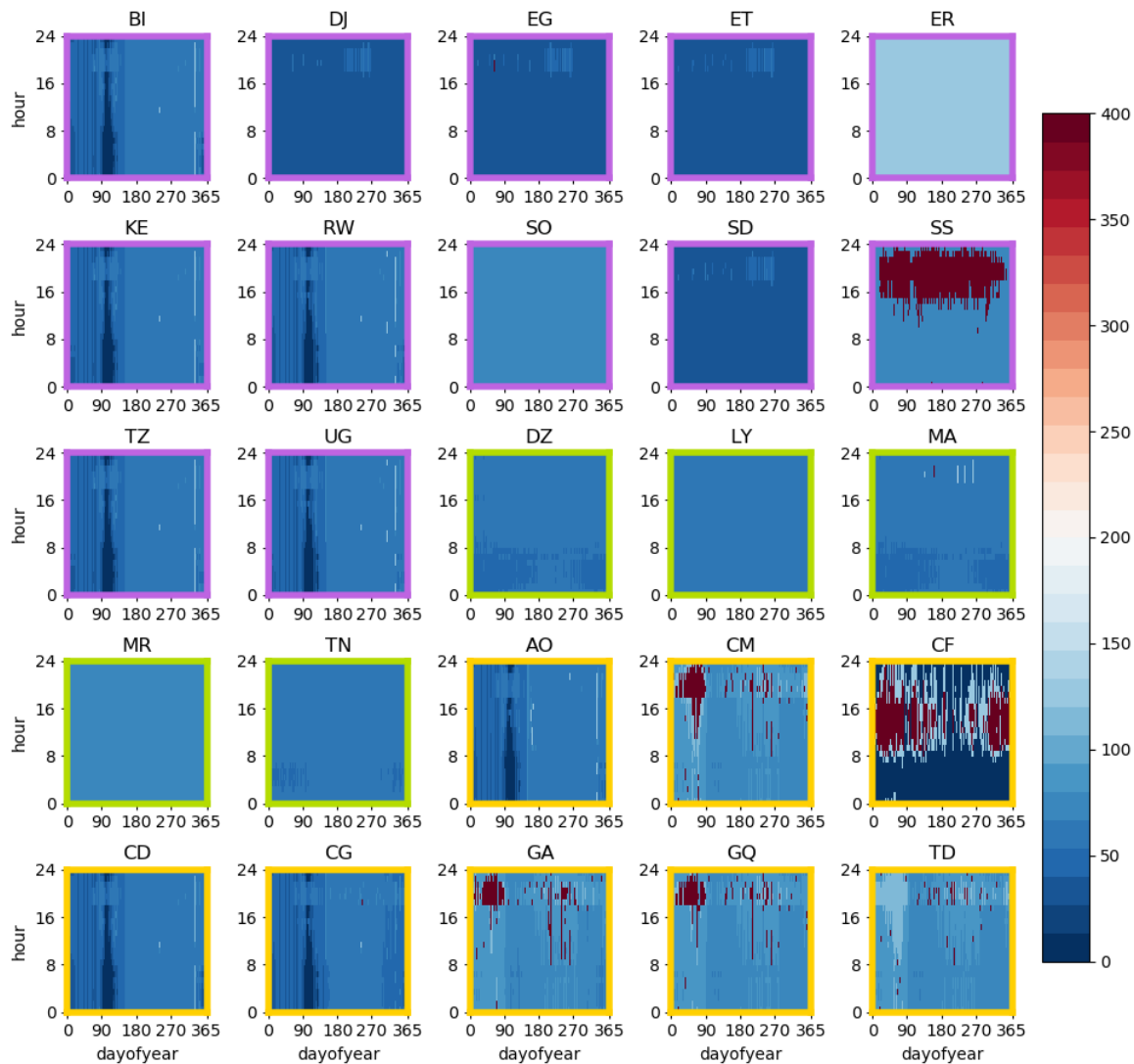
**Figure 48** Heatmap of shadow prices in individual countries for the driest year (2009) in Reference scenario



Source: JRC, 2020

Values on the legend indicate shadow prices in EUR/MWh, blue colours represent variable dispatch costs, red stands for shed load. Purple zones belong to EAPP, green zones belong to NAPP and yellow zones belong to CAPP.

**Figure 49** Heatmap of shadow prices in individual countries for the wettest year (1985) in Reference scenario

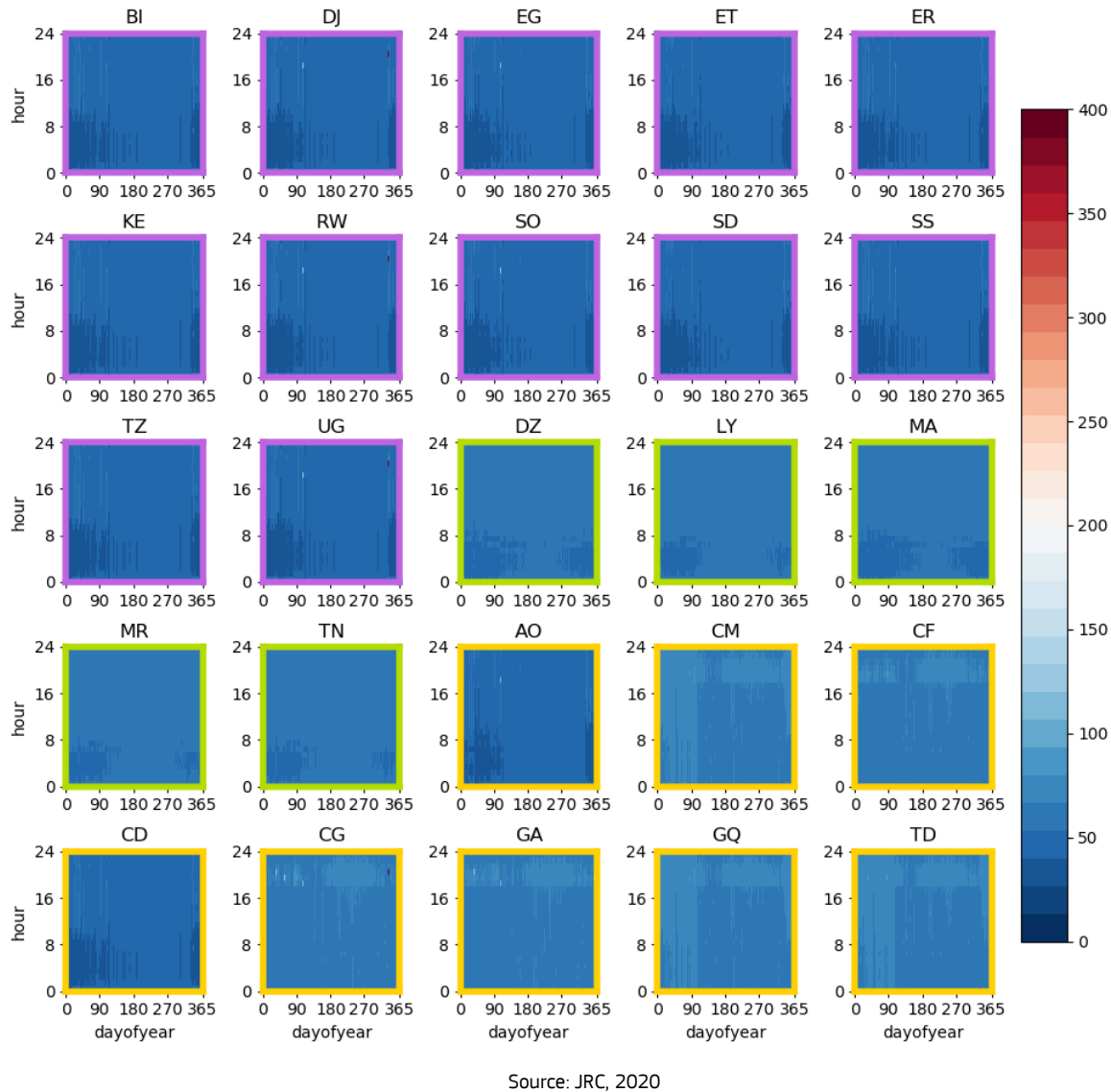


Source: JRC, 2020

Values on the legend indicate shadow prices in EUR/MWh, blue colours represent variable dispatch costs, red stands for shed load. Purple zones belong to EAPP, green zones belong to NAPP and yellow zones belong to CAPP.

## A6.2 Connected scenario

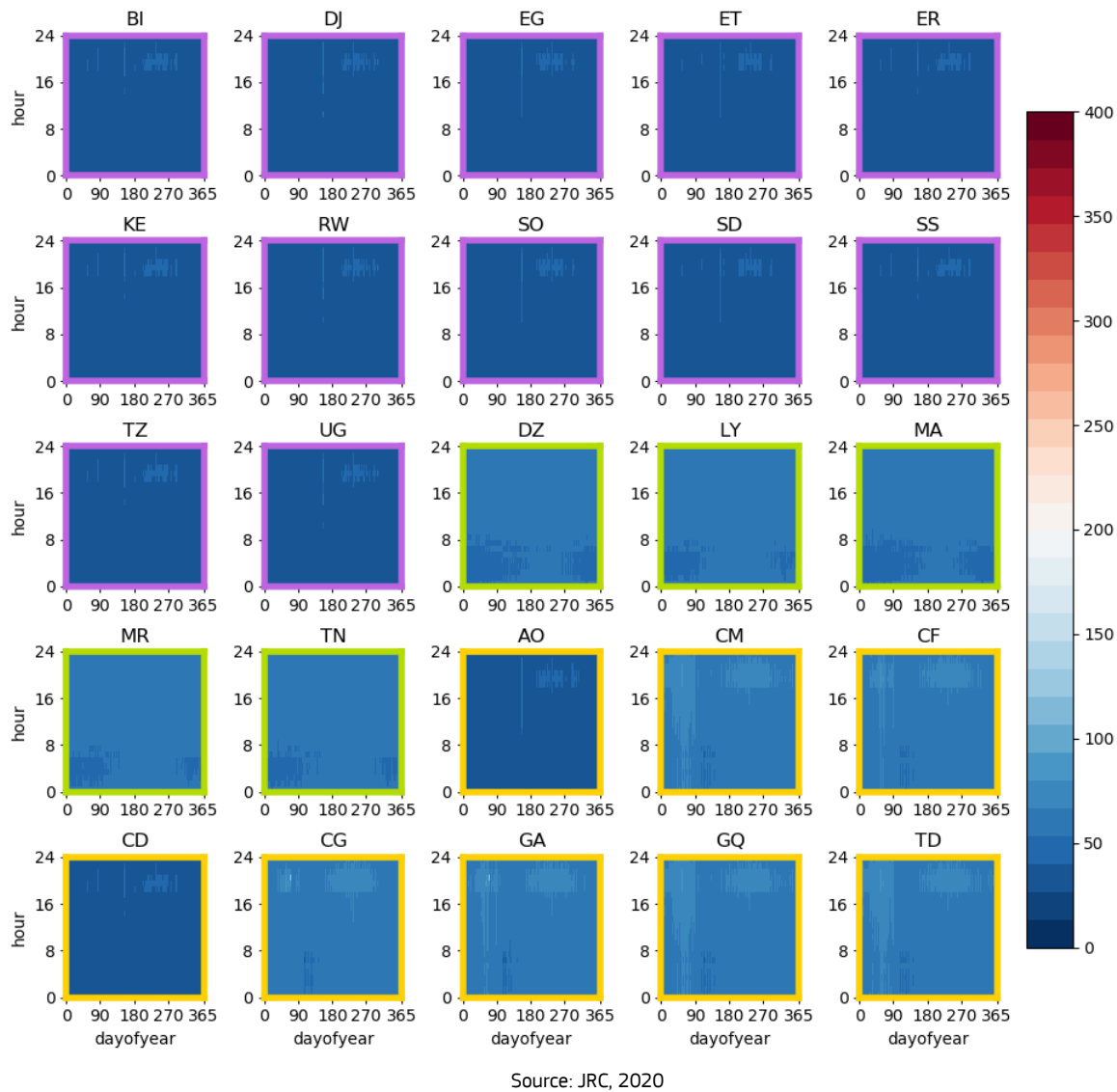
**Figure 50** Heatmap of shadow prices in individual countries for the driest year (2009) in Connected scenario



Source: JRC, 2020

Values on the legend indicate shadow prices in EUR/MWh, blue colours represent variable dispatch costs, red stands for shed load. Purple zones belong to EAPP, green zones belong to NAPP and yellow zones belong to CAPP.

**Figure 51** Heatmap of shadow prices in individual countries for the wettest year (1985) in Connected scenario



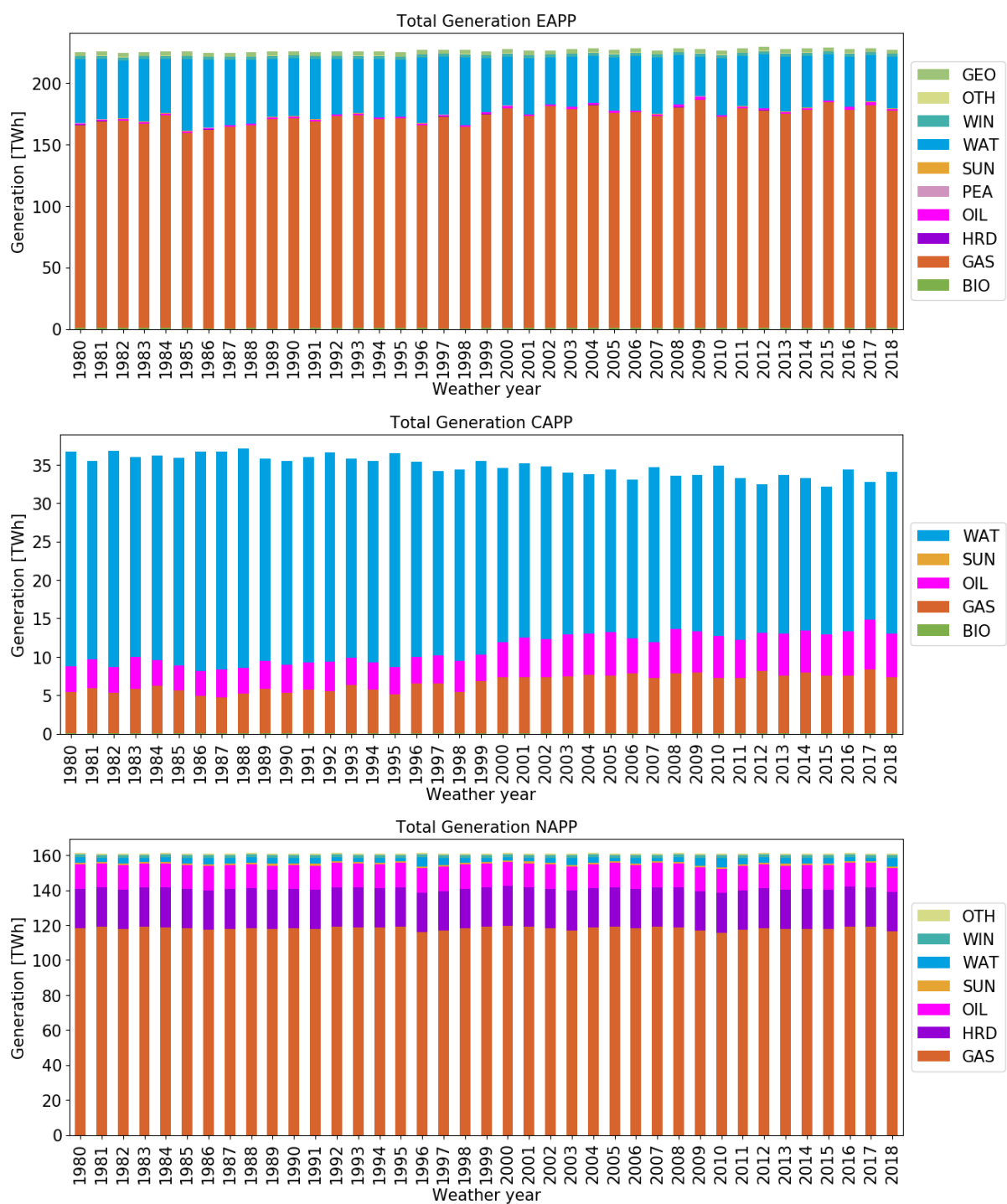
Source: JRC, 2020

Values on the legend indicate shadow prices in EUR/MWh, blue colours represent variable dispatch costs, red stands for shed load. Purple zones belong to EAPP, green zones belong to NAPP and yellow zones belong to CAPP.

## Annex 7. Generation

### A7.1 Reference Scenario

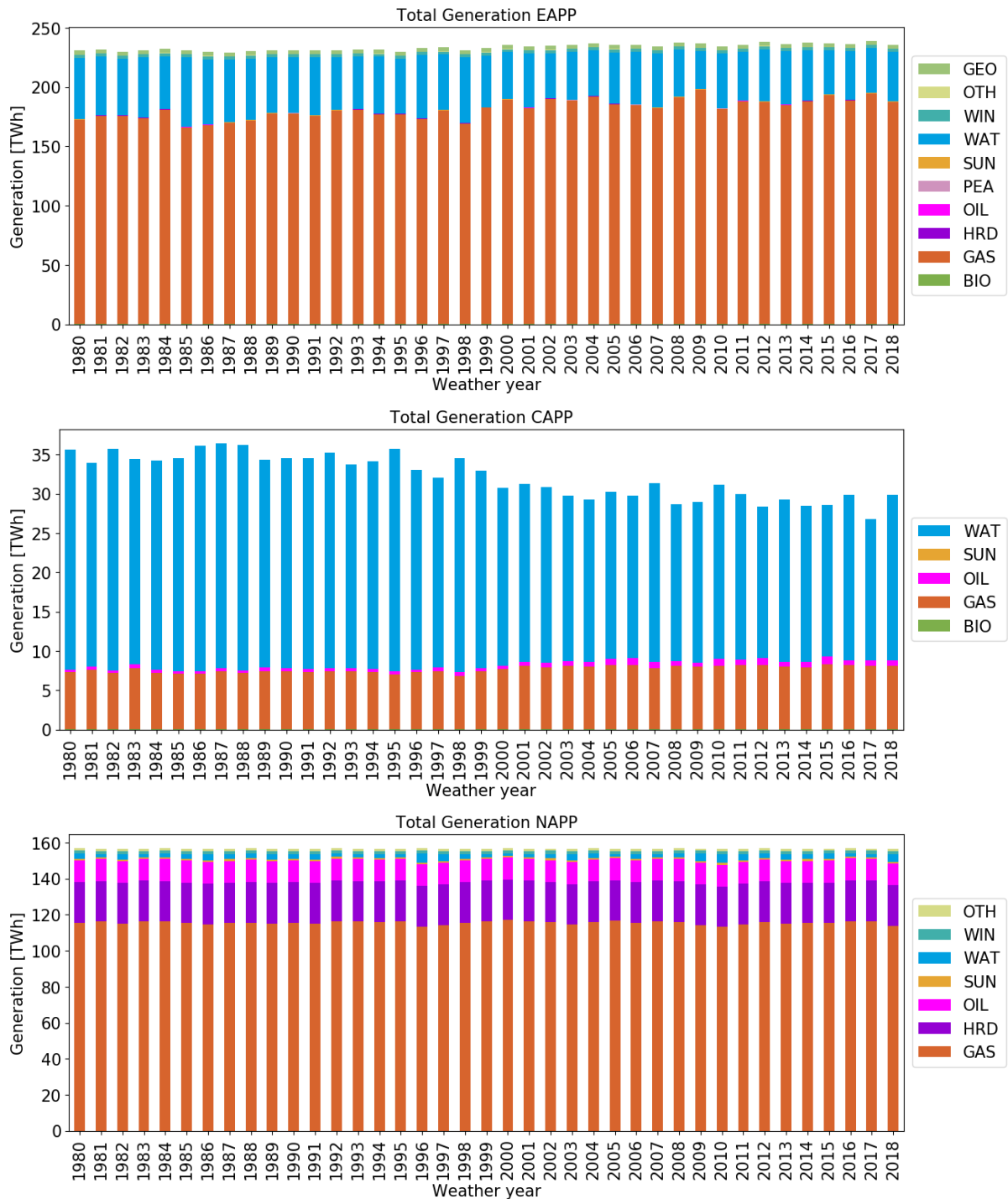
**Figure 52** Generation breakdown for individual power pools in Reference scenario



Source: JRC, 2020

## A7.2 Connected scenario

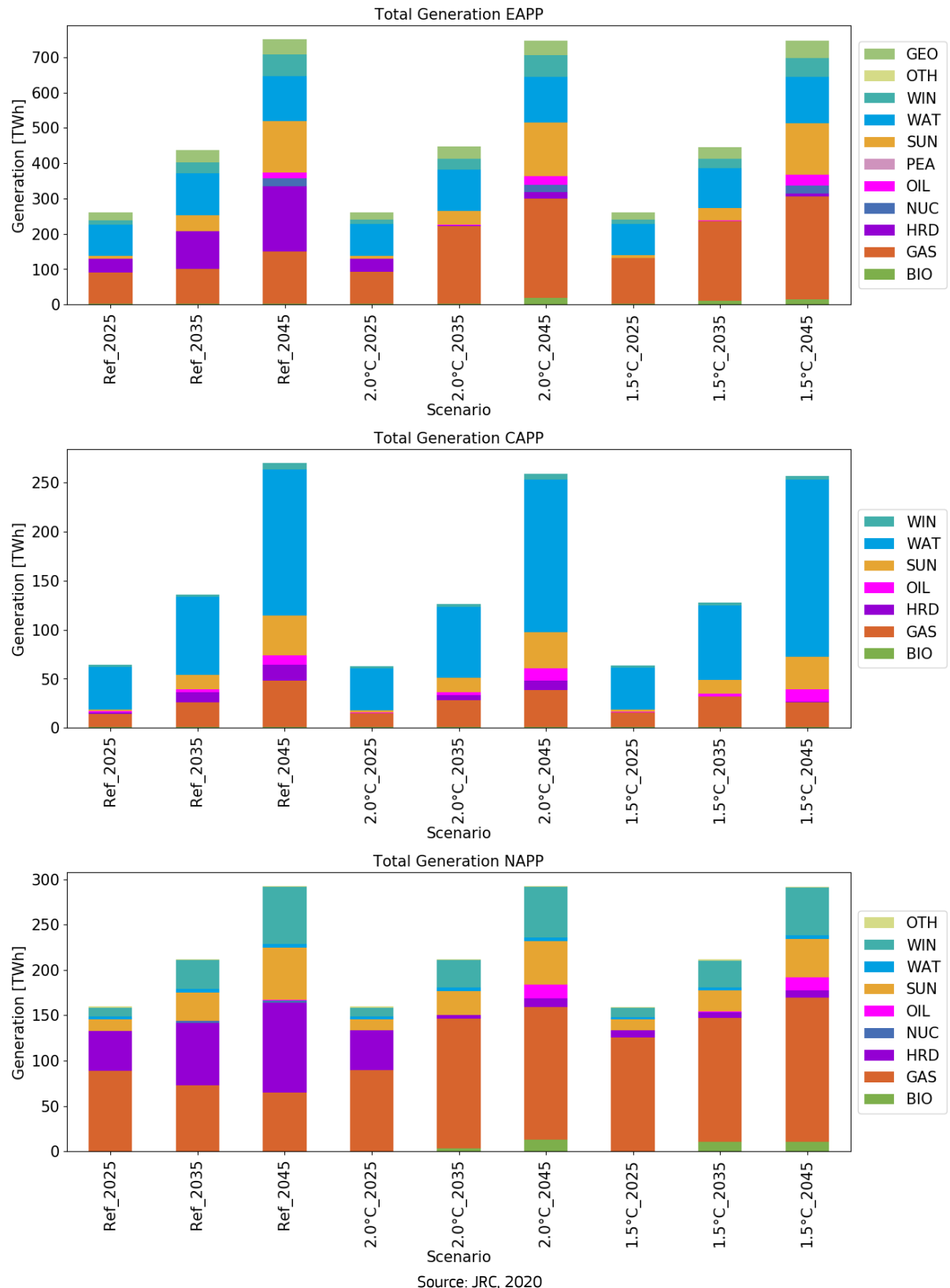
**Figure 53** Generation breakdown for individual power pools in Connected scenario



Source: JRC, 2020

### A7.3 TEMBA scenarios

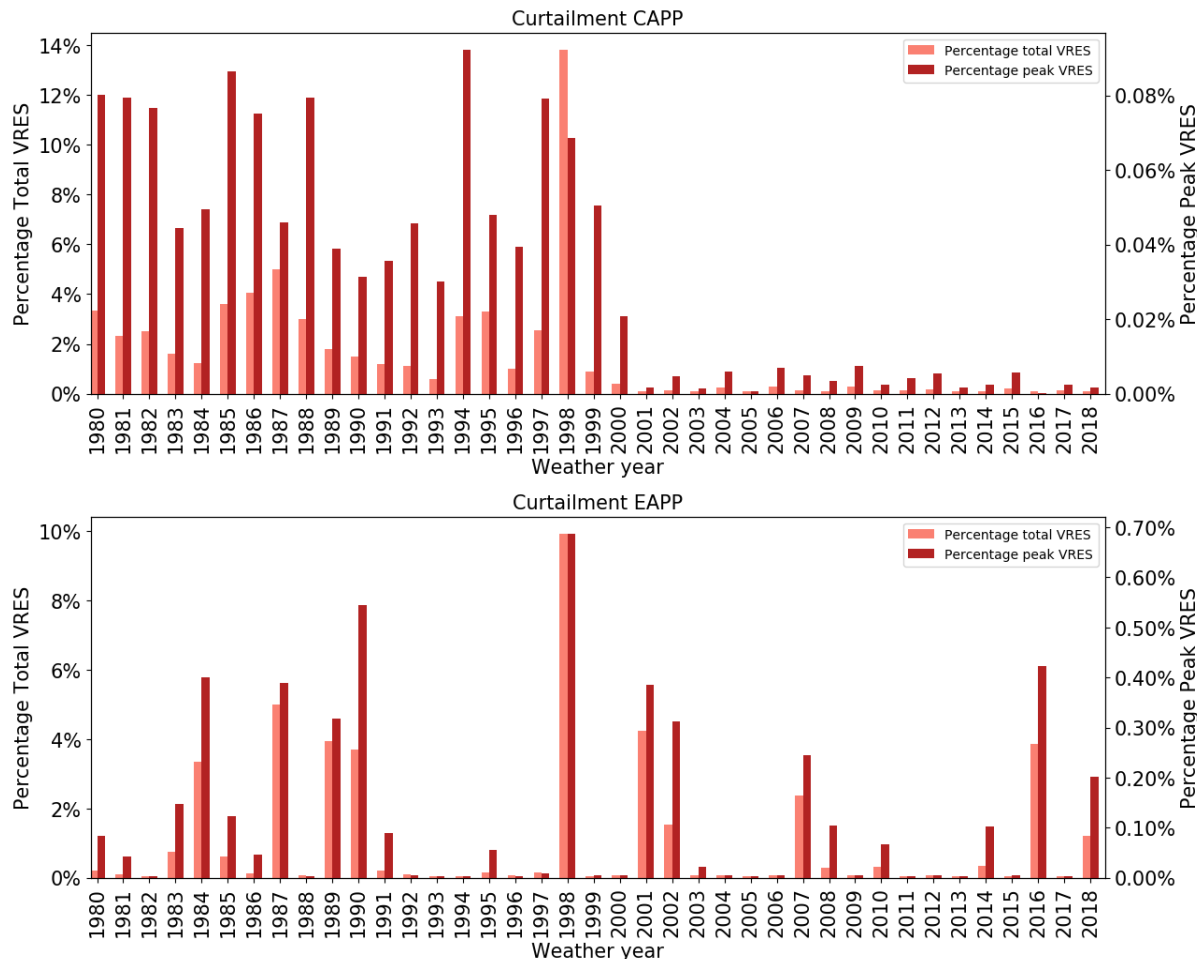
**Figure 54** Generation breakdown for individual power pools in TEMBA scenarios



## Annex 8. Curtailment

### A8.1 Reference scenario

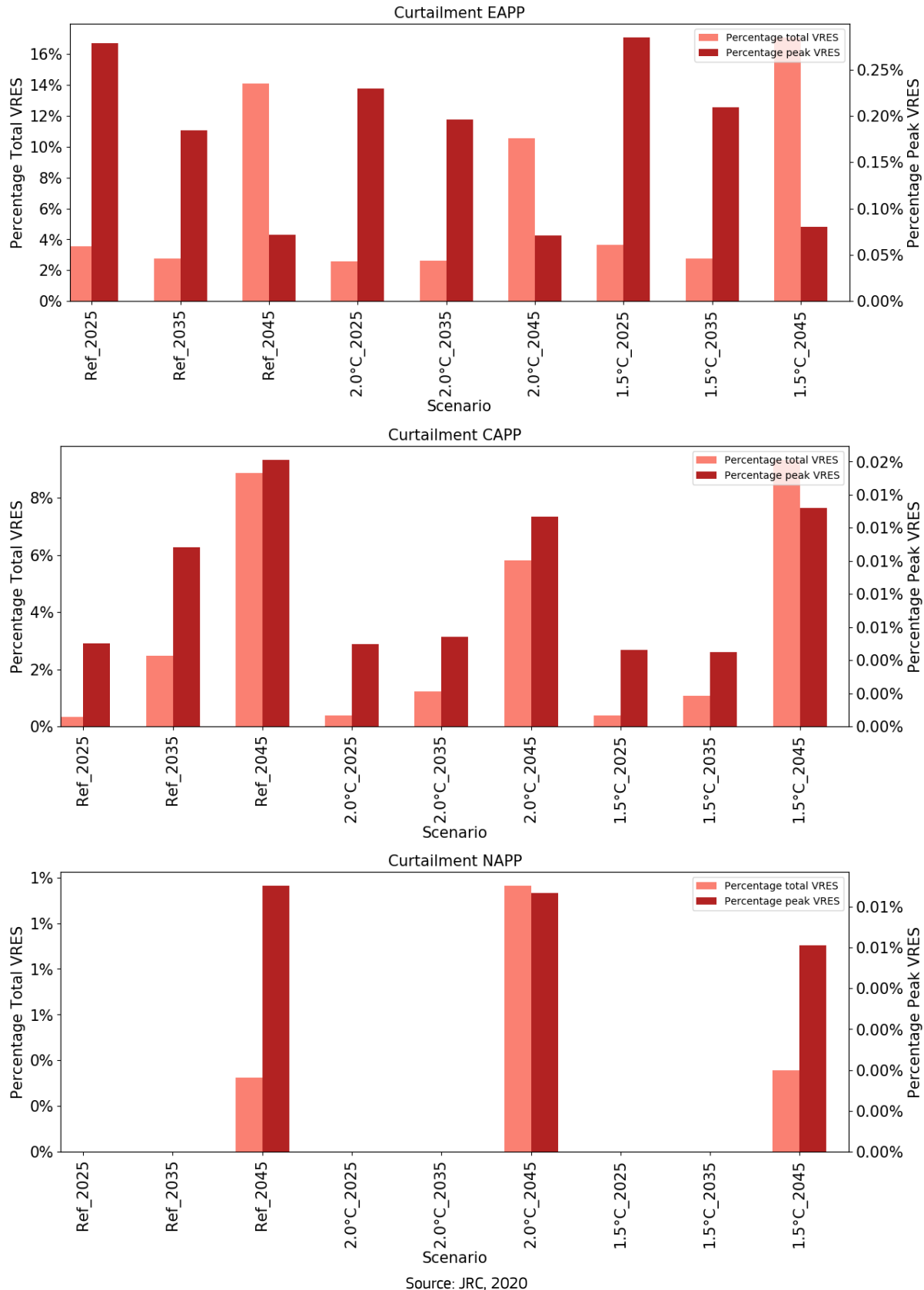
**Figure 55** VRES curtailment for individual power pools and different weather years in Reference scenario



Source: JRC, 2020

## A8.2 TEMBA scenarios

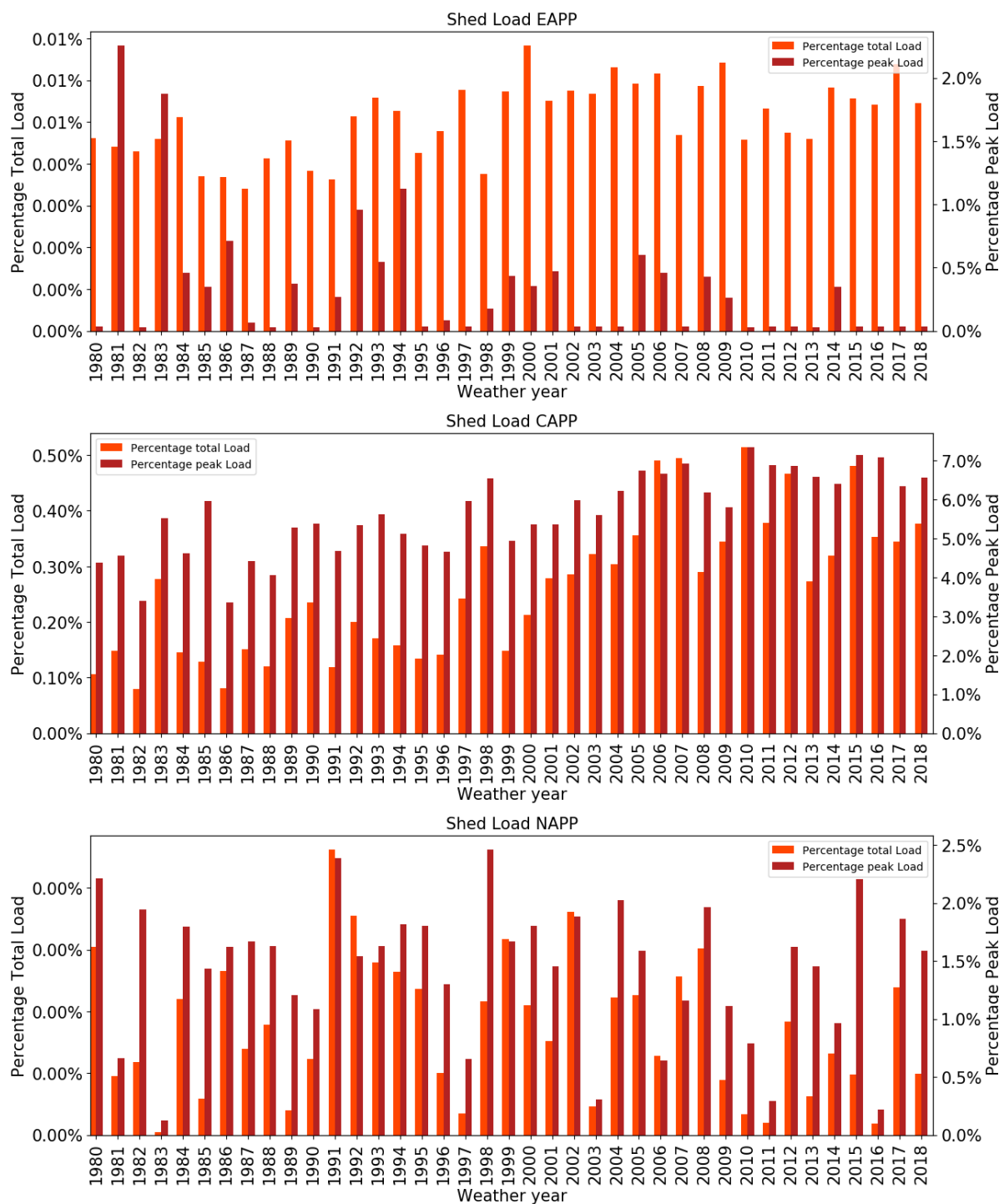
**Figure 56** VRES curtailment for individual power pools and different weather years in TEMBA scenarios



## Annex 9. Load shedding

### A9.1 Reference scenario

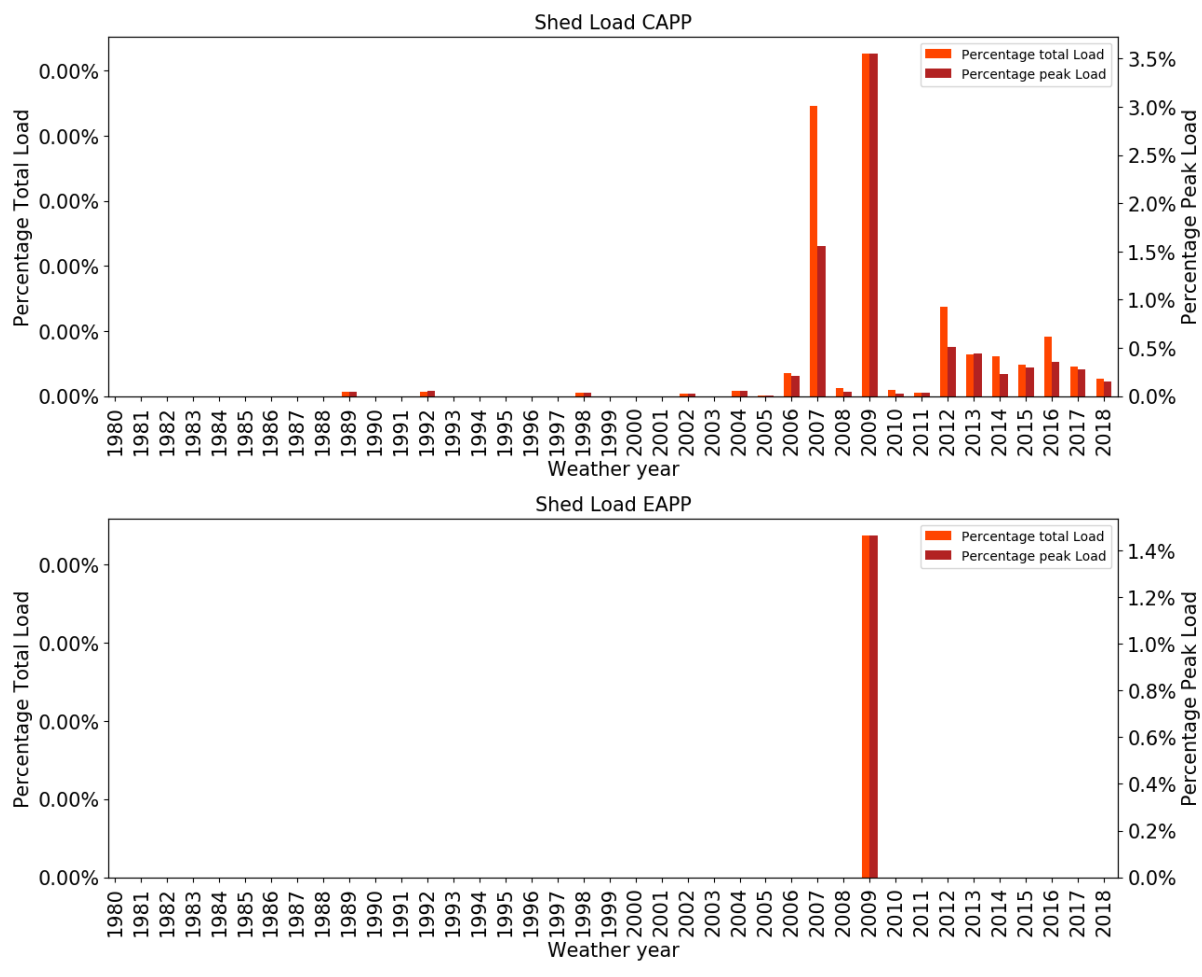
**Figure 57** Load shedding for Reference scenario



Source: JRC, 2020

A9.2 Connected scenario

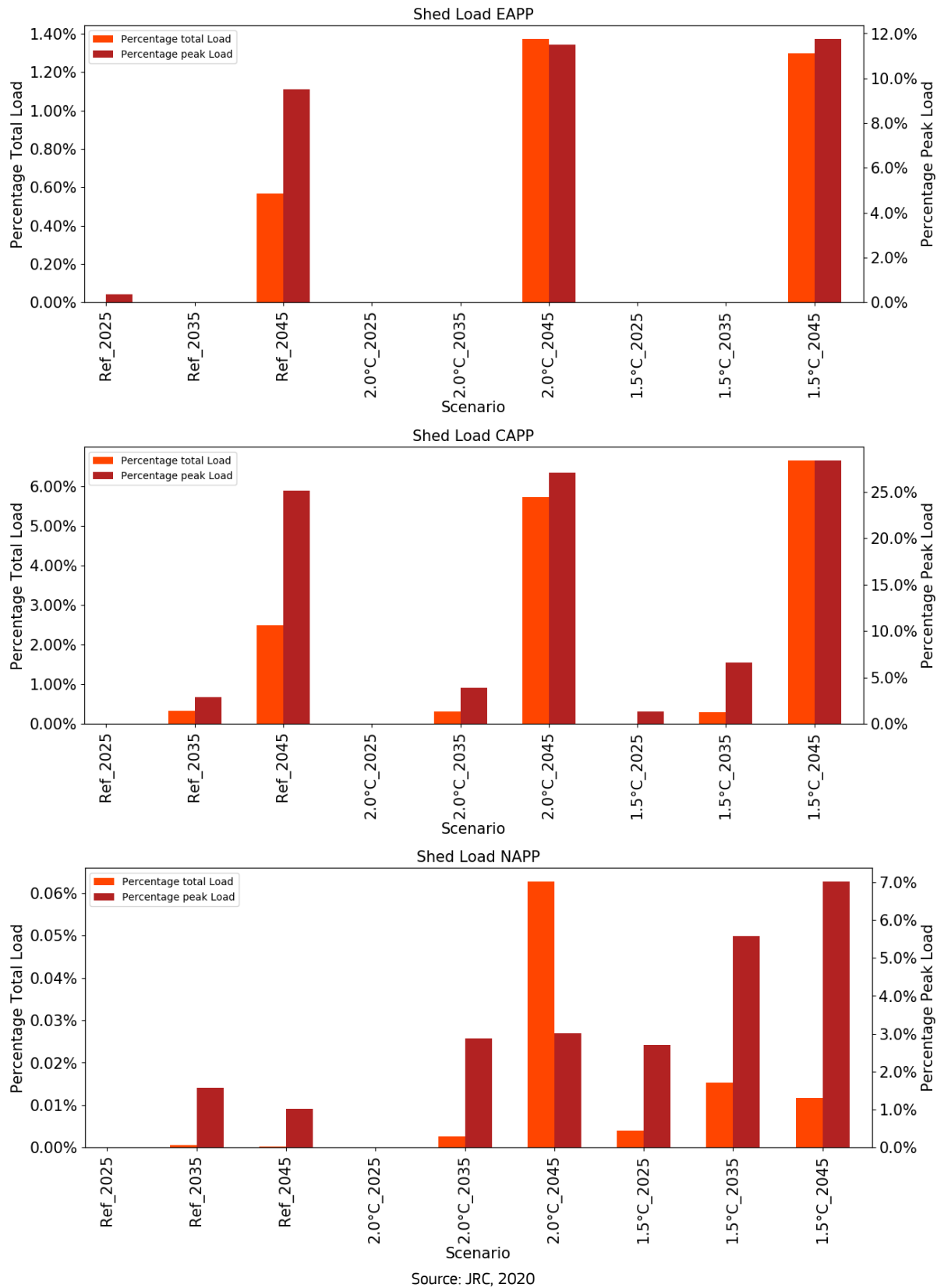
**Figure 58** Load shedding for Connected scenario



Source: JRC, 2020

### A9.3 TEMBA scenarios

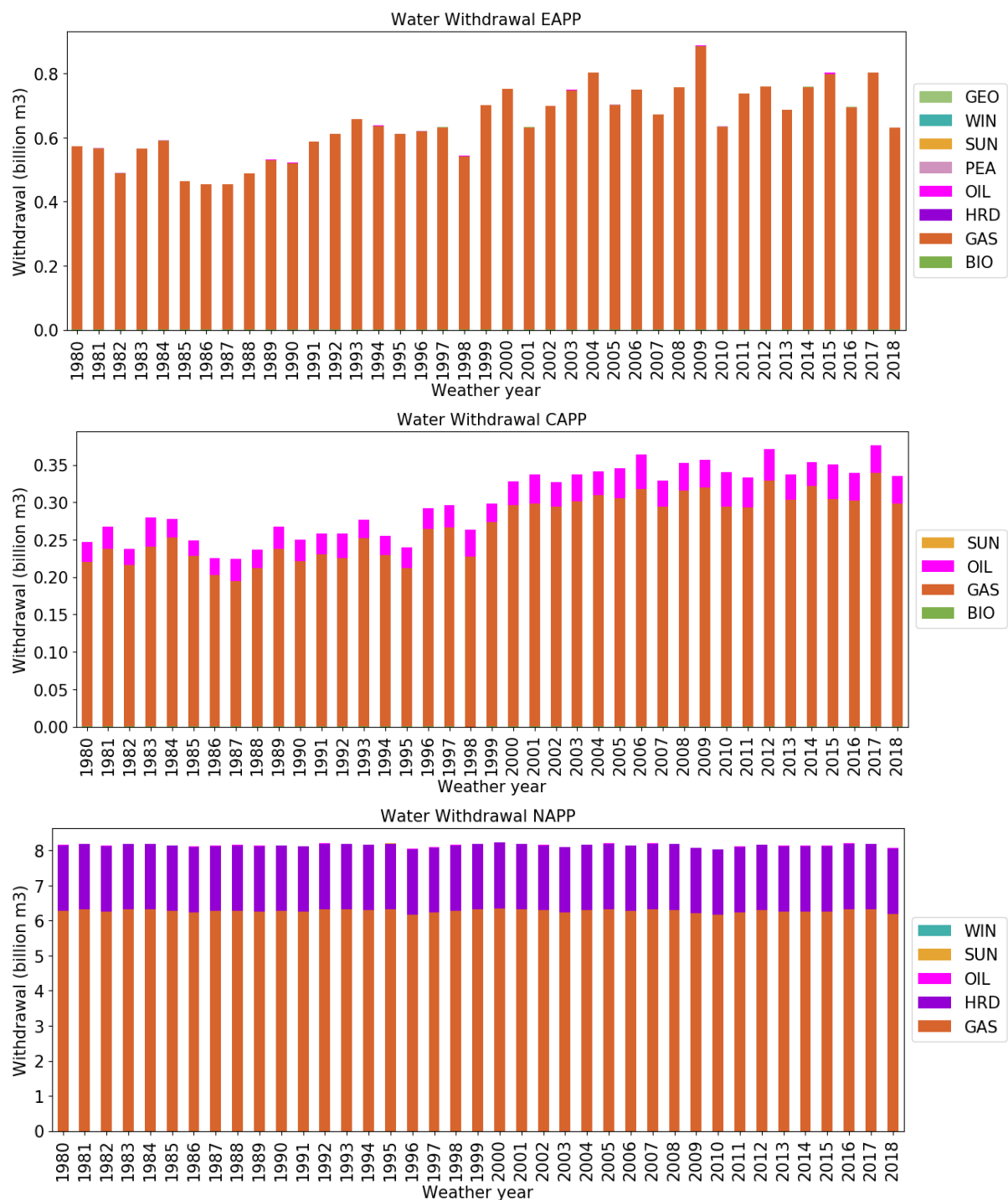
**Figure 59** Load shedding for TEMBA scenarios



## Annex 10. Water indicators

### A10.1 Reference scenario

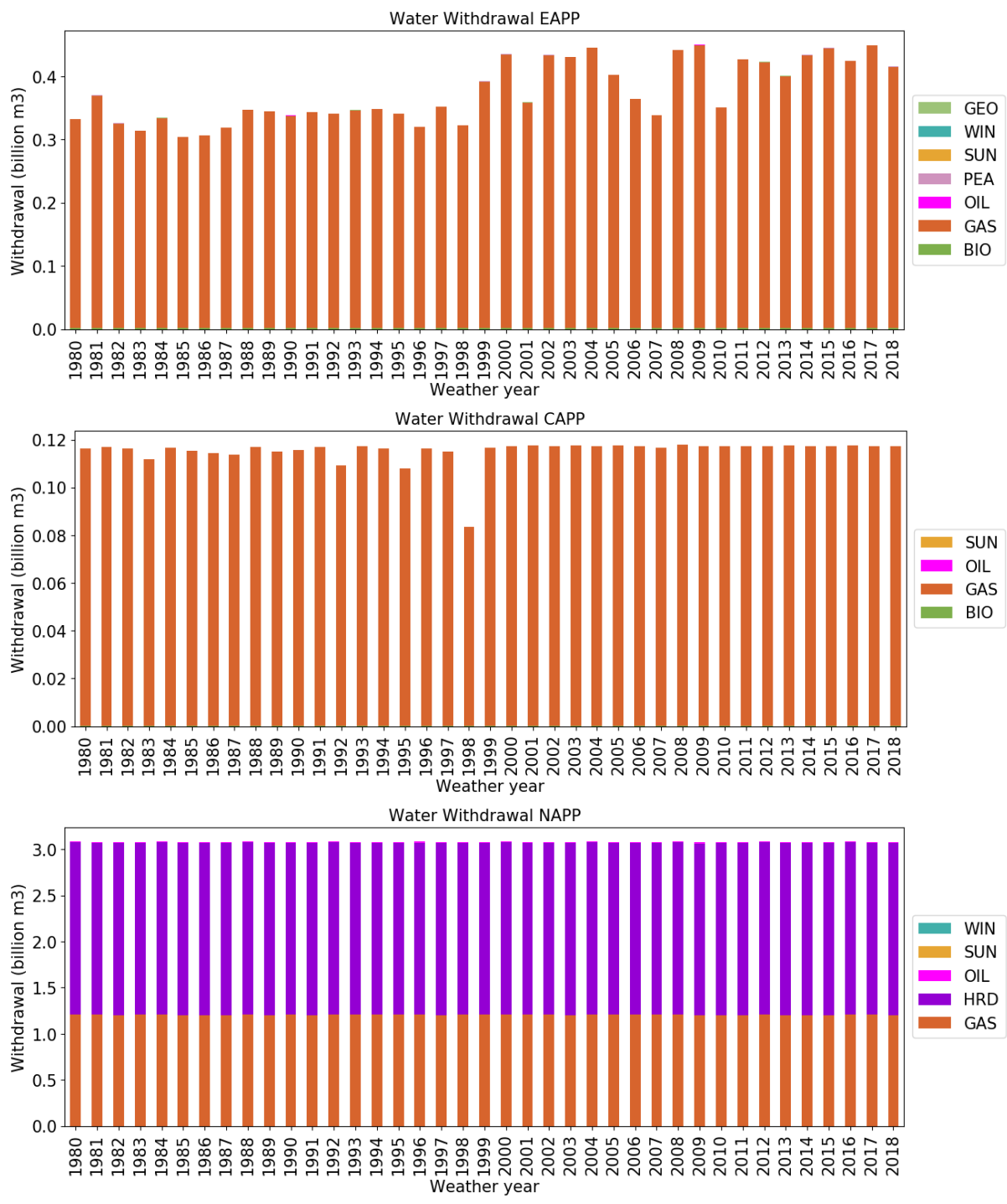
**Figure 60** Water Withdrawal for Reference scenario



Source: JRC, 2020

## A10.2. Connected scenario

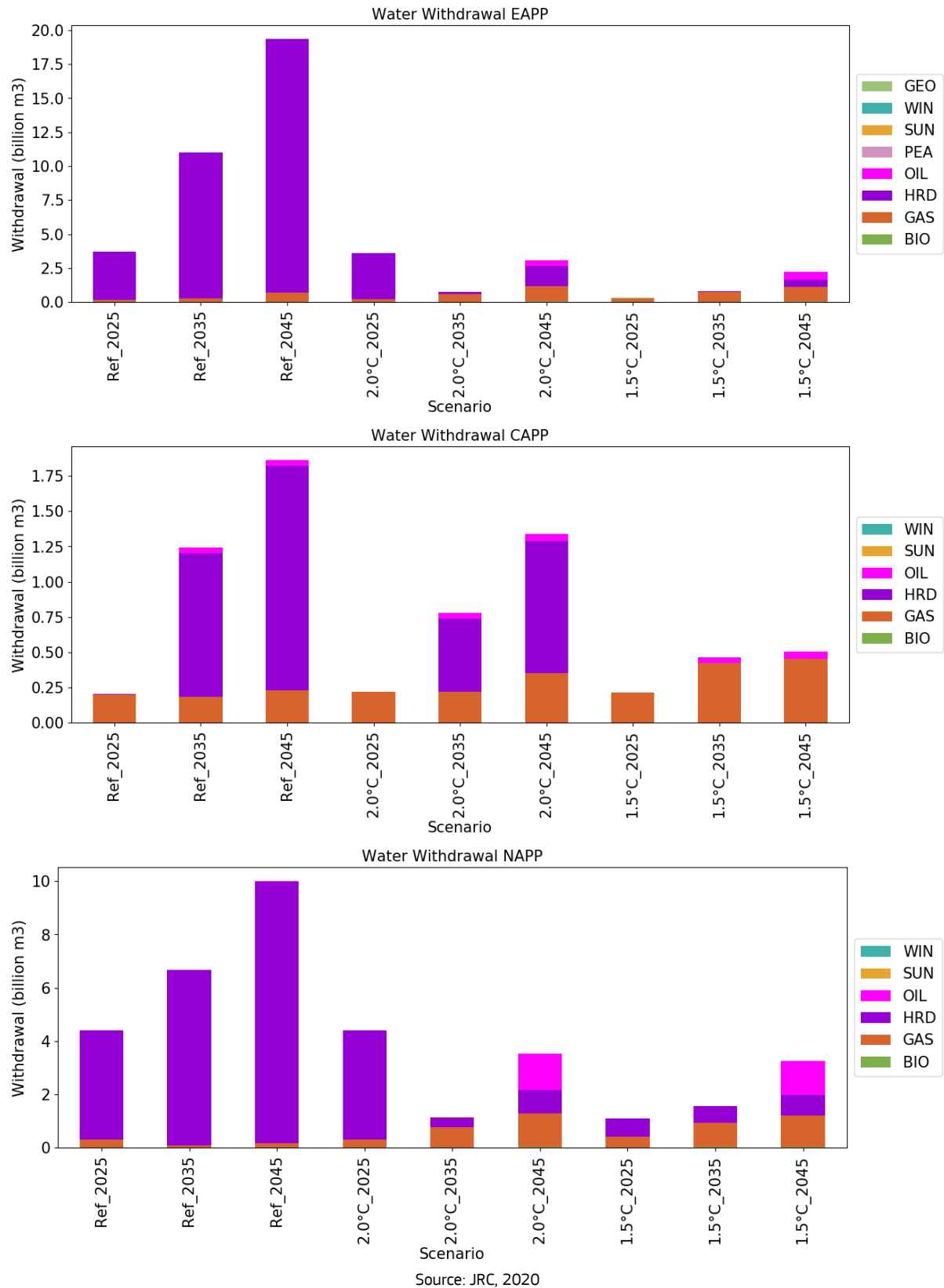
**Figure 61** Water Withdrawal for Connected scenario



Source: JRC, 2020

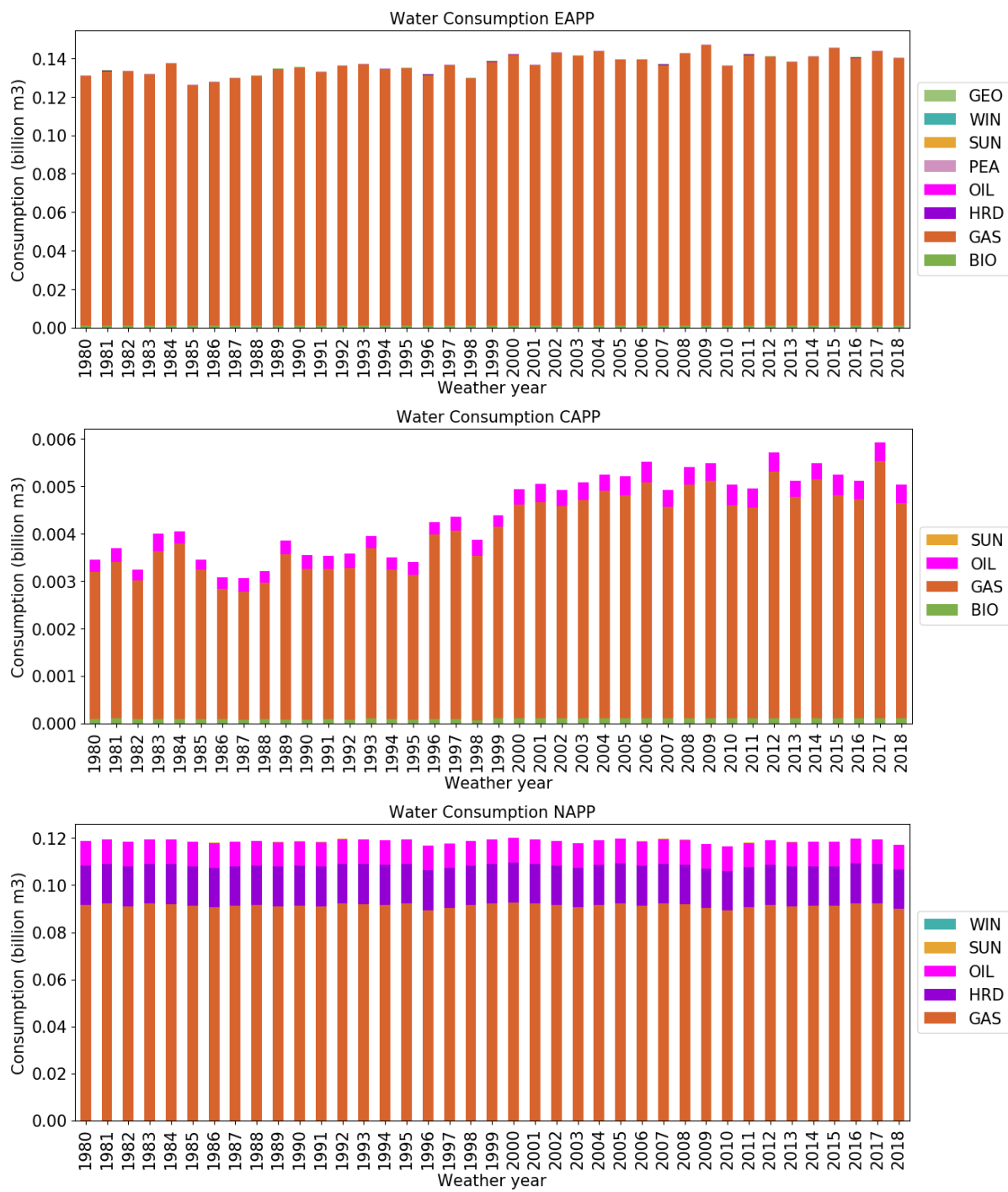
### A10.3 TEMBA Scenarios

**Figure 62** Water Withdrawal for TEMBA scenarios



#### A10.4 Reference scenario

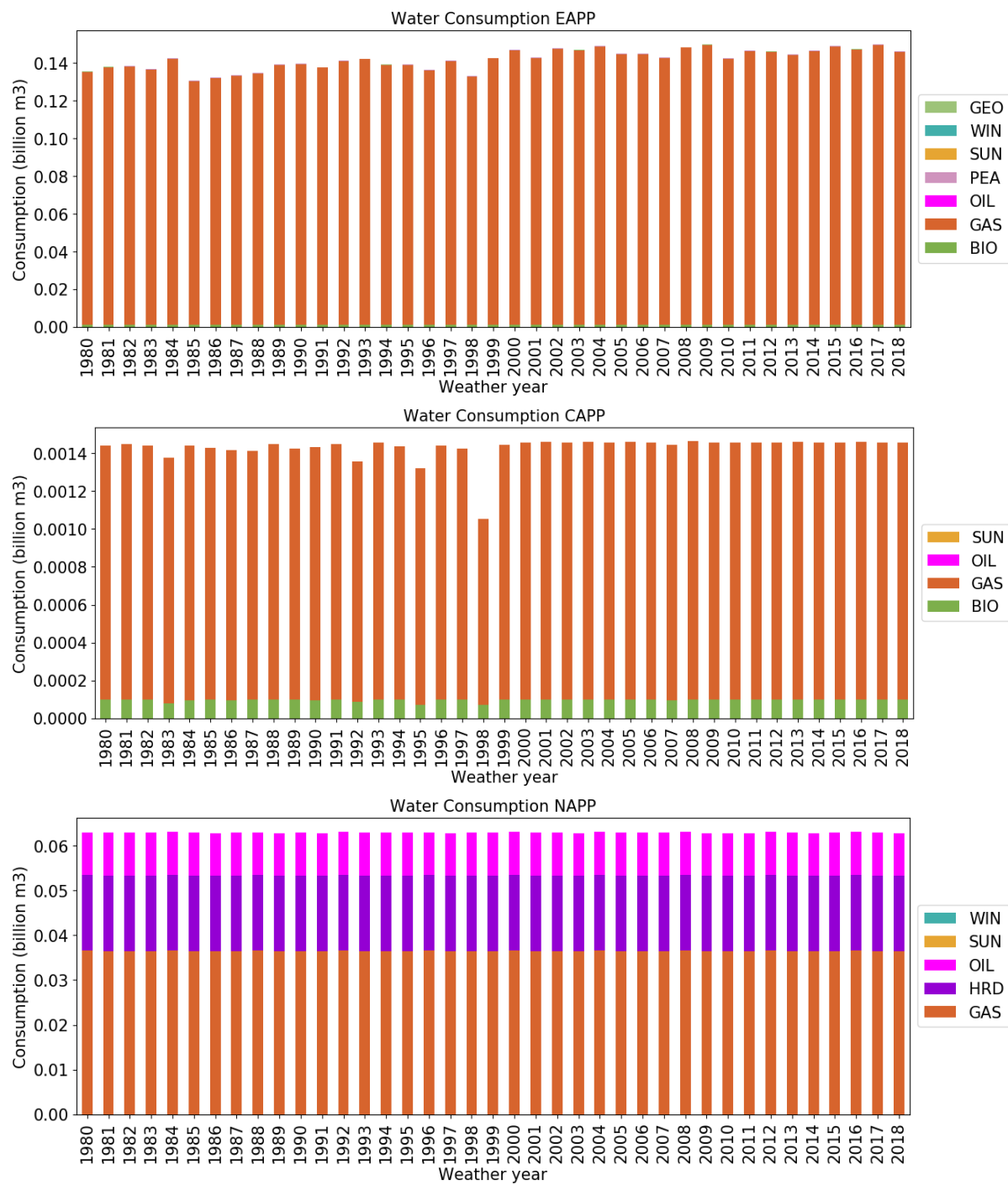
**Figure 63** Water Consumption for Reference scenario



Source: JRC, 2020

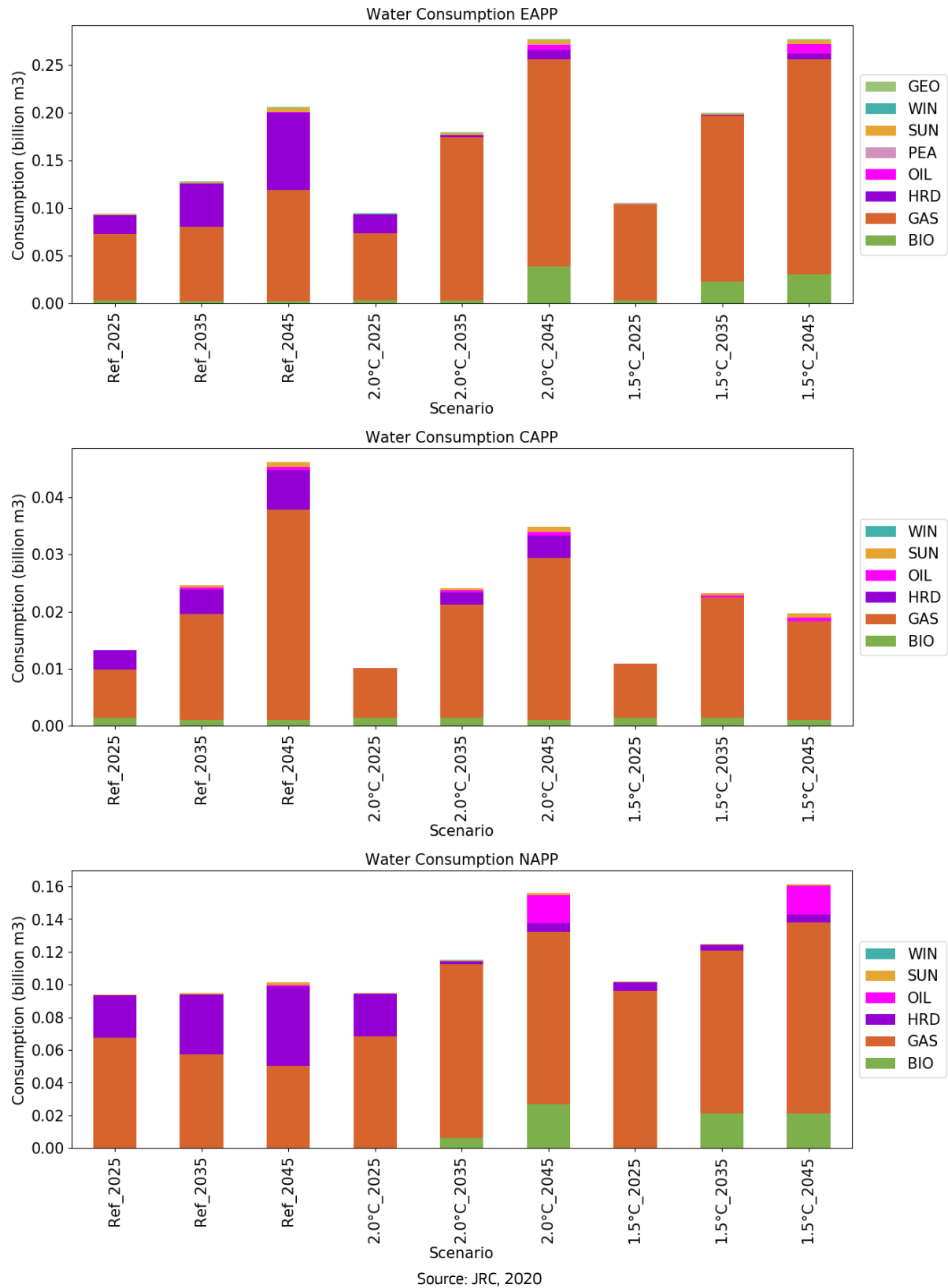
## A10.5 Connected scenario

**Figure 64** Water Consumption for Connected scenario



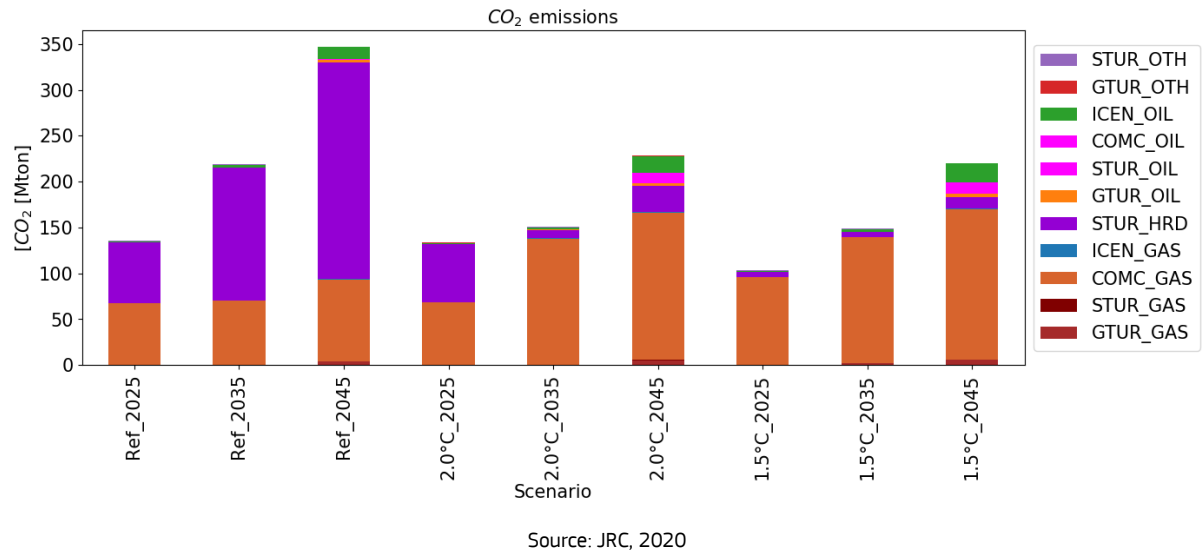
A10.6 TEMBA scenarios

**Figure 65** Water Consumption for TEMBA scenarios



## Annex 11. CO<sub>2</sub> emissions

**Figure 66** Summary of carbon emissions grouped per fuel and per technology type in TEMBA scenarios



## **GETTING IN TOUCH WITH THE EU**

### **In person**

All over the European Union there are hundreds of Europe Direct information centres. You can find the address of the centre nearest you at: [https://europa.eu/european-union/contact\\_en](https://europa.eu/european-union/contact_en)

### **On the phone or by email**

Europe Direct is a service that answers your questions about the European Union. You can contact this service:

- by freephone: 00 800 6 7 8 9 10 11 (certain operators may charge for these calls),
- at the following standard number: +32 22999696, or
- by electronic mail via: [https://europa.eu/european-union/contact\\_en](https://europa.eu/european-union/contact_en)

## **FINDING INFORMATION ABOUT THE EU**

### **Online**

Information about the European Union in all the official languages of the EU is available on the Europa website at: [https://europa.eu/european-union/index\\_en](https://europa.eu/european-union/index_en)

### **EU publications**

You can download or order free and priced EU publications from EU Bookshop at: <https://publications.europa.eu/en/publications>. Multiple copies of free publications may be obtained by contacting Europe Direct or your local information centre (see [https://europa.eu/european-union/contact\\_en](https://europa.eu/european-union/contact_en)).

**The European Commission's  
science and knowledge service**  
Joint Research Centre

**JRC Mission**

As the science and knowledge service of the European Commission, the Joint Research Centre's mission is to support EU policies with independent evidence throughout the whole policy cycle.



**EU Science Hub**  
[ec.europa.eu/jrc](http://ec.europa.eu/jrc)



@EU\_ScienceHub



EU Science Hub - Joint Research Centre



EU Science, Research and Innovation



EU Science Hub



Publications Office  
of the European Union

doi:10.2760/12651

ISBN 978-92-76-20874-7